



Document title:

Validation of the Geomatrix Hanford Seismic Report for Use on the TWRS Privatization Project

Department:

Safety & Regulatory Programs

Contract title:

TWRS Privatization

Contract number:

DE-AC06-96RL13308

Author(s):

**Joe Litehiser Farhang Ostadan James Marrone
Nick Gregor**

Document Number:

RPT-W375-RU00004, Rev. 0

Checked by:

**Ann Tallman Alan Hosler Richard Lee
Richard Smith**

Date of issue:

March 17, 1999

Issue status:

Approved

Approved by:

Don Edwards

Approver's position:

Safety & Regulatory Programs Manager

Approver's signature

BNFL Inc.
TWRS-P Project
2940 George Washington Way
Richland, WA 99352
United States of America
Tel: 509 371 3000
Fax: 509 371 3001



History sheet

Rev	Date	Reason for revision	Revised by
0	03/17/1999	Initial Issue	

Contents

Item	Page Number
Executive Summary.....	vii
1. Introduction.....	1
1.1. Background and Purpose of Validation Report.....	1
1.2. Brief History of Geomatrix Hanford Seismic Hazard Report	1
1.3. Scope of Validation Studies Performed.....	2
2. Survey of Previous Site Hazard Estimates.....	4
2.1. Hanford Site Studies.....	4
2.2. U. S. Geological Survey (USGS) National Maps	5
3. Basis for Geomatrix (1996b) Input	11
3.1. Attenuation Relations	11
3.2. Seismic Sources.....	13
3.2.1. Yakima Fold Belt Sources	14
3.2.2. Sources of the Crystalline Basement.....	18
3.2.3. Cascadia Sources	20
3.3. Recurrence Relations.....	21
3.4. Foundation Soil Column.....	23
3.5. Model Weight Schemes.....	24
3.6. Other Parameters	24
4. Additional or Alternative Model Parameters.....	32
4.1. Additional Data.....	32
4.1.1. Regional Seismicity	32
4.1.2. Search for Local Strong Motion Data	32
4.2. Alternative Attenuation Relations	34
4.2.1. Cascadia Interface Subduction Zone.....	34
4.2.2. Campbell Shallow Crust Attenuation.....	34
4.3. Alternative or Additional Sources – May Junction Structure	35
4.4. Alternative Recurrence Relations - Saddle Mountain Fault Slip Rate	36
4.5. Alternative Weighting Schemes.....	37
4.6. Basin Effects	39
5. Confirmatory Analyses.....	49
5.1. Site Soil Column Amplification	49
5.1.1. Approach / Methodology.....	50
5.1.2. Validation of Calculations	51

Contents

Item	Page Number
5.1.3. Assessment of the Results	52
5.2. Hazard from Selected Sources.....	53
5.2.1. Yakima Fold Belt Faults.....	54
5.2.2. Deep Crystalline Crust	56
5.2.3. Cascadia Interplate Source	57
6. Hazard Sensitivity Results.....	69
6.1. Coupled/Uncoupled Yakima Fold Belt Fault Models.....	70
6.2. Weighting Scheme for Crustal Crystalline Basement Source.....	71
6.3. Effect of Alternative Attenuation Relationships.....	73
6.3.1. Cascadia Interface Subduction Zone	73
6.3.2. Campbell Attenuation Relationships.....	74
6.4. Effect of May Junction Fault	75
6.5. Effect of Higher Slip Rate on Saddle Mountains Fault Segments.....	75
7. Conclusions	97
8. References	99
Appendix A – Responses to Specific DOE RU Questions/Comments.....	109

FIGURES

1-1. Map of the Hanford Site and Location of the Tank Waste Remediation System Phase 1 Demonstration Site.....	3
2-1. Schematic Comparison of Various Soil Classification Criteria	9
3-1. Structural Map of the Pasco Basin and Surrounding Columbia Plateau.....	27
3-2. Sketch Map of Major Tectonic Features of the Cascadia Subduction Zone	28
3-3. Comparison of Truncated Exponential and Characteristic Forms of Magnitude Recurrence Relations.....	29
3-4. Two Composite Soil-Rock Shear-Wave Velocity Profiles for the 200 East Area: H1 + Basalt and its Shannon and Wilson Modification	30
4-1. Plot of Earthquake Epicenters from Geomatrix	42
4-2. Plot of Earthquake Epicenters from CNSS, Covering the Time Period of Early March 1991 to Late December 1998	43
4-3. Plot of Earthquake Epicenters from 1850 to December 1998, a Composite of Figures 4-1 and 4-2	44

Contents

Item	Page Number
4-4. Comparison of Predicted Response Spectra Amplitudes Between Youngs et al. (1993) and Youngs et al. (1997) for a Magnitude 8.5 Earthquake on the Cascadia Subduction Zone Interface Boundary at a Distance of 375 km	45
4-5. Comparison of Predicted Response Spectra Amplitudes Between Campbell (1994) and Campbell (1997).....	46
4-6. Comparison of Predicted Attenuation Uncertainties Between Campbell (1994) and Campbell (1997).....	48
5-1. G/G_{max} vs. Depth Relationship during Earthquake Shaking for Hanford 200 East Area Soil Profile: 'H1 + Basalt'	62
5-2. Effective Shear Strain Distribution during Earthquake Shaking for Hanford 200 East Area Soil Profile: 'H1 + Basalt'	62
5-3. Initial and Strain-Compatible Shear-Wave Velocity Profiles for Hanford 200 East Area Soil Profile: 'H1 + Basalt'	64
5-4. Strain-Compatible Damping Ratios for Hanford 200 East Area Soil Profile: 'H1 + Basalt'	65
5-5. Comparison of Hazard Curves (Annual Frequency of Exceedance) at 200 East Area from the Umtanum – Gable Mtn. Seismic Source.....	65
5-7. Comparison of Hazard Curves (Annual Frequency of Exceedance) at 200 East Area from the Cascadia Interface Seismic Source	68
6-1. Geomatrix (1996b) Mean Equal Hazard Spectrum at 200 East Area for 2,000-Year Return Period (Solid Line) with Confidence Intervals for Spectral Ordinates at PGA (Shown Here at 33 Hz), 0.3 sec (3.3 Hz), and 2.0 sec (0.5 Hz).....	78
6-2. Geomatrix (1996b) Mean Equal Hazard Spectrum at 200 East Area for 10,000-Year Return Period (Solid Line) with Confidence Intervals for Spectral Ordinates at PGA (Shown Here at 33 Hz), 0.3 sec (3.3 Hz), and 2.0 sec (0.5 Hz).....	80
6-3. Sensitivity of Coupled/Uncoupled Weighting of Yakima Folds Seismic Sources on the Total 2,000-Year Mean Equal Hazard Spectrum at 200 East Area	82
6-4. Sensitivity of Coupled/Uncoupled Weighting of Yakima Folds Seismic Sources on the Total 10,000-Year Mean Equal Hazard Spectrum at 200 East Area	83
6-5. Sensitivity of Various Weighting Schemes of the Crystalline Basement Source Models on the Total 2,000-Year Mean Equal Hazard Spectrum at 200 East Area	84
6-6. Sensitivity of Various Weighting Schemes of the Crystalline Basement Source Models on the Total 10,000-Year Mean Equal Hazard Spectrum at 200 East Area....	86
6-7. Modified Version of Figure 4-10 of Geomatrix (1996b)	88

Contents

Item	Page Number
6-8. Variation of Figure 4-10 of Geomatrix (1996b).....	89
6-9. Variation of Figure 4-10 of Geomatrix (1996b).....	90
6-10. Geomatrix Figure 5-4b Supplemented and Extended to Lower Annual Hazard Values to Include the Sensitivity Results for Campbell 1994 (C94) and Campbell 1997 (C97)	91
6-11. Geomatrix Figure 5-4b Supplemented and Extended to Lower Annual Hazard Values to Include the Contribution of the May Junction Fault	92
6-12. Geomatrix Figure 5-4b Supplemented and Extended to Lower Annual Hazard Values to Include the Contribution of the Sensitivity Analysis for the Saddle Mountain Fault	93

TABLES

2-1. Ground Motion Hazard Assessments at the Hanford Site by U.S.G.S.....	8
3-1. Shear Wave Velocity in the Top 30 Meters for Cite Class C	26
5-1. Summary of Degree-of-Fit to Geomatrix Hazard Curves.....	60
5-2. Summary of Degree-of-Fit to Geomatrix Hazard Curves.....	61
6-1. Spectral Ordinates for Alternate Weighting of Basement Models	77
A-1. Preliminary Questions Concerning the Geomatrix Report and Dynamic Analysis (sent by the RU following the 12/3/98 Level 1 Meeting).....	110
A-2. Post Meeting RU Comments (from the RU meeting minutes of the 12/14/98 Topical Meeting).....	113
A-3. Post Meeting RU Comments (from the RU meeting minutes of the 1/7/99 meeting with Geomatrix Consultants)	114

Executive Summary

The purpose of this report is to provide an independent validation of the seismic hazard analysis completed for the Hanford Site by Geomatrix Consultants (Geomatrix 1996b). The 2,000-year return period ground motions predicted by Geomatrix for the 200 East Area are an integral part of the seismic design basis for the TWRS-P Project. Although currently in use at the Hanford Site and previously extensively reviewed, BNFL Inc. has elected to perform its own review of the report using geotechnical experts on the BNFL team.

As discussed in this report, a variety of validation analyses were performed by BNFL Inc. We reviewed a series of the comments, questions, and responses that passed between Geomatrix and the several earlier reviewers of the report to identify areas of potential concern. We surveyed independent estimates of seismic hazard at the Hanford Site, particularly the recent work of Frankel et al. (1996). We reviewed all elements of the fundamental regional model to determine whether the Geomatrix report contains model parameters that might be affected by information developed over the past several years. We conclude that the Geomatrix report addresses and incorporates all questions raised during earlier reviews, that its conclusions match well the latest independent estimates of Hanford Site earthquake hazard, and that the seismic source model developed by Geomatrix is state-of-the-art and is consistent with current data.

The regional earthquake source model specified in the Geomatrix report is detailed and complex. The hazard estimates derived by Geomatrix are the weighted sums of many thousands of hazard curves computed from many hundreds of input assumptions. We made detailed analysis of those sources shown by Geomatrix to be the principal contributors to Hanford Site earthquake hazard. Based on these computations with an independent computational program we are able to validate both the Geomatrix computer algorithms and the principal results.

During the course of our validation effort we have had the benefit of several technical discussions with many of the scientists who worked on the latest (and earlier) version of the Geomatrix report and with DOE personnel and consultants. To address questions raised during these discussions, we performed representative sensitivity checks on selected parameters for selected models with emphasis on those parameters cited during the technical discussions. We find that the Geomatrix results are robust and not significantly altered by creditable variation of the parameters studied for the sensitivity of their variation to the Geomatrix hazard results.

We conclude that the Geomatrix methodology and the results of the Geomatrix report are appropriate for their application to the design of the TWRS-P Facility at the Hanford Site.

1. Introduction

1.1. Background and Purpose of Validation Report

Approximately 54 million gallons of highly radioactive wastes are stored in underground tanks at the Hanford Site near Richland, Washington. The Tank Waste Remediation System Privatization (TWRS-P) Project will be a privatized waste processing facility owned by BNFL, Inc. but located on DOE land in the 200 East Area of the Hanford Site (see Figure 1-1). The TWRS-P Project is currently in the early stages of design and will ultimately provide DOE with waste processing services capable of treating more than half of the Hanford tank wastes (by mass) and approximately 95% of the long-lived radionuclides.

Because the TWRS-P Facility processes and stores radioactive and hazardous materials, it is necessary to ensure that the facility can provide an adequate level of safety to workers and the public. In order to achieve this, the facility must, among other things, have the ability to withstand the effects of severe natural phenomena events such as earthquakes. To that end, the Project has adopted DOE-STD-1020-94 as the seismic standard for the TWRS-P Facility design and, through the use of that Standard, has established the recurrence interval for the facility's design basis earthquake at 2,000 years. In order to perform the facility design, the site-specific peak ground acceleration associated with the 2,000-year recurrence interval must be determined and the corresponding site-specific seismic response spectra must be generated.

The approach chosen to accomplish this is based on a seismic hazard analysis that was recently completed for the Hanford Site by Geomatrix Consultants (Geomatrix 1996b). The Geomatrix report, which is currently in use by DOE's Hanford contractors, has previously been thoroughly reviewed by DOE (Richland and Headquarters), by Westinghouse Hanford Company, and by independent national and international experts. Nevertheless, because of the privatized nature of the TWRS-P Project, BNFL, Inc. has an obligation to perform its own review of the report using geotechnical experts on the BNFL team. The primary purpose of this review was to validate the Geomatrix Hanford Seismic Hazard Report for use on the TWRS-P Project. In addition, specific questions and comments about the Geomatrix Report that have been raised by the DOE TWRS-P Regulatory Unit have been addressed by the BNFL review team.

1.2. Brief History of Geomatrix Hanford Seismic Hazard Report

The October 1996 Geomatrix report presents probabilistic seismic hazard analysis for five areas at the DOE Hanford Site. The analysis presented is the result of development and refinement of a seismic hazard model for the site region that was begun in 1981 (Powers et al.) for the Washington Public Power Supply System's WNP-1/4 and WNP-2 nuclear reactor sites. The 1981 model was subsequently applied, with modification for earthquake recurrence rate assessments, to the DOE Hanford Site (Woodward-Clyde Consultants, 1989).

In the early 1990s, the 1981 Powers et al. and the 1989 Woodward-Clyde Consultants regional hazard models were revisited in support of an Individual Plant Examination of External Events (IPEEE) analysis for WNP-2 and for planned new DOE projects. In order to develop this updated hazard analysis, the regional seismic model was revised by a team of regional geoscience and probabilistic hazard methodology experts from Geomatrix Consultants, Pacific Northwest National Laboratory, Washington Public Power Supply System, and Westinghouse Hanford Company. The revised model (Geomatrix Consultants, 1993) was used to calculate updated estimates at the same DOE Hanford Site locations

considered in the 1989 Woodward-Clyde Consultants report. The 1993 Geomatrix Consultants model was also used to develop hazard estimates for WNP-2 (Geomatrix Consultants, 1994a) that were incorporated into the WNP-2 IPEEE analysis (Washington Public Power Supply System, 1995) and to develop revised hazard estimates for seismic design of the Hanford Waste Vitrification Project.

In 1994 an extensive review of the 1993 Geomatrix Consultants report was begun, with emphasis on its results for the 200 West and 200 East Areas. Reviews were provided to Westinghouse Hanford Company by Mr. C. Fox, Jr. of Ebasco/BNFL and Dr. K. Campbell of EQE International, Inc. and to DOE through Brookhaven National Laboratory by Professors A. Cornell and C. Costantino and Dr. D. Boore. Review comments concentrated on the attenuation relations used in the 1993 report (both for local earthquakes and for more distant earthquakes on the Cascadia-North American plate interface), the proper inclusion of site-specific foundation soil/rock column effects, and the shape of the vertical design response spectrum relative to the horizontal spectrum in the long-period range. These comments were treated in several reports (Geomatrix Consultants, 1994b and 1996a) culminating in the current version of the Geomatrix Hanford Seismic Hazard Report (Geomatrix Consultants, 1996b).

The current version of the Geomatrix Consultants report has been approved by the DOE Richland Operations Office (Wagoner, 1997).

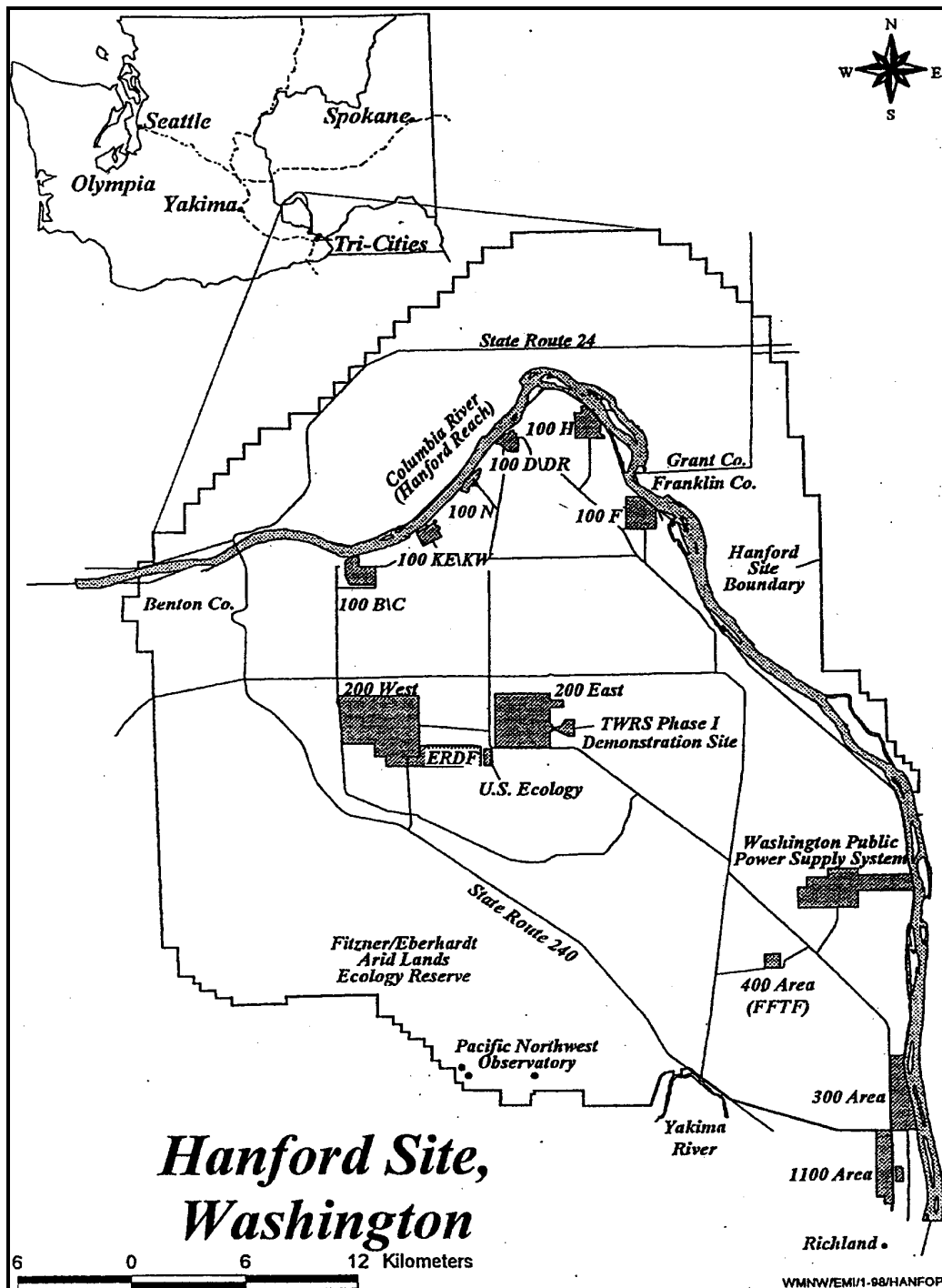
1.3. Scope of Validation Studies Performed

The BNFL team has undertaken a number of tasks to validate the results of the Geomatrix report. We have read a series of comments, questions, and responses that passed between Geomatrix and the several earlier reviewers of the report. We have surveyed independent estimates of seismic hazard at the Hanford Site, particularly the recent work of Frankel et al. (1996). We have reviewed all elements of the fundamental regional model (such as earthquake sources specified, temporal recurrence of earthquakes as a function of magnitude, strong ground motion attenuation with distance, maximum earthquakes anticipated) to determine whether the Geomatrix report contains model parameters that are still current.

The regional earthquake source model specified in the Geomatrix report is detailed and complex. The hazard estimates derived by Geomatrix are the weighted sums of many thousands of hazard curves computed from many hundreds of input assumptions. No attempt has been made to reproduce the entire computational content of the report. However, the Geomatrix report shows that substantial portions of the total seismic hazard come from a relatively few modeled sources. For these selected sources, we have attempted to reproduce the Geomatrix results using a completely independent analytical approach to test our ability to reproduce the outcome for the model input adopted.

During the course of the BNFL validation effort we have had the benefit of several technical discussions with many of the scientists who worked on the latest (and earlier) version of the Geomatrix report and with personnel and consultants of DOE's Regulatory Unit (RU), which is specifically chartered to regulate the radiological, nuclear, and process safety of the TWRS Privatization Program. These discussions often called on us to ponder the scientific basis for particular model characteristics and their uncertainties. To address these questions, we have performed representative sensitivity checks on selected parameters for selected models with emphasis on those parameters cited during the technical discussions.

Figure 1-1. Map of the Hanford Site and Location of the Tank Waste Remediation System Phase 1 Demonstration Site{ TC "1-1. Map of the Hanford Site and Location of the Tank Waste Remediation System Phase 1 Demonstration Site" \f F }



2. Survey of Previous Site Hazard Estimates

The earthquake hazard of the Hanford site has been reported in studies other than Geomatrix (1996b). These other studies have been both regional and site-specific, both direct predecessor and independent of the Geomatrix report, and both earlier and later than the Geomatrix report. Review of these alternative earthquake hazard characterizations shows that the conclusions of the Geomatrix study are conservative.

2.1. Hanford Site Studies

The Geomatrix (1996b) report is the result of development and refinement of a seismic hazard model for the site region that was begun in 1981 (Powers et al.) for the Washington Public Power Supply System's WNP-1/4 and WNP-2 nuclear reactor sites. According to the Safety Evaluation Report for WNP-2 (U. S. Nuclear Regulatory Commission, 1982a), this study was performed in order to account for uncertainties in applying a geologic structure approach to assess the potential vibratory ground motion in the Columbia Plateau. These uncertainties and alternate hypotheses for some of the input parameters (the tectonic model, fault geometry, potential fault segmentation, source activity, and maximum magnitude on each source) were incorporated through the, then new, use of "logic trees" (see, for example, Kulkarni et al., 1984). Additional uncertainties in ground motion attenuation and earthquake recurrence relations were also incorporated into the analysis. The subjective weights applied to the different branches of the logic tree were based on geologic knowledge of Columbia Plateau features. The NRC staff concluded that "the use of the seismic exposure methodology presented a way of dealing with uncertainty in an area of complex regional geology." The staff further cites the applicant's conclusion that "the return period for a peak acceleration of 0.25g at the WNP-2 site is about 10,000 years," but suggests a number of sensitivity tests which would have to be completed before the staff could support a definitive estimate of the SSE ground motion (U. S. Nuclear Regulatory Commission, 1982a).

Direct review of Powers et al. (Figure 5 of their report) indicates that the predicted mean 2000-yr and 10000-yr return period site accelerations at WNP-2 were about 0.10 g and 0.18 g, respectively. These numbers were developed using attenuation relationships intended to properly predict peak ground accelerations from reverse faults on firm soil foundations "generally similar to the soil conditions at the plant site." Only local fault sources were considered, so that neither contributions from the Cascadia subduction zone (which was not generally regarded as active at the time) nor the crystalline basement were included.

At about the same time Tera Corporation (1982) was preparing an estimate for earthquake hazard at Hanford for Lawrence Livermore National Laboratory. This study used area sources and determined the largest magnitude earthquake associated with each source area. The recurrence of earthquakes of various magnitudes was based on historical seismicity. The study was applicable to the whole Hanford Site. There was no unique site location. The mean response spectrum for alluvium presented in WASH 1255 (U.S. Atomic Energy Commission, 1973) was recommended. "Best estimate" 2000- yr and 10000-yr return period peak ground accelerations of 0.14 g and 0.20 g, respectively, were found. The Tera Corporation acceleration hazard curves were adopted by Coats and Murray (1984), and these same curves subsequently used by Kennedy et al. (1990) to specify 500-, 1000-, and 5000-yr return period acceleration for the Hanford Site.

The 1981 model of Powers et al. was subsequently applied, with modification for earthquake recurrence rate assessments, to DOE Hanford Site sites (Woodward-Clyde Consultants, 1989). Separate earthquake hazard curves were developed for the 300 and 400 areas (near WNP-2, see Figure 1-1) and the 100 and

200 areas (near the TWRS-P Facility). The 2000- and 10000-yr peak ground accelerations for the 300 and 400 areas were 0.09 g and 0.18 g, respectively. For the 100 and 200 areas they were 0.10-0.11 g and 0.24 – 0.26 g. As for the Powers et al. study, only local fault sources were considered.

In the early 1990s, the 1981 Powers et al. and the 1989 Woodward-Clyde Consultants regional hazard models were revisited in support of an Individual Plant Examination of External Events (IPEEE) analysis for WNP-2 and for planned new DOE projects. In order to develop this updated hazard analysis, the regional seismic model was revised by a team of regional geoscience and probabilistic hazard methodology experts from Geomatrix Consultants, Pacific Northwest National Laboratory, Washington Public Power Supply System, and Westinghouse Hanford Company. The revised model, which now included both local crystalline crust and Cascadia subduction sources as well as more complex alternative characterizations of faults associated with the Yakima Fold Belt and other surface or near-surface faults, was used to calculate updated estimates at the same Hanford Site locations (Geomatrix Consultants, 1993). The 1993 model was also used to develop hazard estimates for WNP-2 (Geomatrix Consultants, 1994a) that were incorporated into the WNP-2 IPEEE analysis (Washington Public Power Supply System, 1995) and hazard estimates used for seismic design of the Canister Storage Building of the Hanford Site Spent Nuclear Fuel Project (Garvin, 1996).

Results for the 200 East Area are shown in Figure 5-1b of the 1993 Revision 0 version of the Geomatrix report. These curves show peak ground acceleration values for 2000- and 10000-yr return periods of 0.18 g and 0.37 g, respectively. The Geomatrix (1993) report also develops hazard curves for 5%-damped, 0.3 and 2.0 sec period spectral acceleration responses, allowing for the first time specification of uniform or equal hazard design response spectra.

Extensive review of the 1993 Geomatrix report was performed by Westinghouse Hanford Company, Pacific Northwest National Laboratory and DOE-Richland and DOE-Headquarters staff, by a Washington Public Power Supply System geologist, and by off-site experts on geology, probabilistic methodology, and strong ground motion attenuation. These reviews led to revision of the report incorporating alternative, more recent attenuation relationships and (see Chapter 3 below) examining closely the assumptions that had been made about the site foundation conditions in the context of the strong ground motion attenuation relationships that had been used. It is this 1996 Revision 1A Geomatrix report that is the subject of this current validation review. The 200 East Area 2000- and 10000-yr peak ground accelerations for in situ foundation conditions are 0.24 g and 0.44 g, respectively.

2.2. U. S. Geological Survey (USGS) National Maps

The U. S. Geological Survey has been developing earthquake shaking hazard maps for the United States (including, of course, eastern Washington) since 1976 (Algermissen and Perkins, 1976) with revision and extension taking place in subsequent reports (Algermissen et al., 1982; National Earthquake Hazard Reduction Project (NEHRP), 1988; Algermissen et al., 1990; NEHRP, 1991 and 1994; Frankel et al., 1996). The following summary comes from Leyendecker et al. (1995):

Seismic design forces in current United States building codes are effectively based on hazard maps that were included in the report *Tentative Provisions for the Development of Seismic Regulations for Buildings*, prepared by the Applied Technology Council (1978). The Applied Technology Council maps were derived from the 1976 USGS probabilistic peak ground acceleration map of the U. S., with some significant differences, including truncation of peak accelerations in the western U. S. and creation of "velocity-based" maps. In spite of the differences, the ATC maps are often referred to as USGS maps.

Beginning in 1976 the USGS maps have taken the form of probabilistic maps of peak acceleration. New maps in 1982, 1988, and 1990 added maps of peak velocity to those of peak acceleration. Now maps of spectral response ordinates at natural periods of 0.3 and 1.0 seconds for a reference site condition (soil profile S2, see below) are available for the United States (NEHRP, 1991 and 1994; Frankel et al., 1996). The spectral response maps are for a 10 percent probability of exceedance for exposure times of 50 and 250 years (return periods of 474 and 2372 years). These maps are revisions of spectral response maps first prepared in 1991. The 1994 NEHRP and 1996 Frankel et al. maps give recognition to the increased likelihood of occurrence of large earthquakes on the Cascadian subduction zone.

The use of uniform-hazard spectra for design offers a procedure that equalizes the hazard of design ground motion exceedance across all building periods for all regions of the country. However, it would be too cumbersome for building code purposes to require the large number of contour maps needed to define the complete spectrum. Accordingly, an approximate uniform-hazard response spectrum requiring fewer maps has been developed by the USGS (Frankel et al., 1996). The short-period response of the *approximate uniform-hazard response spectrum* is defined by the 0.3-second ordinate while response at longer periods varies as a function of the 1.0-second ordinate and the period, T . Selection of these mapped spectral-response ordinates is based, in part, on studies of complete uniform-hazard spectral response shapes (spectral ordinates for periods ranging from 0.05 sec to 4.0 sec) for the selected cities in different seismic environments across the U. S. Results show that the *complete uniform-hazard response spectrum* can be approximated using the two mapped spectral values. These results, supplemented with results for peak ground acceleration, can be compared with Hanford-specific results.

Since 1976 the USGS maps have taken the form of probabilistic maps expressing the earthquake hazard as a probability of exceeding a specific measure of ground motion in a specific time period. For example, the first such map was for the 10 percent probability of exceeding the peak accelerations shown in a 50-year time period. In fact, all of the maps of seismic zones or ground motion in the current editions of the documents listed in the preceding paragraphs originated, albeit with changes based on the approval process used by the preparing organizations, from the 1976 U. S. Geological Survey (USGS) map of peak acceleration.

In order to compare the USGS and Hanford-specific results we prepared the table below. This table lists, for the most recent USGS reports, peak ground acceleration and 5%-damped spectral acceleration responses at published return periods (475, 975, or 2475 years corresponding to motions with a 10% chance of exceedance in 50, 100, and 250 years, respectively) and comparable values interpolated to the 2000-yr return period of interest for the TWRS-P Facility. (No USGS map shows ground motions for a return period greater than 2475 years, and we have not attempted to extrapolate beyond this to 10000 years, believing that any such attempt could well lead to unreliable results.) The specific sources cited are Algermissen et al. (1990 – peak ground acceleration and velocity maps), NEHRP (1991 – 0.3 and 1.0 sec response spectral ordinates; 1994 – improved 0.3 and 1.0 sec response spectral ordinates including consideration of the Cascadia subduction zone), and Frankel et al. (1996 – peak ground acceleration and 0.2, 0.3, and 1.0 sec spectral ordinates).

The peak ground acceleration and spectral acceleration values specified in Table 2-1 apply to “rock” or “firm foundation” conditions. To compare these with the Geomatrix (1996b) results for Hanford, we evaluated how foundations implied in these studies might be compared and, if different, compensated.

Recent seismic codes, using the USGS maps discussed in this section, have moved toward more explicit definition of the site foundation conditions since they are now recognized to have an important effect on ground motions, particularly at intermediate and long periods. In the 1996 Frankel et al. hazard maps the

reference site condition used is specified to be the boundary between NEHRP site classes "B" and "C" (NEHRP, 1994; Martin and Dobry, 1994), meaning it has an average shear-wave velocity of 760 m/sec in the top 30 m. This corresponds to a typical "firm-rock" site for the Western United States.

Both Boore et al. (1997) and Campbell (1997) discuss site conditions considered in recent ground motion attenuation relationships and how these relate to the NEHRP site classes. Campbell specifically compares the site classifications used by most of the authors of the attenuation relations used in Geomatrix (1996b) (see the discussion on attenuation in Chapter 3.0), from which he concludes that the site conditions implied by the "soil/firm soil" attenuation relations used in the Geomatrix report correspond to the NEHRP site class "D". Schematic comparisons of several soil classification criteria including NEHRP (1994), the 1997 edition of the Uniform Building Code (International Conference of Building Officials, 1997), and those addressed by Campbell (1997) are shown in Figure 2-1.

A comparison of Frankel et al. (1996) and Geomatrix (1996b) response spectral values is made in Figure 2-2. As shown above in this figure, the 2000-year spectral response ordinates from Frankel et al. hazard maps fall below those given by Geomatrix. A portion of this difference may be attributed to the difference in site conditions assumed by the two studies. In Figure 2-2 is also shown the Frankel et al. spectral ordinates scaled to the equivalent site conditions for the NEHRP site class D. The scaling factors were derived by considering the spectral shapes presented in the UBC (1997) for Zone 2B, the UBC seismic zone in which the TWRS-P Facility is located. UBC (1997) uses the same site classification scheme as NEHRP. By considering the spectral shape for UBC Sd (equivalent to NEHRP site class D, see Figure 2-1) and the log-average of the UBC spectral shapes for Sb and Sc (equivalent to NEHRP site classes B and C, respectively), spectral scaling factors were developed to allow scaling the Frankel et al. spectral ordinates from site conditions corresponding to the site class boundary B-C to site class D. The resultant scaled Frankel et al. spectral ordinates are close, though slightly less than, the 2000-year spectrum given by Geomatrix (1996b).

**Table 2-1. Ground Motion Hazard Assessments at the Hanford Site by U.S.G.S.
(Algermissen et al., 1990; NEHRP, 1991 and 1994; Frankel et al., 1996){ TC "2-1.
Ground Motion Hazard Assessments at the Hanford Site by U.S.G.S.
" \f T }**

PGA(g) @ Return Periods (years)

Year	475	975	<i>2000</i>	2475
1990	0.04	-	<i>0.11</i>	0.13
1991	-	-	-	-
1994	-	-	-	-
1996	0.087	0.125	<i>0.176</i>	0.194

Sa(g) for 0.2s @ Return Periods (years)

	475	975	<i>2000</i>	2475
1990	-	-	-	-
1991	-	-	-	-
1994	-	-	-	-
1996	0.192	0.281	<i>0.397</i>	0.440

Sa(g) for 0.3s @ Return Periods (years)

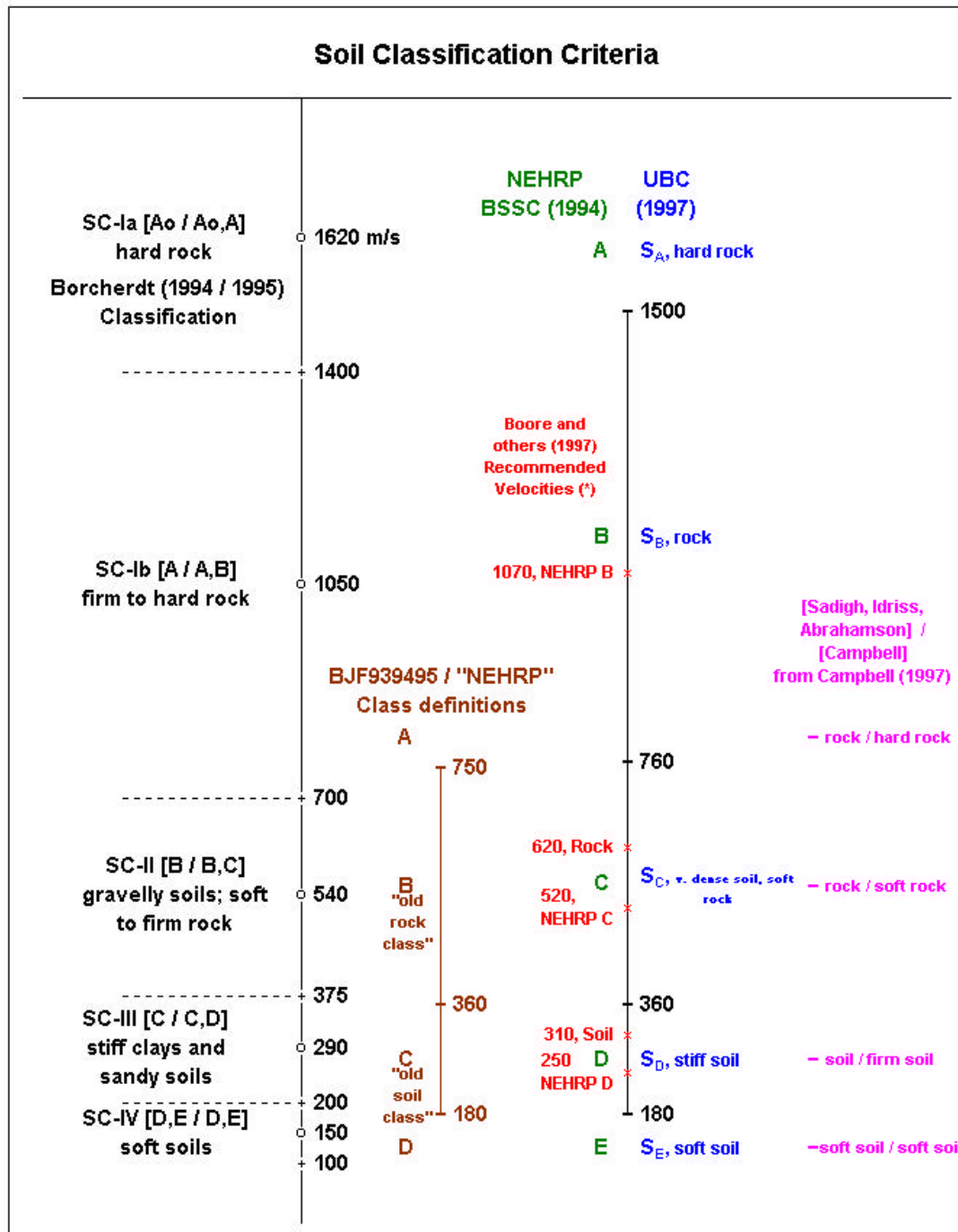
	475	975	<i>2000</i>	2475
1990	-	-	-	-
1991	0.20	-	<i>0.35</i>	0.38
1994	0.26	-	<i>0.39</i>	0.42
1996	0.178	0.259	<i>0.363</i>	0.402

Sa(g) for 1.0s @ Return Periods (years)

	475	975	<i>2000</i>	2475
1990	-	-	-	-
1991	0.10	-	<i>0.17</i>	0.19
1994	0.11	-	<i>0.19</i>	0.20
1996	0.062	0.091	<i>0.127</i>	0.140

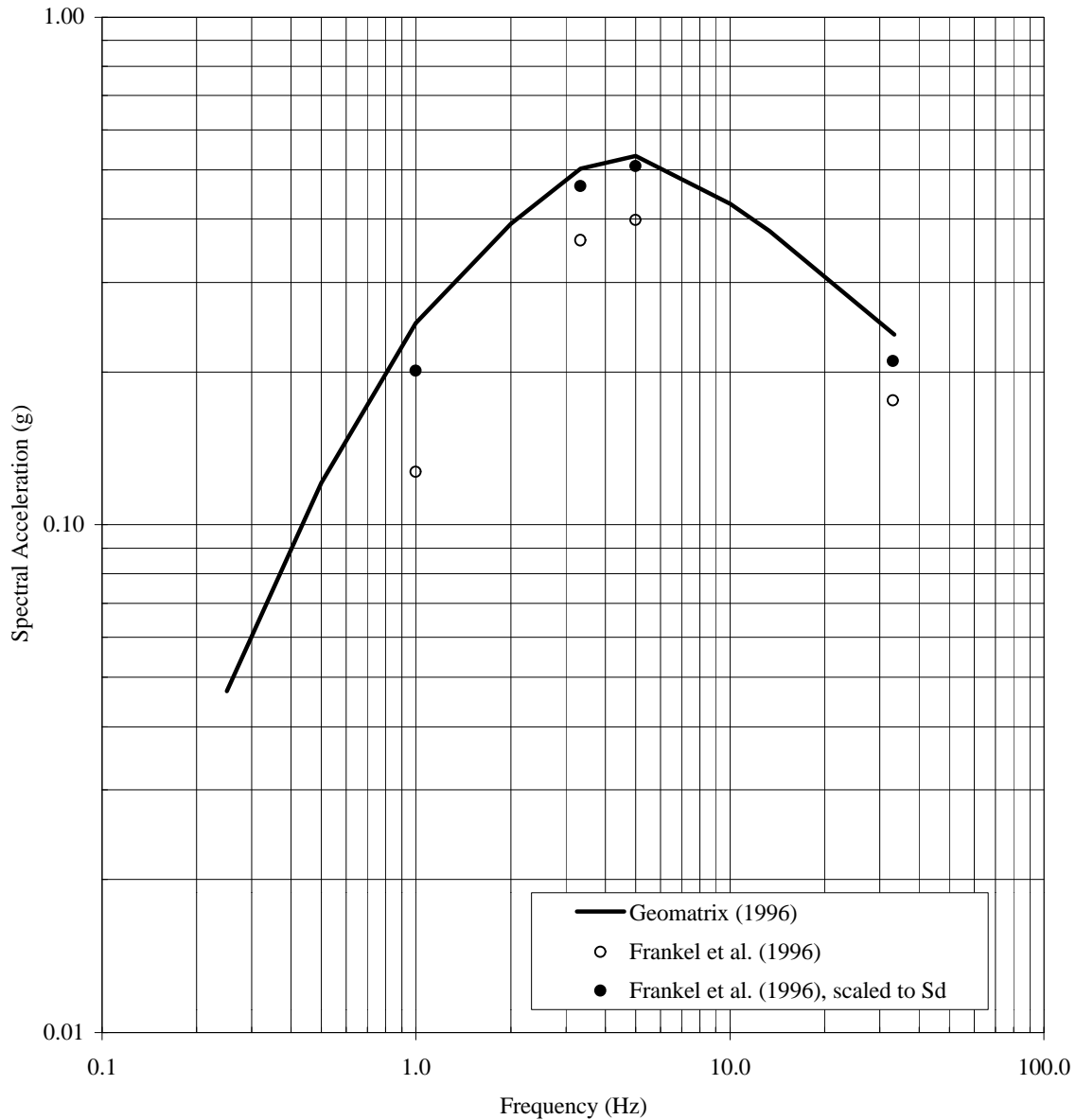
All ground motion values assume stiff soil/soft rock foundation conditions.

**Figure 2-1. Schematic Comparison of Various Soil Classification Criteria{ TC "2-1.
Schematic Comparison of Various Soil Classification Criteria" \f F }**



Note that the specification of “between NEHRP site classes B and C” of Frankel et al. (1996) corresponds to 760 m/s and “rock/hard rock” in the attenuation relations noted by Campbell (1997), while “soil/firm soil” in Campbell’s cited relationships corresponds to NEHRP site D and a shear-wave velocity of about 250 m/s.

Figure 2-2. Comparison of Geomatrix (1996b) equal hazard response spectrum for the 200 East Area with uncorrected Frankel et al. (1996) and Frankel et al. corrected to Geomatrix-equivalent soil column (NEHRP soil-type D)



The uncorrected Frankel et al. hazard values have been interpolated to the 200 East Area location from 0.1 degree grid values taken from <http://geohazards.cr.usgs.gov/eq>.

3. Basis for Geomatrix (1996b) Input

The probabilistic approach used in the 1996 Geomatrix report (and its predecessors) requires models of local and regional strong ground motion attenuation, models of geologic structures or areas of the earth's crust where future earthquakes are expected to occur, estimates of how large those earthquakes will be, and some explicit distribution of how often the earthquakes on a structure or within an area will occur as a function of their magnitude. Where the numbers representing these models or estimates are imperfectly known, a range of values is proposed and considered. The probabilistic approach provides a formal mechanism with which to treat model uncertainty quantitatively.

In this chapter the basis for the earthquake source model of the Hanford Site region is specified as this is used to evaluate the earthquake hazard potential characterization for the site in the Geomatrix report.

3.1. Attenuation Relations

Despite intermittent deployment of strong motion instruments in support of waste isolation and other DOE projects on the Hanford Site, and despite general deployment of triaxial strong motion detectors with a low (0.01 g) trigger level at the WNP-2 nuclear power plant in compliance with U. S. Nuclear Regulatory Commission (1974) requirements, there are no known records of strong ground motion on the Hanford Site in association with any earthquake (see Chapter 4.0).

Given the lack of empirical strong ground motion data in the region around Hanford, there are no published region-specific empirical strong ground motion attenuation relationships for southeastern Washington. For the Geomatrix (1996b) hazard analysis and its immediate predecessors (Geomatrix 1993 and 1996a), a suite of empirical attenuation relationships were used that were the then-current state-of-knowledge.

For crustal sources (that is, for sources other than the Cascadia subduction zone) Geomatrix (1996b) uses four empirical attenuation relationships for horizontal ground motions on site foundation conditions appropriate for the Hanford Site. These four empirical attenuation relationships - Abrahamson and Silva (1995), Boore et al. (1995), Sadigh (1996), and the pair of sources Campbell and Bozorgnia (1994) and Campbell (1990) - are based predominately on strong ground motion data recorded in California and the western United States. (The Campbell and Bozorgnia, 1994 and Campbell, 1990 pair define attenuation of peak ground acceleration and spectral acceleration, respectively.) Each attenuation relationship was given an equal weight in the Geomatrix hazard analysis. Only the Campbell and Bozorgnia (1994)/Campbell (1990) attenuation relationship pair has been modified noticeably since the latest version of the Geomatrix report (see Chapter 4.0).

A recent compilation of empirical strong ground motion attenuation relationships has been published (Abrahamson and Shedlock, 1997) and represents the current state-of-knowledge of all of the four crustal attenuation relationships used in the Geomatrix (1996b) study. Based on comparative plots of predicted ground motions for a suite of magnitudes and distances, the Abrahamson and Silva (1995) is identical to the Abrahamson and Silva (1997) attenuation relationship and the Sadigh (1996) is identical to the Sadigh et al. (1997) empirical relationship.

For the Boore et al. (1995) attenuation relationship, sites were classified as either soil type B (rock) or C (soil) site conditions. (Comparisons of these classifications with the current NEHRP and UBC foundation

classification system are discussed in Chapter 2.0.) For the Geomatrix (1996b) analysis, a site classification of C was used. In the more recent Boore et al. (1997) attenuation relationship, the site condition term is dependent on the average shear wave velocity of the top 30 meters below a given site. For Boore et al. (1997), the following functional form was fit to the site classification coefficient term of the old relationship:

$$b_7 = b_v * \ln (V_s/V_A)$$

where V_A is a period dependent reference velocity and V_s is the average shear wave velocity in the top 30 meters beneath a site. Although the current Boore et al. (1997) attenuation relationship has a different functional form than the Boore et al. (1995) attenuation relationship for the site condition term, the equations predict very similar ground motion values given an average shear wave velocity in the top 30 meters of a site which would correspond to a site class C of the old attenuation relationship. The values of V_s which correspond to a site class of C can be computed by solving the above equation for V_s (see Table 3-1). Based on this calculation, the average shear wave velocity for the top 30 meters over all periods is 267 m/sec.

Two additional spectral acceleration periods ($T=0.075$ and 4.0 seconds) were added to the Boore et al. (1995) attenuation relationship for the Geomatrix hazard analysis. An interpolation procedure was used for the estimation of the $T=0.75$ sec coefficients taking the standard error for $T=0.1$ seconds. For the $T=4.0$ sec, the coefficients at $T=2.0$ sec were extrapolated taking the standard errors of the $T=2.0$ seconds case. These new spectral coefficients were estimated to provide a smooth spectral shape.

The fourth crustal attenuation relationship for peak ground acceleration used in the Geomatrix (1996b) study was developed by Campbell and Bozorgnia (1994). This relationship was generalized to spectral acceleration values using (SA/PGA) ratios from Campbell (1990). Campbell (1997) represents a more current empirical attenuation relationship that has a different functional form for spectral acceleration. This alternative relationship is discussed in Chapter 4.0.

The variation in crustal source hazard estimates caused by use of the identified attenuation relationships is modest (Geomatrix, 1996b, Figure 5-8b). All hazard curves cluster quite closely to the mean for all attenuation relations.

A concern at the time of the Geomatrix (1996b) hazard analysis was the ability of the four crustal attenuation relationships to predict the empirically observed higher ground motions associated with blind thrust earthquakes in some near source region earthquake source models. This concern arose from ground motions recorded in the near source region of the 1994 Northridge earthquake which were generally greater than predicted by attenuation relationships current at the time of the earthquake. Both the Abrahamson and Silva (1995) and Sadigh (1996) attenuation relationships of the 1996b Geomatrix report use the Northridge data. Indeed, one important difference between the Revision 0 version of the Geomatrix report (Geomatrix, 1993) and the current Revision 1A version (Geomatrix 1996b) is the addition of the Abrahamson and Silva and updated Sadigh attenuation relationships. The Boore et al. (1995) and Campbell and Bozorgnia (1994)/Campbell (1990) attenuation relationships do not include the Northridge data in their regression analyses. Geomatrix (1996b) performed a residual analysis between rock peak ground acceleration motion and median peak ground acceleration motion from the four attenuation relationships for thrust and reverse earthquakes. No significant statistical bias was found from the analysis. (It should be noted that the Campbell (1997) and Boore et al. (1997) still do not contain Northridge data as part of their regression analysis.)

Separate empirical attenuation relationships were used in the Geomatrix (1996b) hazard analysis for the Cascadia subduction zone seismic source. As was the case for the crustal attenuation relationships, a suite of published relationships was used. Five attenuation relationships were considered: Youngs et al. (1993), Crouse (1991), Iai et al. (1993), Fukushima and Tanaka (1990), and Molas and Yamazaki (1995).

Youngs et al. (1993) developed an attenuation model for rock and soil site conditions from subduction zone strong ground motion data for peak ground acceleration and spectral acceleration for both interface and intraslab events. Numerical simulations for magnitude and distance ranges that were lacking from the empirical data were also used in the regression. A more recent version of this model (Youngs, et al., 1997), based on a regression with additional data, is discussed in Chapter 4.0.

Both the Crouse (1991) and Iai et al. (1993) attenuation models for soil site conditions were based on data primarily from Japanese subduction events. The Crouse model was for peak ground acceleration as well as spectral acceleration. The spectral acceleration regression was based on fewer data points than the peak ground acceleration regression due to the lack of digitization for subduction event time histories. Crouse (1991) performed a regression for both peak ground acceleration and spectral acceleration using only that data available for both and found a bias when compared to the regression using all of the data. To reduce this bias, Geomatrix (1996b) modified the Crouse (1991) attenuation model by performing a regression on the reduced data set to get a spectral shape for soil sites. This spectral shape model was then applied to the peak ground acceleration regression of Crouse (1991) using the full data set. The defined distance is closest distance to the center of the energy release. However, for the hazard analysis, Geomatrix used the closest distance to the rupturing fault plane, which could lead to a more conservative hazard estimate for the Cascadia source due to the closer distance from the source to the site. The depth of the earthquake was set at 25 km.

The Iai et al. (1993) regression contained a mixture of interface and intraslab ground motion data from Japan. The attenuation relationship is based on the JMA (Japan Meteorological Agency) scale that was assumed to be equivalent to the moment magnitude scale in the hazard analysis (Katsumata, 1996). This model was extended to spectral acceleration by taking the average spectral shape predicted by the modified Crouse (1991) and Youngs et al. (1993) attenuation relationships. The standard errors for spectral periods were also extended from the modified Crouse (1991) and Youngs et al. (1993) relationships.

The empirical relationship of Fukushima and Tanaka (1990) was also considered. Their data set consisted of shallow (depth less than 30 km) crustal and subduction zone earthquakes from Japan. The distance range for the attenuation relationship is 300 km based on the lack of data for larger distances. Due to this distance limit and the corresponding low levels of ground motion predicted compared to the other subduction attenuation relationship, the Fukushima and Tanaka (1990) relationship was not used in the Geomatrix hazard analysis.

Only an update to the Youngs et al. (1993) subduction attenuation model has been published (see Chapter 4.0). All attenuation relationships were given equal weights in the hazard analysis.

3.2. Seismic Sources

The 1996 Geomatrix report evaluates earthquake ground shaking potential at the Hanford Site from local sources in the Columbia Basin and from the Cascadia subduction zone to the west. The various parameters needed to model these sources for earthquake hazard analyses were gathered using a combination of state-of-the-art literature and input from an expert team of geoscientists familiar with the

geology, tectonics, and seismicity of the site region. Good summary discussions of earthquake sources may be found in the Geomatrix (1996b) report itself. More detailed discussions of these parameters appear in several reports for various Hanford facilities (Washington Public Power Supply System, 1981, 1995; U. S. Nuclear Regulatory Commission, 1982a and others as cited below) and in the open scientific literature (also as cited below). The most significant parts of this material are summarized in this section.

Earthquake activity in the Columbia Basin is attributed to three sources within the seismogenic crust: (1) the Yakima Folds related thrust/reverse faults; (2) the shallow basalt source which accounts for the observed seismicity within the Columbia River basalt that is not spatially associated with the Yakima Folds; and (3) the crystalline basement source region that extends from the top of the crystalline basement to the base of the seismogenic crust. Of these sources, the ones contributing most to the earthquake hazard potential at the TWRS-P Facility on the Hanford Site are (for higher frequency motions) the faults associated with the Yakima Fold Belt and deep crystalline basement sources and (for longer period motion) the Cascadia subduction zone interface earthquakes (see Figures 5-2b and 5-3b in Geomatrix 1996b).

Among the Yakima Fold faults, the Umtanum-Gable Mountain and Saddle Mountains faults are treated in some detail below as the greatest Yakima Fold Belt fault contributors to TWRS-P Facility earthquake hazard (see Figure 5-4b in Geomatrix 1996b) and the rift model of deep crystalline basement sources is discussed because it would predict the highest hazards from these sources (see Figure 5-13b in Geomatrix 1996b) if it had been given higher weighting among potential deep crystalline sources models.

3.2.1. Yakima Fold Belt Sources

The Hanford Site lies in the Pasco Basin, one of the larger structural basins near the eastern limit of the Yakima Fold Belt (see Figure 3-1). The Yakima Folds have been investigated as potential seismic sources for nearly 50 years in support of the siting of nuclear facilities on the Hanford Site. Extensive detailed investigations were completed for the siting, construction, and operation of nuclear power reactors (Washington Public Power Supply System 1981, Puget Sound Power and Light Co. 1982, U. S. Nuclear Regulatory Commission 1982a and 1982b). The Department of Energy also completed geologic studies of the Yakima Folds to support the siting, construction, and operation of a research reactor (Department of Energy, 1975 and U. S. Nuclear Regulatory Commission, 1978) and in the site characterization of a potential civilian nuclear waste repository (Department of Energy, 1988).

The Yakima Fold Belt consists of asymmetrical anticlinal ridges and synclinal valleys. The anticlines are typically segmented and usually have a north vergence, although some folds have a south vergence. Synclines are typically asymmetrical with a gently dipping north limb and a steeply dipping south limb. Fold length is variable ranging from several km to over 100 km; fold wavelengths range from several kilometers to as much as 20 km. Structural relief is typically about 600 m but varies along the length of the fold. The greatest structural relief along the Frenchman Hills, the Saddle Mountains, Umtanum Ridge, and Yakima Ridge occurs where they intersect the north-south trending Hog Ranch-Naneum Ridge anticline (Reidel et al., 1989).

In general, the axial trends produce a "fanning" pattern across the fold belt. Anticlines on the western side of the fold belt generally have a N 50° E trend (Swanson et al., 1979). Anticlines in the central part of the fold belt have east-west trends except along the Cle Elum-Wallula deformation zone (CLEW) where a N 50° W trend predominates. The Rattlesnake Hills, Saddle Mountains, and Frenchman Hills have overall E-W trends across the fold belt but Yakima Ridge and Umtanum Ridge change eastward from E-W to N 50° W in the zone of the CLEW. In the central part of the fold belt, the Horse Heaven

Hills, the Rattlesnake Hills and the Columbia Hills have eastward terminations against the CLEW. There is no evidence for continuation of any anticline to the northeast across the CLEW.

3.2.1.1. Fold and Fault Geometry

Within the Hanford Site and surrounding area, the geometry of the anticlines typically consists of steeply dipping to overturned north flanks and gently dipping (< 5 degrees) south flanks. Exceptions, however, include the doubly plunging anticlines within the Rattlesnake-Wallula alignment (RAW) of the CLEW and the conjugate box-fold geometry of parts of the anticlines such as the Smyrna segment of the Saddle Mountains (Reidel, 1984). The main variable in fold profiles is the width of the gently dipping limb. The widths of the gently dipping limbs vary from as little as 5 km to as much as 35 km.

Segmentation of the anticlines is common throughout the fold belt and is defined by abrupt changes in fold geometry or by places where regional folds die out and become a series of doubly plunging anticlines. Segment lengths are variable but average about 12 km (ranging from 5 to 35 km) near Hanford; some of the larger segments contain subtler changes in geometry such as different amplitudes that could also be considered segment boundaries. Segment boundaries are often marked by cross or tear faults that trend N 20° W to north-south and display a principal component of strike-slip movement (for example, the Saddle Mountains, Reidel, 1984). Near Hanford these cross faults are confined to the anticlinal folds and usually occur only on the steeper limb, dying out onto the gentler limb. Segment boundaries may also be marked by relatively undeformed areas along the fold trend where two fold segments plunge toward each other. For example, the Yakima River follows a segment boundary where it crosses the RAW at the southeast termination of Rattlesnake Mountain (see Figure 3-1).

The steep limb of the asymmetrical anticlines is almost always faulted. Near Hanford the steep limb is typically the northern flank, but elsewhere, as at the Columbia Hills (Swanson et al., 1979), the south limb is faulted. Where exposed, these frontal fault zones have been found to be imbricate thrusts as, for example, at Rattlesnake Mountain, Umtanum Ridge near Priest Rapids Dam (Bentley, 1977; Goff, 1981; Swanson et al., 1979), the Horse Heaven Hills (Hagood, 1986) and the Saddle Mountains near Sentinel Gap (Reidel, 1984 and 1988).

Yakima Folds have emergent thrust faults at the ground surface. The tops of the youngest lava flows at the earth's surface serve as a plane that becomes a low angle thrust fault; the structural attitude of the surface flow controls the angle of the emergent fault plane. This type of apparent structural control led many investigators to conclude that faults associated with the Yakima Folds are low-angle thrust faults with detachment surfaces either within the Columbia River Basalt Group, in the sediments below the basalts, or at the basalt-sediment contact. Where erosion provides deeper exposures into the cores of folds, the frontal faults are observed to be reverse faults (for example, the Columbia water gap in the Frenchman hills, 45 degrees south (Grolier and Bingham, 1971); the Columbia Hills at Rock Creek, WA, 50-70 degrees north (Swanson et al., 1979); the Saddle Mountains, 60 degrees (Reidel et al., 1989).

Although it is difficult to assess, total shortening increases from east to west across the Yakima Fold Belt. At about 120° W longitude, it is estimated to be greater than 15 km but less than 25 km (Reidel et al., 1989) or about 5% (Reidel et al., 1994, Table 2). Typically, shortening on an individual anticline due to folding is approximately 1 to 1.5 km. The amount of shortening on faults expressed at the surface is generally unknown. Estimates range from several hundred meters to as much as 3 km (Reidel et al., 1994, Table 3).

The first comparative tectonic evaluation required in the seismic hazard assessment is the relative probability of activity for the individual fold sources. As with fault activity assessment, the fold activity is based on such things as association with historical seismicity, evidence for late Quaternary fault displacement, geomorphic evidence for geologically recent deformation, association with neighboring structures showing evidence for Quaternary activity, pre-Quaternary history of deformation, and the orientation relative to the present stress field. The two-end member structures are Toppenish Ridge which was assigned a probability of activity of 1.0 (that is, certainly active) and the Hog Ranch-Naneum Ridge, assigned a probability of activity of 0.1 (that is, having only one chance in ten of being active). Holocene faulting has been mapped on Toppenish Ridge and all the criteria listed above are present (Campbell and Bentley, 1981). Landslides and faults are present on neighboring ridges and there are Native American legends that support the occurrence of earthquakes and landslides. Further, there is more structural shortening at Toppenish than in Yakima Folds in the Pasco Basin. The Hog Ranch-Naneum Ridge anticline was active in late to middle Miocene as demonstrated by thinning of basalt flows across it (Reidel et al., 1989) but the east-trending Yakima Folds show no apparent offset by the cross structure (Campbell, 1989; Tabor et al., 1982; Keinle et al., 1977; Reidel et al., 1989). There is no definitive evidence of Quaternary deformation or associated seismicity. A relative probability of activity of 0.25 is assigned to all other Yakima Folds except the Saddle Mountains. The Saddle Mountains is assigned an activity probability of 0.50 based on the presence of more evidence for Quaternary deformation than all Yakima Folds other than Toppenish Ridge. However, Saddle Mountains folds contain significantly less evidence for Quaternary deformation than Toppenish Ridge.

The Saddle Mountains and the Umtanum Ridge-Gable Mountain are two Yakima Folds that significantly contribute to the seismic hazard at the Hanford Site. The aspects of these structures that determine contribution to the seismic hazard are described below. The information presented is amplification of that presented in Geomatrix (1996b).

3.2.1.2. Saddle Mountains

Grollier and Bingham (1971) mapped the Saddle Mountains and surrounding areas to the north and east. Reidel (1984, 1988) followed with more detailed mapping. Additional mapping in the Smyrna Bench-Saddle Gap area of the Saddle Mountains was recently completed by West and others (1996). The following tectonic model description is based upon these studies.

The Saddle Mountains anticline can be modeled as coupled (fault extends from the surface or near-surface basalt to the crystalline basement) or uncoupled (faulting only within the basalt layer). Evidence which may suggest coupling is the thinning of the sub-basalt sediments near the Saddle Mountains (Glover, 1985, Ludwin et al., 1992). An argument for the structure being uncoupled is that the basalt structure, with 300 to 600 m of relief, is separated from the crystalline basement by greater than 1 km of sediment which provides mechanical decoupling to the crystalline basement. In addition, the structure's east-west orientation is more aligned to the regional stress field during formation to present time (U. S. Department of Energy, 1988). The probability of coupling is assessed to be 0.6. The only Yakima Fold assessed to be higher is Toppenish Ridge at 0.95 which displays Quaternary indicative of large earthquakes.

Segmentation of the Saddle Mountains was mapped by Reidel (1988) and includes five segments based on fold geometry, vergence along strike, crosscutting faults, and cross cutting folds which suggest that the underlying fault is segmented. Later work by West et al. (1996) used the same segmentation as designated by Reidel. Rupture lengths are estimated by measuring the length of each segment. The probability that the structure is segmented is estimated to be 0.6 and 0.4 that it is not segmented.

The dips of faults beneath the anticlines in the Yakima Fold Belt are generally not well constrained. The dips of seismogenic reverse faults worldwide, derived from the pattern of earthquake aftershocks and focal mechanisms, indicate that dips of between 30° and 60° are typical (Wells and Coppersmith, 1991). Based on these observations, average dips of 30°, 45° and 60° are equally applied to the Yakima Folds where there are no constraining field data. Hydrocarbon exploration boreholes provide direct evidence for the dips of the frontal faults at Saddle Mountains. Reidel et al. (1989) have shown that the Saddle Mountains fault must dip more than 60° where the Shell-ARCO BN 1-9 borehole was drilled. This supports high weight for the steeper dip than on folds where there are no constraining data. The weights assigned to the Saddle Mountains fault dips are 30° (0.1), 45° (0.3), and 60° (0.6).

The Columbia River Basalt flows are identified and have been age dated making it possible to determine the long-term deformation rate during and since the eruption of the basalt. The long-term slip rate is determined by measuring the vertical and horizontal offset of mapped units of known age or ages. The slip rate is then calculated for the dips discussed above. For the Saddle Mountains considered as a whole, slip rates so calculated range from 0.030 to 0.138 mm/yr. Individual segment slip rates vary from 0.007 to 0.021 mm/yr (Eagle Lakes) to 0.046 to 0.175 mm/yr (Sentinel Gap) (see Geomatrix, 1996b, Table 3-4).

3.2.1.3. Umtanum Ridge-Gable Mountain

Gable Mountain was mapped by Fecht (1978), and Price (1982) studied the structural evolution of the Umtanum Ridge as part of the tectonic assessment for a potential civilian nuclear waste repository deep in the Columbia River Basalt. Concurrently, the Washington Public Power Supply System had three nuclear power reactors in various licensing stages and the Puget Sound Power and Light Co. was conducting siting studies at the Hanford Site to move two planned reactors from the Skagit Valley, Washington to the Hanford Site. The results of these studies (Golder 1981a, U. S. Nuclear Regulatory Commission, 1982a and 1982b) concluded that faults on Gable Mountain (Central Fault, South Fault, North-Dipping Reverse Fault, West Fault, and DB-10 Fault) were capable (U. S. Nuclear Regulatory Commission, 1973) but of relatively low seismic potential. They found that the Southeast Anticline Fault is capped with unfaulted Ringold Formation and is not capable and that the Umtanum Ridge is likely not capable.

The structural relief of the Umtanum Ridge-Gable Mountain decreases from west (Umtanum Ridge) to the east where the southeast extension of the Gable Mountain disappears. The approximately 4 km thick basalt layer is underlain by an equal or greater thickness of sediments which provide a mechanical uncoupling from faulting in the basement. Unlike the Saddle Mountains, discussed above, there is no indication of a basement structure rise near Umtanum Ridge-Gable Mountain. Though coupling to crystalline basement is considered possible, there is no direct evidence to support a coupled model and strong stratigraphic evidence against it. The coupled model is given a weight of 0.15 and the uncoupled model 0.85. With the exception of Saddle Mountains, all east-west Yakima Folds in the Pasco Basin are give 0.15 probability of coupling.

Golder Associates (1981a, and 1981b) concluded that the Umtanum Ridge-Gable Mountain structural trend is a bedrock high that is composed of five segments. These are the western, central and eastern Umtanum segments, the Gable Mountain-Gable Butte segment and the Southeast Anticline segment. The segmentation of the Umtanum Ridge is based on discontinuities of faulting and changes in fold vergence along the axis of the anticline. The Gable Mountain-Gable Butte segment is based on a change in structural style to a broader, lower relief structure of the first order fold and the development of second and third order folds. Distinctive gravity and magnetic signatures also suggest the segment (Weston, 1981). The Southeast Anticline, the easternmost segment, is a subsurface, low-amplitude, anticlinal

ridge at the eastern end of the Gable Mountain-Gable Butte segment. Rupture lengths are estimated from the length of each segment.

The geometry of secondary faults in the Umtanum anticline (Price and Watkinson 1989) suggest that faults increase in dip with depth to about 40° to 70°. The dips and assigned weights for the Umtanum Ridge-Gable Mountain structure are 30° (0.2), 45° (0.4) and 60° (0.4). These dips are weighted slightly towards the larger dips to make some accommodation for Umtanum Ridge field observations by Price and Watkinson (1989).

3.2.2. Sources of the Crystalline Basement

Rocks older than the Columbia River Basalt Group (CRBG) are exposed primarily along the margin of the Columbia Basin and vary widely in age, lithology, and structure. It is this complex stratigraphy and structure that underlies the CRBG of the Columbia Basin and Hanford Site, and that are the probable sources for seismic hazards under basalt. Because of the thick basalt cover, the stratigraphy and types of the structure under the Hanford Site are constrained by only a few deep boreholes outside the Hanford Site and indirect evidence from geophysical data developed from as seismic, magnetic-electric, and gravity surveys.

Along the north and northwest margins of the Columbia Basin in early Tertiary time, a series of sedimentary basins formed in the accreted terranes of the North Cascades (Campbell, 1989). These basins are now separated by tectonic "blocks" or uplifts that have a northeast- to northwest-trending structural grain and trend toward the Hanford Site.

The crystalline basement at the Hanford Site lies beneath the relatively low-velocity sub-basalt sediments. The low-velocity sediments are not thought to be a seismic source in themselves because of their lower strength relative to the basalt layer above and the crystalline basement below. However, they may participate in displacements initiated in the stronger layers. The occurrence of earthquakes within the crystalline basement (Geomatrix, 1996b, Figure 3-25) indicates that the basement is seismogenic. The crystalline basement is probably composed of accreted terranes overlying ancient oceanic floor. Little is known about the nature of basement structures, in the accreted terranes and overlying sediments. However, inferences can be made from structure surrounding the Columbia Plateau and from limited geophysical data including a seismic refraction line (Catching and Mooney, 1988; Rohay et al., 1985; Glover, 1985) and gravity data (Weston Geophysical, 1981). Three alternative models, the failed rift model, the basement block model and the random basement model are discussed below.

3.2.2.1. Failed Rift Model

The failed rift model was proposed by Catchings and Mooney (1988) based on a crustal cross-sectional velocity model developed along a seismic refraction line through the southern Columbia Basin and on analogies to known intra-continental rifts. This model is based on a single seismic refraction line across the inferred rift structure. The inferred rift's orientation in the present stress field is not known. Assessment of the reactivated rift model requires information on the orientation of the rift.

A north-south orientation of the proposed rift is suggested by the regional gravity, the western gradient probably related to the Naneum-Hog Ranch structure, and the eastern gradient edge of the craton (Reidel et al., 1994). In-situ stress measurements indicate the principal stress direction is north-south (Kim et al., 1986) and the focal mechanism data for deeper events in this area are predominantly north-south compression. Reactivation of a north-south oriented rift is incompatible with a north-south stress regime.

The Naneum-Hog Ranch structure is not offset by strike-slip movement indicated in the rift model, and Saltus (1993) suggests that it is no longer active.

The northwest-southeast oriented rift was modeled with two alternative rift zone widths; a narrow model where the source zones are specified by the most inward faults and a wide model where the source zones are specified by the limits of the region within which 50 percent necking of the crystalline crust.

The base of the seismogenic crust is approximately 21 km, defined by the 95 percent cut-off in seismicity. The depth to the top of the basement is interpreted to be 8 to 9 km in the Columbia Plateau (Rohay et al., 1985; Catchings and Mooney, 1988; Glover, 1985), resulting in a seismogenic thickness of about 13 km.

The maximum earthquake magnitudes for the rift model were estimated based on conjectured fault rupture dimensions. There are no large earthquakes in the historical record to support this estimate. The maximum magnitude distribution is assessed to be between 6.5 and 7.0. Outside the rift, the basement structures are likely to be smaller and the maximum magnitudes are distributed in the 6 to 6.5 range.

The slip rate for the rift zone is based on the total rate of shortening inferred from the individual fold slip rate assessments along three north-south cross-sections across the Columbia Plateau (Reidel et al., 1994). Assuming that this rate of shortening occurs within the crystalline basement and is expressed as dextral strike-slip faulting along a fault having a northwest orientation, a slip rate was determined. Because there is no information on the slip rate on individual faults, the slip rates are for the entire rift zone and are used to estimate the average recurrence across the entire zone.

The uncertainty in rift orientation, the evidence for reverse rather than strike-slip faulting, the lack of a signature in the seismicity, the lack of an offset of the Naneum-Hog Ranch structure, and the uninterrupted sediment package across the Cascade range are the primary reasons that the failed rift is given low weight (0.1).

3.2.2.2. Basement Block Model

This model recognizes a depression in the crystalline basement around the Pasco Basin. The basement is divided into two source zones or blocks, the inner down-dropped zone and the zone outside the down-dropped block. The down-dropped inner zone is distinguished by generally deeper crystalline crust and increased levels of observed seismicity relative to the outer area. Two interpreted basement structures provide the north and east boundaries for this model (Geomatrix, 1996b; Figure 3-25).

The first proposed structure (fault) lies along the Ice Harbor Dike Swarm which may coincide with the crustal discontinuity that marks the transition from shallow, stable cratonic basement and the subsided region to the west. Reidel et al. (1994) consider this feature to be a long-lived major crustal boundary that may have originated as a suture zone separating the North American craton from accreted terrane to the west. An alternative interpretation for the location of this structure is provided by regional seismic refraction data (Rohay et al., 1985; Glover, 1985).

The other proposed fault forms the northern boundary, separating the subsided crystalline crust from the shallower, more stable basement to the north. The northern boundary fault is based on seismic refraction data that indicate a down-to-the-south step in the basement between the Frenchman Hills and the Saddle Mountains (see Figure 3-1) (Rohay et al., 1985; Glover, 1985; Catching and Mooney, 1988).

The probability that these two faults are seismogenic is assessed to be 0.5. There is little evidence either for or against activity so the maximum state of uncertainty is applied. If considered active, the earthquake recurrence rates are assessed using estimated subsidence rates in the Columbia Basin of 0.003 mm/yr (Reidel et al., 1989). The maximum magnitude distribution is assumed to be the same as that assessed for the rift zone. The seismicity rates for the crustal regions located within and outside the basement block are determined from the observed seismicity. A weight of 0.1 is assigned to this model.

3.2.2.3. Random Basement Model

This model assumes a random occurrence of basement earthquakes and assumes that neither the rift model nor the block model provides an appropriate representation of the seismic sources in the basement. Random occurrence of seismicity within a source area indicates that the causative structures are not known. Because of the low level of confidence that either of the two structural models provide an appropriate representation of the current basement tectonic deformation, the random model is given the highest weight (0.8)

3.2.3. Cascadia Sources

The Cascadia subduction zone lies along the west coast of North America, from Cape Mendocino, California, to Vancouver Island, Canada. A sketch of the plate tectonic elements making up this zone is shown in Figure 3-2. An interesting and useful review of the plate tectonic characterization of the Pacific Northwest beginning with the pioneering work of Raff and Mason (1961) and continuing through the state-of-knowledge in the mid-1970's is presented in Riddihough (1978). In the mid-1980's the most important question was whether or not the Juan de Fuca – North American plate contact could be the site of future, very large earthquakes (Heaton and Kanamori, 1984) larger than any occurring during the brief historical record.

By the early 1980's the favored interpretation of the relative motions of regional tectonic plates implied that the crust offshore the Pacific Northwest coast was converging towards the onshore crust at a rate of several cm/yr (Nishimura et al., 1984). This implied active subduction of the Juan de Fuca plate beneath the North American plate with a zone of contact between the two plates east of the Cascadia subduction zone and beneath the North American plate crust. This is termed the megashear zone because it is along this part of the contact between overthrust and subducted plates in many parts of the world where very large earthquake are generated.

No historic earthquakes have occurred along the megashear zone in the Pacific Northwest region. Beginning from the apparent active subduction of the Juan de Fuca plate and the absence of very large earthquakes of the megashear type historically associated with that subduction, Heaton and Kanamori (1984) compared physical characteristics of many worldwide subduction zones and concluded that the Cascadia subduction zone is most similar to other subduction zones that have experienced great earthquakes. Heaton and Hartzell (1986) extended these studies and concluded that the Cascadia subduction zone is most similar to the subduction zones of southern Chile, southwestern Japan, and Colombia each of which have experienced sequences of very large, shallow subduction (megashear) earthquakes of moment magnitudes ranging from 8 to 9.5.

Detailed paleoearthquake studies of the next several years concluded that very large prehistoric earthquakes had occurred on the Cascadia subduction zone at intervals ranging from a few hundred years to about 1000 years and averaging about 500 years (Atwater and Hemphill-Haley, 1996; Geomatrix, 1995; Atwater et al., 1995). By the early 1990's, these megashear-type earthquakes began to be

incorporated into regional earthquake hazard studies (Leyendecker et al., 1995; Geomatrix, 1995; Frankel et al., 1996).

The model of the Cascadia megashear seismic source zone is similar in all current hazard studies. The details of this model parameters considered by Geomatrix (1996b) are summarized below. Geomatrix also considers earthquakes occurring not at the interface between the subducting Juan de Fuca and overriding North American plates but within the subducting Juan de Fuca plate ("intraslab" earthquakes). The intraslab earthquakes are smaller and somewhat farther away from the Hanford Site than the interface earthquakes. Calculations of relative contributions to hazard from all sources (Geomatrix, 1996b, Figure 5.2b) show that intraslab earthquakes contribute very little to the shaking potential at Hanford. The several USGS studies (see Chapter 2.0) do not appear even to treat this Juan de Fuca plate intraslab as a distinct source. It is not treated separately in this validation report for these reasons.

The cross-section geometry of the subducting Juan de Fuca plate is well constrained. For purposes of earthquake strong ground motion potential calculation, the only geometric variable is the extent of the seismogenic portion of the interface contact zone – defined by both its updip and downdip horizons. Two alternatives for both horizons are considered in the Geomatrix (1996b) report which, when combined, lead to four geometric models (see Figure 3-29 of the Geomatrix report). These models are quite similar and are essentially identical at the distance of the Hanford Site.

Maximum magnitudes of earthquakes on the Cascadia interface source were estimated for several alternative assumptions about what portion of the source would rupture during an earthquake and, given the rupture area or length, what magnitude would be expected from empirical relations. Rupture segment lengths were estimated from modeled rupture zone width and empirical relations between width and rupture length (the "aspect ratio"), from observation of distances between significant changes in interface zone trend or deformation pattern (modeled as acting singly or in concert with adjacent segments), or simply considering the entire subduction front. Maximum segment lengths so modeled ranged from 150 to 1100 km and magnitudes from about 8 to 9-1/4 with a median maximum magnitude estimate just under 8.5 (see Geomatrix 1996b, Figure 3-30). The greatest weights were assigned to intermediate rupture segment lengths of 450 km (0.5) and 250 km (0.3) with 0.1 weights for the end point lengths of 150 and 1100 km. Maximum magnitudes were estimated from these various rupture lengths using one magnitude-length and two magnitude-area formulas, equally weighted.

Finally, several recurrence models were adopted, all defined such that a single very large or some combination of smaller megashear earthquake would be expected to rupture the entire 1,100 km length of the Cascadia interface on the average of every 450 years, based on the paleoearthquake evidence cited above. Some details of these recurrence rate models are discussed in the next section.

These maximum magnitudes and recurrence rates are very similar to one adopted in both Leyendecker et al. (1995) and Frankel et al. (1996).

3.3. Recurrence Relations

Geomatrix generally considers the frequency of earthquakes by magnitude for a given source to follow one of two conventional distributions. For areal sources (such as the random basement source discussed above) the recurrence relations were based on recorded seismicity and the truncated exponential magnitude distribution (Cornell and Van Marke, 1969) was used. For fault sources (such as the Umtanum-Gable Mountain or Saddle Mountains structures discussed above) the earthquake recurrence rate is based on an assessment of fault slip rate and a translation of the slip rate to seismic moment rate.

Both exponential and characteristic (Youngs and Coppersmith, 1985) models are used to partition the moment rate into earthquakes of various sizes. Outlines of these methods are presented in chapter 2 of the Geomatrix (1996b) report. Some minor variations of these two methods were adopted in the Geomatrix study, and are elaborated here. A less conventional third magnitude-frequency recurrence relation, referred to as the “aspect ratio” method, is considered by Geomatrix in developing magnitude recurrence relations for the Cascadia subduction zone interface source. This is also discussed here.

When considering the seismic activity of an area that likely encompasses multiple, but unspecified, structures, the cumulative frequency distribution of earthquakes has been seen to generally follow a log-linear relationship, truncated at the maximum magnitude observed or as tectonically appropriate for the area. Figure 3-3 shows the simple truncated exponential recurrence relation (heavy gray line) for a maximum magnitude 7, a b-value (slope of the log-linear portion) of 0.8, and an activity rate of one magnitude 4 or greater earthquake per year.

For certain single fault sources, it has been observed that a small range of maximum size earthquakes occur, as well as more frequent small magnitude events, but with few intermediate size events relative to what would be expected from an exponential recurrence distribution. Youngs and Coppersmith (1985) discuss this “characteristic” magnitude distribution, which shows a relatively flattened portion in the cumulative magnitude frequency distribution within the intermediate magnitude range. Figure 3-3 shows the characteristic magnitude frequency distribution for the same seismic moment rate implied by the exponential distribution. (The seismic moment rate is a measure of the strain energy release rate that is often considered fundamentally constant for a given tectonic source.) In Figure 3-3 are also shown both the constituent small magnitude, exponentially-distributed portion of the characteristic frequency distribution and the cumulative distribution of the high or “characteristic magnitude” events that generally occur within about a magnitude range of about 0.5.

Figure 3-3 shows that, in keeping the seismic moment rate constant, the increase in the relative numbers of characteristic earthquakes comes at the expense of a significant number of smaller magnitude events. Seismic hazard evaluations can be significantly affected by this variation in magnitude recurrence, so that Geomatrix considered both of these viable representations of magnitude recurrence. Figure 5-14b of the Geomatrix (1996b) report shows that the magnitude distribution parameterization is an important component in the total uncertainty of the hazard evaluation for the 200 East Area, particularly for high frequency spectral ordinates. It may be that the diminished influence of magnitude distribution for the long periods – 2 sec. period is attributable to the dominance of the Cascadia subduction zone interface seismic source in the total hazard, where the “aspect ratio” magnitude distribution function, as discussed below, replaces the exponential distribution in the consideration of alternate magnitude distribution models.

Some subtle variations of exponential and characteristic magnitude distributions have been used by Geomatrix (1996b) which we found important in our efforts to reproduce the Geomatrix results for selected sources. In Youngs and Coppersmith (1985) the range of characteristic events is presented to occur over a 0.5 magnitude interval width, the “maximum magnitude” of a characteristic distribution refers to the high magnitude end of this half-magnitude interval. In Figure 3-3 the characteristic magnitude distribution considers characteristic events ranging between magnitudes 6.5 and 7.0, and the magnitude recurrence asymptotically approaches zero events at the maximum magnitude of 7.0. In the 1996b Geomatrix report, the maximum magnitude, M_{\max} , of a characteristic distribution is re-defined to apply to the center of the half-magnitude interval because it is reasoned (Youngs, personal communication) that a maximum characteristic magnitude should be defined as “ $M_{\max} \pm 0.25$ ”. Therefore, in considering the maximum magnitudes shown in tables and figures in the Geomatrix (1996b)

report, one must consider that the magnitude frequency relation asymptotically approaches zero at 0.25 magnitude units higher than the M_{\max} tabulated in the report. For example, in Figure 3-3 presented here, the Geomatrix report would have tabulated the maximum magnitude to be 6.75.

For an exponential magnitude frequency distribution there should be less confusion about the meaning of maximum magnitude. For the appropriately truncated exponential relation, the recurrence relation asymptotically approaches zero at M_{\max} . In the Geomatrix report, it is noted that an inconsistency in the exponential and characteristic recurrence relations can be introduced if each implies a different M_{\max} . To “provide a consistent interpretation for the exponential model”, the Geomatrix report refers to Youngs et al. (1987) for a definition of the “modified exponential” relation. This “nearly exponential” relation has high magnitude asymptote at $M_{\max}+0.25$. The exact formulation of the modified exponential, as presented in the Geomatrix report, is complicated and cannot be incorporated exactly into commercial seismic hazard evaluation programs. However, the modified exponential may be approximated by simply keeping the number of minimum magnitude events constant as obtained using the tabulated maximum magnitude (and other recurrence parameters) and then increasing the maximum magnitude by 0.25 magnitude units when performing the integrated hazard analysis.

For the seismic hazard contribution of the Cascadia subduction zone interface seismic source, Geomatrix considers two magnitude recurrence formulations. Besides the characteristic distribution, as discussed above, Geomatrix also uses what is called the “aspect ratio” method. The details of this method given in Geomatrix (1996b) are minimal, as repeated here *in toto*:

The second approach [of recurrence modeling] was to use the statistics of observed aspect ratios of interface ruptures to simulate sequences of events needed to completely rupture the margin. The average distribution of event sizes over a large number of simulations was used to construct a recurrence relationship.

Figure 3-32 of the Geomatrix report shows a plot of the mean characteristic and “aspect ratio” recurrence relations used for the Cascadia Subduction Interface source. The “aspect ratio” recurrence, similar to the characteristic recurrence relation, shows a flattened portion to the recurrence, but the flattening is more prominent. That is, the flattened portion of the aspect ratio recurrence is flatter and covers a wider magnitude range in which the cumulative frequency is nearly a constant.

There is insufficient detail given in the Geomatrix report to replicate the aspect ratio recurrence relationships specified for the Cascadia interface source. We asked for and obtained from Geomatrix the digital versions of these aspect ratio recurrence relations, but found that this form and format are not easily incorporated into commercial seismic hazard routines.

3.4. Foundation Soil Column

The scope of the Geomatrix (1996b) seismic hazard study is Hanford Site-wide without a great deal of specific foundation information at any particular site. What is specified for the subsurface is in the context of arguments for the appropriate use of available strong ground motion attenuation relationships. In this context the Geomatrix report concludes that the Hanford Site is underlain by “stiff to very stiff alluvial soils overlying the Columbia River Basalts” for which use of attenuation relationships developed from firm alluvial sites in California are appropriate.

The general subsurface conditions at Hanford are characterized as alluvial soils of Holocene loess and Pleistocene and Holocene sands and gravels underlain by the Ringold Formation, which consists of dense

gravels and gravelly silts and clays. Depth to basalt is given as about 200 to 600 feet. A recent summary discussion in more detail may be found in Reidel et al. (1994).

To quantitatively justify the use at Hanford of attenuation relationships developed from California data, comparative site response studies are referenced from an earlier WNP-2 report (Washington Public Power Supply System, 1985) and performed in Appendix A to the 1996b Geomatrix report. The conclusion of these analyses is that the empirical strong motion data from firm alluvial sites in California are appropriate for the Hanford Site. We have performed an independent review of this Appendix A as part of the current validation report, and results of that review are presented in Chapter 5.0 below.

What is known to date about the details of shallow subsurface materials in the 200 East Area is summarized in Appendix A of the Geomatrix report. Two composite soil-rock shear-wave velocity profiles have been selected: "H1 + basalt" and a second profile with the upper 100 feet of the H1 + basalt profile modified using the most recent velocity measurements (Shannon & Wilson, 1994). These two profiles are shown in Figure 3-4. The Shannon & Wilson data show a time-averaged shear-wave velocity in the upper 100 feet of the 200 East Area of 580 m/s. This, when compared with the soil classification criteria of Section 2.2 indicates NEHRP soil type C.

3.5. Model Weight Schemes

The earthquake source model presented in the Geomatrix (1996b) report was developed with input from Geomatrix Consultants, Westinghouse Hanford Company, Pacific Northwest National Laboratory, and Washington Power Supply System. The individuals involved in the assessments of potential earthquake sources are listed in the introduction of the Geomatrix report. Many of them have provided input to this validation report.

The models, parameters, and their relative weights as presented in the Geomatrix report represent a consensus of the team developed through multiple meetings and discussions, and represent the team's assessment of the then-current state of scientific knowledge about the seismic potential and earthquake ground motion characteristics of the Hanford region. The weights are typically based on subjective judgement.

The Geomatrix report carefully tabulates all weights adopted as part of its hazard analysis for several Hanford Site sites. It does not document specifically how particular weights were chosen. This can be deduced in part from the additional discussion of selected weights for alternative branches of logic tree analysis for specific potential earthquake sources as presented above in this chapter. Sensitivities of results to weighting of selected parameters for several specific sources are presented in the Geomatrix report (Geomatrix, 1996b, Figures 5-10 through 5-13). Finally, additional parametric examination of alternative weighting schemes for two input variables (coupled/uncoupled characterization for Yakima Fold Belt features and the credibility of the Deep Crystalline Basement Rift source) are further examined in Chapter 6.0 of this current report.

3.6. Other Parameters

Two parameters that affect the computed hazard results are not discussed in the Geomatrix report: minimum magnitude and truncation of the ground motion attenuation relations.

The number of earthquakes within a given areal source or on a given fault source is specified in terms of number of events equal to or greater than some minimum value. This minimum magnitude value has

been variously selected in the past. For example, Algermissen et al. (1982, 1990) use a lower bound magnitude of 4.0 and 4.6, respectively; Bernreuter et al. (1985) and EPRI (1986) adopt values of 3.75 and 5.0 in their respective studies of earthquake hazard in the Eastern North America, and Frankel et al. (1996) use a value of 5.0. Kennedy (1989) argues that ground motions from earthquakes of magnitude less than 5.0 are of short duration, limited energy content, generally lack low frequency power and appear to be generally incapable of damaging well-engineered structures and equipment.

The Geomatrix report also adopts a value of 5.0, in agreement with current convention, as the “minimum magnitude of engineering significance.”

Little has been written about appropriate ground motion attenuation truncation. The following is summarized from Reiter (1990, p. 214 et seq.). The convention of truncating ground motion attenuation relationships arises from the argument that, while there is theoretically no limit to the amplitude of ground motion that is modeled by a lognormal equation with statistical uncertainty included, there must be some physical limitation on the strength of ground motion that a given earthquake can generate, both from the perspective of the strength of rocks storing the elastic energy released during an earthquake and from limits on the ability of near-surface materials to transmit elastic energy. In probabilistic analyses the issue of where and how one truncates the high range of ground motion must be dealt with. One way to treat this issue is to limit the absolute value of ground motion. This is a choice used in a limited way, for example, for the New Madrid region in Frankel et al. (1996). Another way of implementing this cutoff is to limit the number of standard deviations (σ 's) used in calculating ground motion. Algermissen et al. (1990) specify a value of 6 σ . In Bernreuter et al., (1989), for example, one ground motion expert proposed that the limit be set at 2.5 σ while another thought that 4 σ was appropriate. The basis for any of these choices is limited. In addition, the effect is generally not important for probabilistic ground motions with return periods well in excess of return periods (roughly 500 to 2500 years) generally of interest for engineering applications.

The Geomatrix (1996b) report truncates all ground motion attenuation relationships at 3 σ .

**Table 3-1. Shear Wave Velocity in the Top 30 Meters for Site Class C{ TC "3-1.
Shear Wave Velocity in the Top 30 Meters for Cite Class C" \f T }**

Period (sec)	b7	bv	V _A	V _s
0.03	0.251	-0.371	1400	294.83
0.10	0.136	-0.212	1110	253.40
0.20	0.279	-0.292	2120	234.89
0.30	0.356	-0.401	2130	275.80
0.50	0.439	-0.553	1780	286.13
1.00	0.517	-0.698	1410	256.17
2.00	0.537	-0.655	1790	271.02
Mean =				267.46 m/s

b7, b_v, and V_A are period-specific attenuation regression parameters from Boore et al. (1995 and 1997). V_s is the average shear wave velocity in the top 30 m of foundation material underlying a site, related to the other parameters as discussed in the text. For Boore et al. soil class C, the value of V_s averaged over all periods is about 267 m/s.

Figure 3-1. Structural Map of the Pasco Basin and Surrounding Columbia Plateau{ TC "3-1. Structural Map of the Pasco Basin and Surrounding Columbia Plateau" \f F }

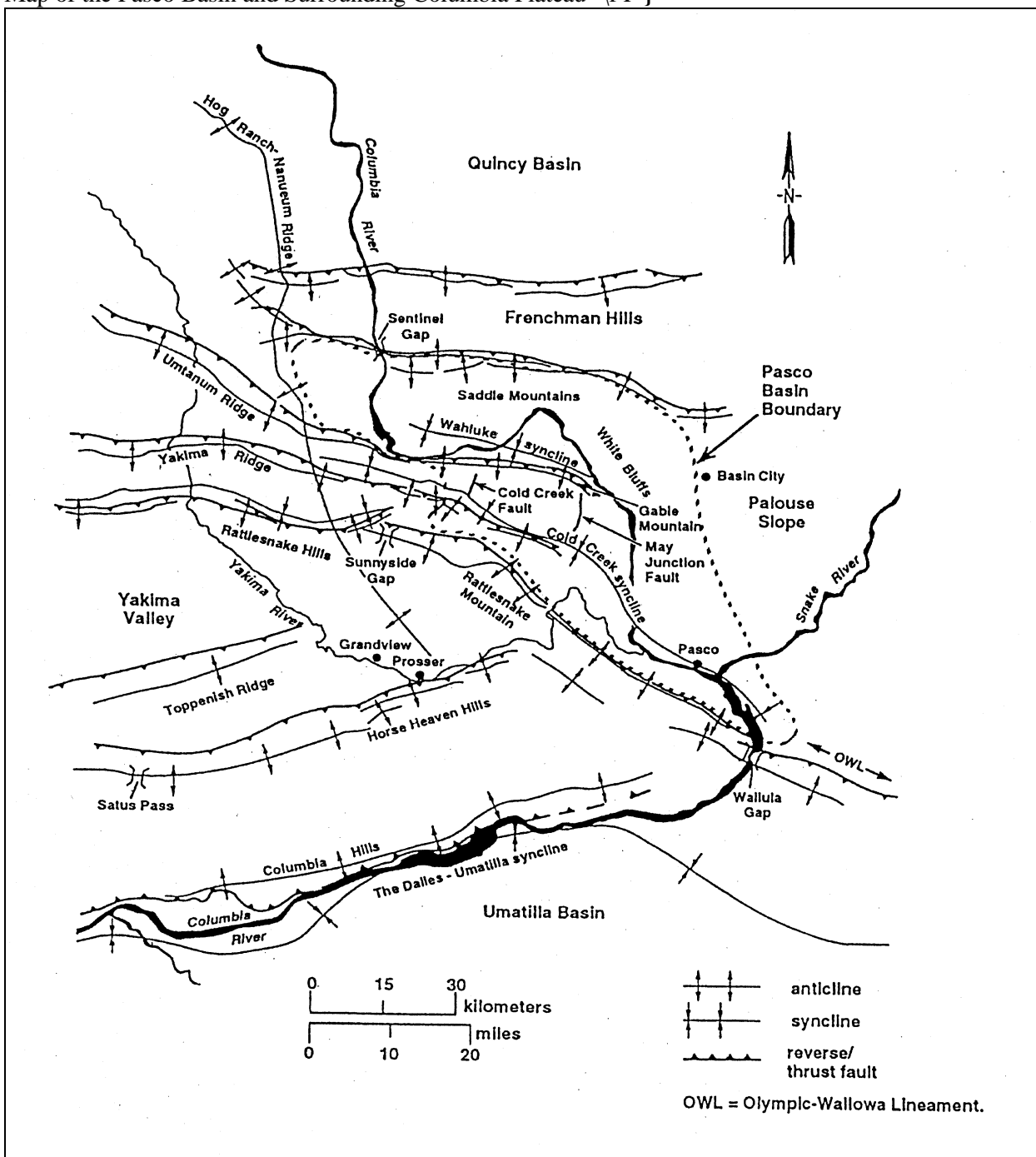
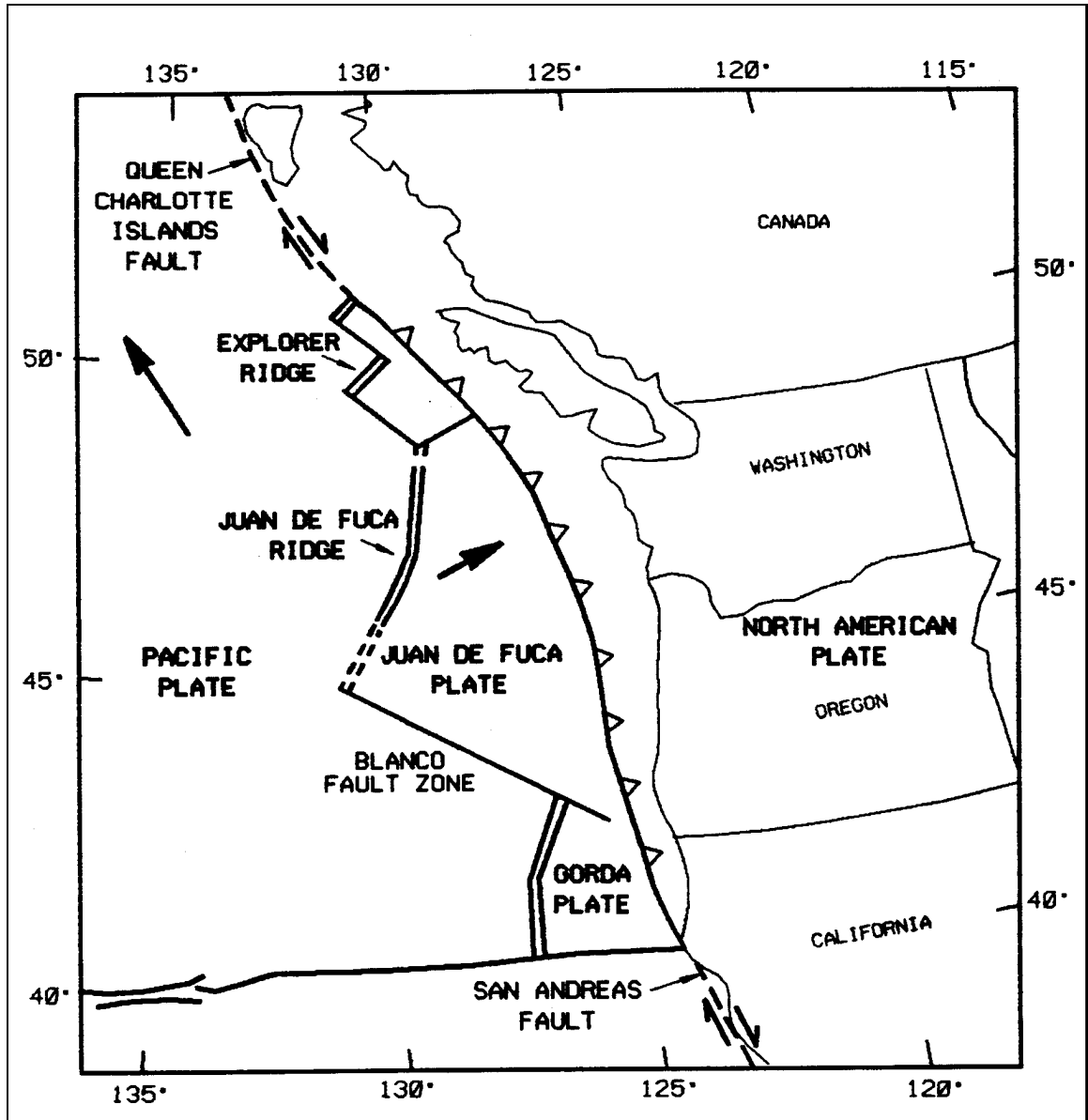
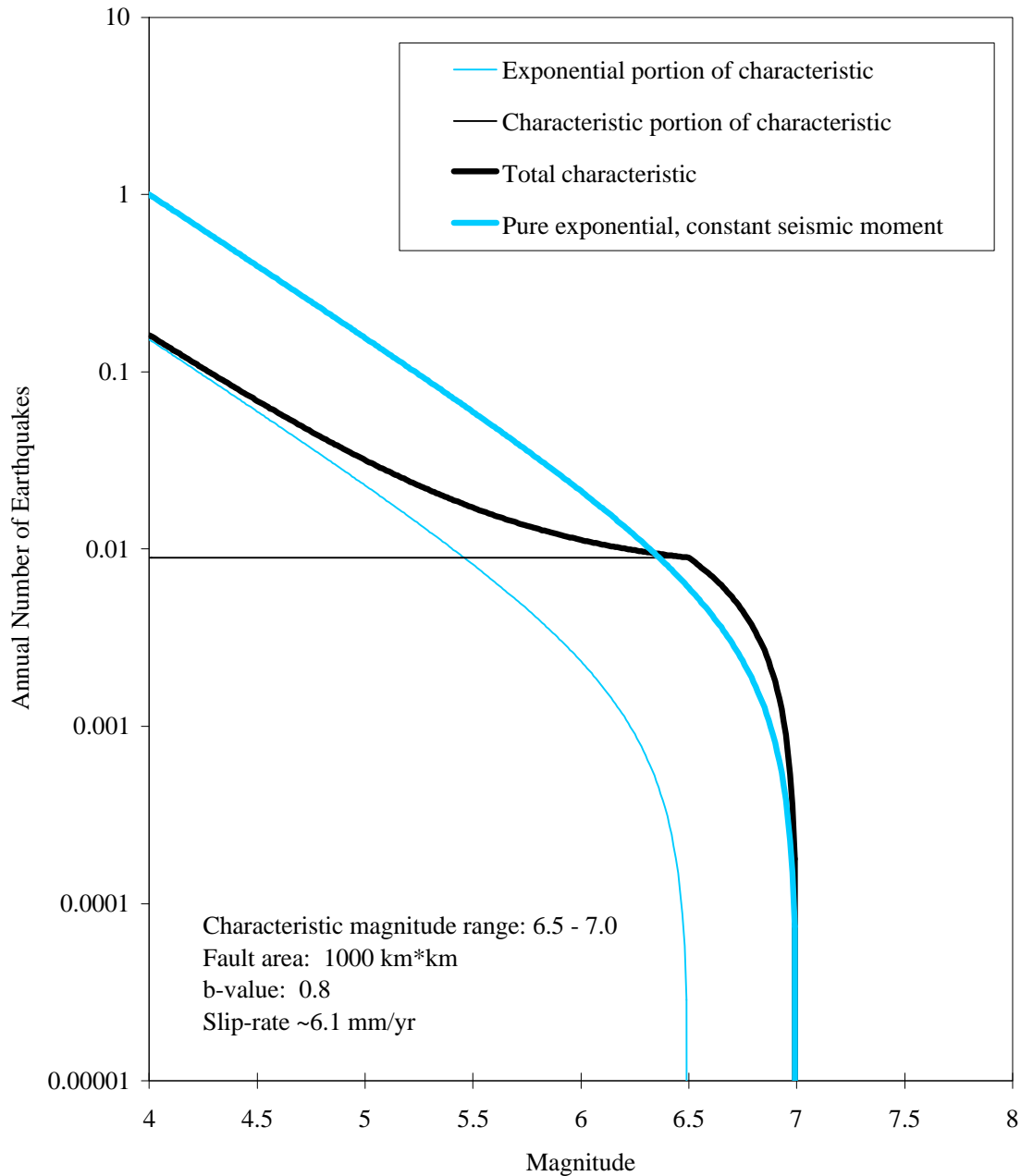


Figure 3-2. Sketch Map of Major Tectonic Features of the
 Cascadia Subduction Zone{ TC "3-2. Sketch Map of Major Tectonic Features of
 the Cascadia Subduction Zone" \f F }



Large arrows show plate motion of the Pacific (about 5 cm/yr) and Juan de Fuca (about 3 cm/yr) plates relative to the North American plate. Adapted from Chandra (1974), Riddihough (1978), and Heaton and Hartzell (1987).

Figure 3-3. Comparison of Pure Exponential and Characteristic Forms of Magnitude Recurrence Relations
TC "3-3. Comparison of Truncated Exponential and Characteristic Forms of Magnitude Recurrence Relations"



The Geomatrix (1996b) report uses the exponential form for area sources and both the exponential and characteristic form for fault sources. The characteristic model is made up of an exponential and characteristic portion, and these are split out in the figure.

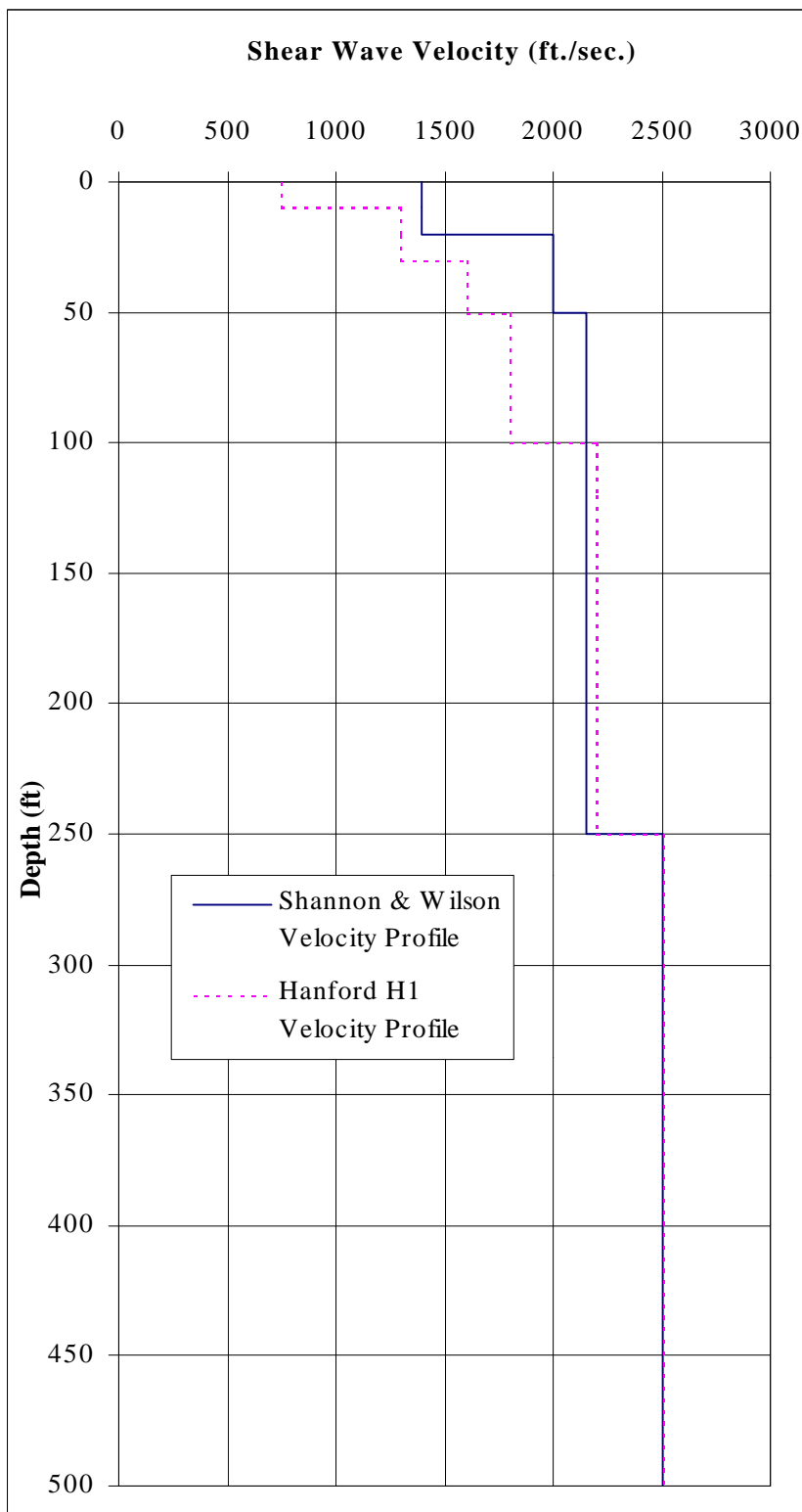
Figure 3-4. Two Composite Soil-Rock Shear-Wave Velocity Profiles for the 200 East Area: H1 + Basalt and its Shannon & Wilson Modification{ TC "3-4. Two Composite Soil-Rock Shear-Wave Velocity Profiles for the 200 East Area: H1 + Basalt and its Shannon and Wilson Modification" \f F }

Shannon Wilson Velocity Profile

Depth (ft)	Vs (ft/s)
0	1400
10	1400
10	1400
20	1400
20	2000
30	2000
30	2000
50	2000
50	2150
100	2150
100	2150
120	2150
120	2150
250	2150
250	2500
500	2500

Hanford H1 Velocity Profile

Depth (ft)	Vs (ft/s)
0	750
10	750
10	1300
20	1300
20	1300
30	1300
30	1600
50	1600
50	1800
100	1800
100	2200
120	2200
120	2200
250	2200
250	2500
500	2500



4. Additional or Alternative Model Parameters

4.1. Additional Data

The Geomatrix report concludes that the spatial distribution of regional historical earthquakes (see Geomatrix, 1996b, Figure 3-1) through March 1991 (the most recent data available at the time of the 1993 Revision 0 version of the report) is scattered and not generally associated with any particular identified structure. The Geomatrix report also specifies that no strong motion data have been recorded in the study region. In this section, these two assertions are revisited in the light of any more recent data.

4.1.1. Regional Seismicity

Geomatrix (1993, 1996b) compiles a regional earthquake catalog from two sources: 1) the catalog presented in the FSAR for Washington Public Power Supply System's WNP-2 power plant for the time period of 1850 to 1969; and 2) from University of Washington seismic records for the period of 1969 through March 1991. Figure 3-1 of the Geomatrix report plots the seismicity data that lies within the site region, defined as the geographic window of 118° - 121° W, 45.5° - 47.5° N. We obtained this earthquake catalog from Geomatrix, and replotted these data in Figure 4-1. There are 3124 earthquakes plotted, the largest a magnitude 5.75 event on July 16, 1936 about 115 km from the TWRS-P Facility.

The University of Washington contributes seismicity data maintained by the Council of the National Seismic System (CNSS) [<http://quake.geo.berkeley.edu/cnss/>]. On the recommendation of Alan Rohay of Pacific Northwest National Laboratory (personal communication), this database was searched for all events occurring since the end time (March 28, 1991) of the Geomatrix catalog. Within the site region 987 additional earthquakes were found through December 29, 1998, the largest of which is a magnitude 4.3 event on November 28, 1991 also about 115 km from the TWRS-P Facility. A procedure for identifying and removing dependent events from the earthquake catalog was not performed for this supplemental data set. Figure 4-2 is a plot of the additional seismicity (March 1991 to December 1998), and Figure 4-3 is a composite of all events from 1850 to December 1998.

The spatial distributions of earthquakes before and after March 1991 are similar so that the more recent data would not alter the original assessment of their association with identified or conjectured geologic structures.

It is interesting to note, that the epicenters of the July 1936 and November 1991 events, referred to above, apparently occurred near one another within a cluster of seismic activity along the Washington-Oregon state border, just east of the mapped ends of the Horse Heaven Hills and Rattlesnake-Wallula Yakima Folds.

For either the original or time-supplemented Geomatrix regional seismicity catalog, the largest historical felt earthquake at Hanford is the M5.7 in Milton-Freewater, Oregon, event of 1936. This earthquake occurred about 115 km from TWRS-P Facility and resulted in a Hanford Site peak ground acceleration (PGA) estimated to have been $< 0.05g$

4.1.2. Search for Local Strong Motion Data

The Washington Public Power Supply System's WNP-2 nuclear plant is located on the Hanford Site approximately 18 km east-southeast of the TWRS-P Facility (see Figure 1-1). WNP-2 includes seismic

monitors to meet regulatory requirements (U. S. Nuclear Regulatory Commission, 1974). These instruments include three triaxial strong-motion accelerographs located: 1) on the reactor building foundation (422' MSL), 2) higher in the reactor building at elevation 522' MSL, and 3) in the free field at least 1000 ft. from any large structure. The two sensors located in the reactor building are rigidly mounted to the building.

All three sensors transmit electrical signals to the main control room where the data are recorded on magnetic tape. The recorders are activated by a seismic trigger unit mounted on the reactor building foundation close to the triaxial strong-motion accelerograph sensor. The trigger is also triaxial, broadband, and set to trip at 0.01g (Washington Public Power Supply System, 1998). Activation of the seismic trigger is indicated in the main control room. These instruments have been in operation since the initial fuel load of WNP-2 on December 25, 1983.

We asked the Washington Public Power Supply System whether the triaxial time-history accelerographs had ever been triggered by an earthquake. The response was negative (Hosler, 1998).

As an additional check, a search of the global earthquake database of the Council of the National Seismic System (CNSS) was made for all earthquakes in the site region from January 1984 through December 1998. A 781 events were found within 50 kilometers of WNP-2, ranging in magnitude from 1.0 to 3.5. For each of these events, a peak ground acceleration was estimated at WNP-2 from the four crustal attenuation relationships used in Geomatrix (1996b). The six earthquakes with the largest calculated site peak ground accelerations were identified for further investigation of possible triggering of the WNP-2 strong motion instrumentation.

The six seismic events were:

EVENT (PACIFIC STANDARD TIME)					LAT N	LON W	DEPTH km	DIST* km	MAG
CNSS	1988	Dec	15	13:52:52.84	46.459	119.291	0	3.5	2.00
CNSS	1989	Feb	5	8:28:00.65	46.455	119.302	0	3.0	1.70
CNSS	1989	Feb	11	14:43:31.98	46.456	119.299	0	3.2	2.20
CNSS	1989	March	24	0:42:44.03	46.489	119.274	1	4.9	2.10
CNSS	1989	April	3	8:42:59.89	46.487	119.261	2	5.8	2.50
CNSS	1995	June	11	17:48:24.40	46.404	119.263	1	9.3	3.30

* DIST is epicentral distance from WNP-2.

For each of the above dates, the operability of the seismic monitors "at all times" was a requirement of the plant Technical Specifications (Washington Public Power Supply System, 1996) (the seismic monitor Technical Specification was relocated to the Licensee Controlled Specifications in March 1997). Washington Public Power Supply System provided copies of the Control Room Operators Logs for the shifts that cover the six above-listed times which specify that the triaxial time-history accelerographs and their seismic trigger were not declared inoperable at these times. In addition, review of the Control Room Operators Logs by the Supply System gave no indication of activation of the seismic annunciators or other reports of seismic activity for the times provided (Hosler, 1999). The only mention of an earthquake is an entry at 2008 hours on June 11, 1995 that describes a notification of the control room several hours after the earthquake occurred. The log entry reads as follows.

"Emergency management reports via security a 3.3 Richter scale earthquake, 9.9 miles N. of Richland; there was no indication of earthquake in the plant; equip. operators walked their areas for negative results."

Therefore, to the best of our ability to determine, there are currently still no strong motion accelerometer records from any earthquake in the Hanford Site region.

4.2. Alternative Attenuation Relations

The evolution of Hanford Site earthquake hazard estimates beginning with Powers et al. (1981) has resulted in significant part from adoption of alternative updated empirical strong ground motion attenuation curves incorporating new data, principally from earthquakes in California. For this validation report, we have considered whether new attenuation relationships, developed since the latest version of the Geomatrix report, have been developed.

4.2.1. Cascadia Interface Subduction Zone

As discussed in Chapter 3.0, the 1996b Geomatrix report used several attenuation relationships for the Cascadia subduction zone interface source. Only one of these, Youngs et al. (1993) has been updated. Youngs, et al. (1997) publish a more recent relationship based on a regression with additional data. The 1993 and 1997 models are identical for all spectral periods except for 0.2 and 0.3 seconds. A comparison of the two attenuation models is shown in Figure 4-4 for a magnitude 8.5 interface earthquake at a distance of 375 km (depth of the hypocenter of 25 km). The updated attenuation relationship predicts higher ground motion between the 0.1-0.5 seconds period range. The sigma values for the two models are identical at all spectral periods. The comparison shown was selected because the Geomatrix hazard analysis used a depth of 25 km for the interface hazard estimates and the 8.5 magnitude and 375 km distance are reasonable choices for the central measure of model maximum magnitudes and minimum distances used for the Geomatrix Cascadia interface earthquake source model (see Figures 3-29 and 3-30 of Geomatrix 1996b).

The possible effect of the difference shown in Figure 4-4 is discussed in Chapter 6.0 of this report.

4.2.2. Campbell Shallow Crust Attenuation

One of the four crustal attenuation relationship for peak ground acceleration used in the Geomatrix (1996b) study was developed by Campbell and Bozorgnia (1994). This relationship was generalized to spectral acceleration values using (SA/PGA) ratios from Campbell (1990). Campbell (1997) represents a more current empirical attenuation relationship that has a different functional form for spectral acceleration. The Campbell (1997) attenuation model is based on a combination of previous attenuation models by the author. Hence the functional form for PGA is exactly the same between the Campbell and Bozorgnia (1994) and Campbell (1997). For spectral attenuation on soil sites, however, the Campbell (1997) and Campbell and Bozorgnia (1994)/Campbell (1990) models predict slightly different ground motions.

As an example, the median spectral acceleration for earthquakes of magnitude 5.5, 6.5, and 7.5 at a distance of 10 km are shown in Figure 4-5a for a depth to basement of 0.6 km. For periods greater than 0.2 seconds, the Campbell (1997) attenuation relationship predicts lower ground motion for all three magnitudes with the largest difference occurring at 1.0 second for a magnitude 6.5. For a depth to basement of 8 km, the spectral acceleration values are shown in Figure 4-5b. At this depth to basement the two attenuation models are quite similar. These two examples are relevant to the Geomatrix (1996b) report because Geomatrix actually computes hazards using the Campbell relations for the two separate depth-to-basement values specified above (Youngs, personal communication). The comparison is made

for the close distance of 10 km because it is the closer earthquakes that contribute most significantly to hazard from crustal sources (see Figures 5-6b and 5-7b of Geomatrix, 1996b).

The standard error for the Campbell (1997) attenuation relationship is no longer period dependent as was the case for the earlier attenuation relationship. Figure 4-6 shows the comparison between the Campbell (1997) and Campbell and Bozorgnia (1994)/Campbell (1990) standard error for the same three magnitudes at a distance of 10 km. Both attenuation models predict similar sigma values as would be expected, the newer Campbell values being a little higher on average, generally enveloping the previously published period-dependent values.

The possible effect of the difference shown in Figure 4-5a and 4-5b is discussed in Chapter 6.0.

4.3. Alternative or Additional Sources – May Junction Structure

The seismic sources model used in the Geomatrix report was developed by a panel of geologists and seismologists expert in these topics for the Hanford Site region and with access to all known relevant regional research. During this review of the Geomatrix report we contacted these experts and asked if there were any additional sources of potential ground shaking for the Hanford Site, and for the 200 East Area in particular, not already considered by Geomatrix. One such potential feature – the May Junction structure – emerged as a candidate additional source to consider.

The May Junction structure is not a new feature. It was first recognized by Golder and Associates (1982) (who called it the May Junction monocline) based on anomalies in the aeromagnetic signature of the area. Golder drilled a series of boreholes across the feature and identified it as a sharp flexure in the surface of the buried basalt. These boreholes bracketed, but none penetrated, the feature. As early as 1982 this evidence suggested the possibility of faulting both to the NRC staff and to its advisor, the U.S. Geological Survey (U. S. Nuclear Regulatory Commission, 1982b).

Reidel and Fecht (1994) reviewed the available data and interpreted the lineament as a concealed fault based on comparison of its aeromagnetic signature to other faults in the area, the steep closure of contours on the top of the basalt that are constrained by the two nearest Golder boreholes, and professional judgement based on over 20 years experience mapping basalt structure in Washington. The May Junction fault, taken from its characterization in Reidel and Fecht appears on the Geologic Map of Washington (Schuster et al., 1997). It also appears on the “Structural and Tectonic Map of the Columbia Basin” in annual Hanford seismic reports (for example, Hartshorn et al., 1998) which has been reproduced in this current validation study as Figure 3-1.

The following is the current best characterization of this feature for purposes of seismic source modeling (Tallman, 1999). The May Junction fault is approximately 3 km east of the 200 East Area. It is buried by sediments of the Ringold Formation and Hanford formation, is approximately 6-km long, and trends generally in a north-south direction. The fault dies out to the north before reaching Gable Mountain. Its southern extent is difficult to estimate because borehole coverage is sparse in that region. Two wells that straddle the projection of the fault about 3 km south of its projected end indicate no offset.

The May Junction fault extends through the Columbia River basalt (4 km). The maximum displacement of the fault is about 60 meters measured on the surface of the Columbia River Basalt Group (CRBG) which is 10.5 Ma and overlying Ringold Formation sediments (approximately 7Ma). However, it is thought that the fault was active during the eruption of CRBG. Offset on the overlying Hanford formation (1 Ma to 10 ka) cannot be estimated using available data, but by comparing the elevations of

subunits of the Hanford formation any offset must be minor. The youngest movement of the fault is not known.

The May Junction fault is a normal fault that forms the western boundary of the Wye Barricade depression, a basin that lies between Gable Mountain and Rattlesnake Mountain east of the termination of Yakima Ridge. The Wye Barricade depression is a subfeature of the Cold Creek syncline and Pasco Basin. These structures have been subsiding since the Miocene.

Based on the size of the May Junction fault (4 km by 6 km), it has a characteristic magnitude of 5.5. Its long-term slip rate is very low and does not support a very high probability that it is active. The model for this fault is based on stratigraphic offset across the structure. It has never been drilled. Based on the interpreted origin (basin subsidence), the subsidence rate of the Pasco Basin (0.003 mm/yr) and the slip rate of the proposed fault (0.009 mm/yr), the probability of activity is assumed to be much lower than the surrounding Yakima Folds. A value of 0.1 is assigned.

4.4. Alternative Recurrence Relations - Saddle Mountain Fault Slip Rate

The characterization of the Saddle Mountains faults given in the Geomatrix report is summarized above in Chapter 3.0. A fundamental feature of that characterization is the long-term slip rates adopted for the fault and its five segments. In the Geomatrix (1996b) model, these slip rates depend on alternative estimates for the ages of offset stratigraphic horizons, whether or not folds are modeled as “fault propagation” or “fault-bend” features (see Geomatrix, 1996b, p. 3-25), and the dip assumed for the fault segments. For the Saddle Mountains considered as a whole, slip rates so calculated range from 0.030 to 0.138 mm/yr. Individual segment slip rates relevant to the discussion below vary from 0.054 to 0.144 mm/yr (Smyrna Bench) and 0.035 to 0.094 mm/yr (Saddle Gap) (see Geomatrix, 1996b, Table 3-4).

For a number of years, Michael West and his colleagues have been performing field investigations of the north flank of the Saddle mountains. The most recent easily available summary of this work may be found in West et al. (1996). Work more recent than that reported in the 1996 reference may be viewed on the Internet (West, 1998). In both the 1996 and 1998 references, it is concluded that information found in trenches excavated for the purpose of investigating the recent tectonics of Saddle Mountains indicate minimum slip rates for the Smyrna Bench and Saddle Gap segments of the Saddle Mountains faults of 0.33 to 0.65 mm/yr, “2.3 to 9.4 times greater than slip rates used in a recent seismic hazard analysis for the Hanford Site.” (The reference here is to Geomatrix, 1993, which contains the same slip rates as Geomatrix, 1996b.)

The regional experts who provided geologic, tectonic, and seismologic input for the Geomatrix (1996b) study have been following the West work, which began more than ten years ago (see, for example, West and Shaffer, 1989). At our request, the following summary (through the three bullets below) was provided.

West et al (1996) propose strain rates of 0.33-0.65 mm/yr. for the Saddle Mountains fault (assuming a dip of 30°) based on 6.5 m of normal fault displacement of 20,000-40,000 year old sediments in the Smyrna graben. All strain is attributed to faulting with none accounted for by folding. If the strain is separated into the vertical and horizontal components, the vertical uplift component is 0.17 mm/yr. Taking the top of the Priest Rapids Member (14 Ma) as a datum, and using the 0.17 mm/yr. as the uplift rate since Priest Rapids time, the Priest Rapids Member should have been uplifted a minimum of 7,800 feet from its undisturbed position north of the Saddle Mountains. The measured uplift on the top of the Priest Rapids is 2000 feet, a minimum of 5,800 feet less than predicted by West et al (1996). If the fault angle is

increased to 60° to match the fault angle determined from the BN 1-9 exploratory borehole, the amount of predicted uplift increases. If the angle is reduced to 15° the predicted uplift is still over 2000 feet more than the observed uplift.

There are several possible explanations for the difference between predicted and observed uplift.

- Calculation of slip on the Saddle Mountains fault based on 6.5 m of normal fault movement is incorrect. The Saddle Mountains is folded and the Smyrna graben is an extensional graben due to folding above the fault. An uplift rate of 0.04 mm/yr. would produce the 2000 feet of observed uplift; this translates into 0.08 mm/yr. of slip on the Saddle Mountains fault. Slip of 0.08 mm/yr. would produce 1.6 m of offset on the normal fault. The remaining 4.9 (6.5-1.6) m of normal fault slip is a result of extensional folding.
- The slip rate proposed by West et al is not a long-term slip rate but a short-term slip rate. The time between earthquakes that produce this amount of slip is much greater than presently estimated (at least 4 times greater). The long-term uplift rate is still 0.04 mm/yr.
- Normal fault movement measured by West et al. (1996) is a result of slumping off the toe of the hanging wall. Over steeping of the hanging wall (basalt flows are vertical to overturned) results in slumping producing extension. A model of this type, assuming 60° dips typical of normal faults, produces a horizontal extension half that of the vertical (3.25 m), and slip on the 30° toe of about 0.375 m, or a slip rate of 0.09-0.19 mm/yr. This may not necessarily be tied to the slip rate of the deeper, causative seismogenic fault, but may be broadly (order of magnitude) indicative.

The regional experts stand by the slip rate estimates of the Geomatrix study and recommend that, if a sensitivity run is made, slip rates on the Smyrna and Saddle Gap segments of the Saddle Mountains fold may be doubled (Tallman, 1999).

4.5. Alternative Weighting Schemes

The weights applied to alternative models of the various input parameters of a probabilistic earthquake ground motion hazard may be important to the quantification of both the preferred (mean or median) result and to the range in the derived hazard characterization. Issues of specific weights adopted for Crystalline Basement and Yakima Fold Belt fault properties were raised during several meetings with the Regulatory Unit of DOE (see Appendix A of this report). The addition of some potential contribution to earthquake hazard from the May Junction fault and from alternative slip rate values on certain segments of the Saddle Mountains fold faults constitute alternative weights (from zero to some non-zero value) to these possibilities (see immediately preceding sections). The effects of these alternative weights are examined in Chapter 6.0. The panel of regional experts reviewed and decided to retain the Geomatrix (1996b) report weights for alternative Crystalline Basement sources.

Another way to consider the effects of altering weights selected for any given model parameter is to compare mean hazard curves that have resulted from the actual weighting scheme used with the mean hazard curve that would have resulted if a given branch of the suite of branches representing alternative options for that parameter had been assigned a weight of 1.0 while all other branches had been assigned zero weight. Comparisons of this type are made in Figures 5-10 through 5-13 of the Geomatrix report. We review and elaborate on this type of comparison for the two model parameters coupled/uncoupled for the Yakima Fold Belt faults (Geomatrix, 1996b, Figure 5-10b) and Deep Crystalline Basement features (Geomatrix, 1996b, Figure 5-13b) in Chapter 6.0 below.

In addition to questions of specific weights adopted for specific pieces of the earthquake source model of the Geomatrix report, we asked our consultant, Allin Cornell, to comment on the use of weights to properly capture hazard estimate uncertainty and on what could be said about capturing the uncertainty in the hazard result caused by the use of subjective weights. The remaining paragraphs of this section are from his response (Cornell, 1999).

The quantification of the uncertainty in each of the basic individual elements (seismicity and ground motion model parameter values, alternative forms or types of some sub-model, and so on) is conducted in various ways. Some cases (for example, uncertainty in mean historical seismicity rates) are the simple products of classical statistics – a science that deals with inference from finite samples. Others must of necessity be based on the judgements of experts in the field by, for example, giving relative “weights” (degrees of belief”, or likelihoods) on alternative parameter values or contending models representing their current professional characterizations of the state of the professions knowledge. Alternative ways of doing the latter have been carefully outlined in a multi-year study referred to as the SSHAC report (1997). The level of effort can range from (a) having one senior professional assign weights designed to reflect his/her reading of the central estimate and breadth of the profession’s uncertainty as indicated, for example, by the frequency of literature citations or frequency of application by knowledgeable specialists, through (b) soliciting opinions from a collection of experts, to (c) conducting a time-and-resource-intensive program of facilitated meetings, white papers, and panels.

The Geomatrix Hanford PSHA central estimates and uncertainties are based on the use of a panel of geoscience experts although the report pre-dates the SSHAC report. The process used is representative of the moderate to high level of resource commitment identified by SSHAC. It is quite consistent with the recommendations of that panel. In short, a significant effort was made to obtain a sample of opinions of regionally knowledgeable geoscientists; their judgements were captured (‘elicited’) and represented by uncertainty distributions on several important parameters and models. This is a much higher level of effort, for example, than went into the USGS maps to reflect the uncertainties in seismic hazard.

As to the question, “Why not put uncertainties on the weights, i.e., on the uncertainties?” the short answer is that “two levels are all there are”. The first level is nature’s randomness and the second is “our” uncertainty about the parameters and/or bottom-line probability results. It should be remembered that in combining the results from a panel of experts the expert-to-expert deviations as well as the “within expert” uncertainty bands are reflected in the final (“total”) uncertainty bands. That is why the result can be said to reflect the profession’s uncertainty, not just an expert’s uncertainty or even an average expert’s uncertainty.

A more complete answer could be that, while it is true that the process of eliciting expert opinion (that is, weights, uncertainties) may not be perfectly reproducible, the weights may (perfectly legitimately) change with time (that is, with new evidence), the uncertainties may change somewhat if a different sample of recognized experts is empanelled, and so on, experience suggests that there is little to be gained in practice by pursuing this third level further. In the SSHAC (1997) report there is discussion of the question in the context that, because the uncertainty there is supposed to represent the profession’s uncertainty and because it is feasible to only “sample” the whole profession via a panel, can one estimate the “panel-to-panel” variability one might see if he were to repeat the process several times with different panels? The answer is that under some circumstances, perhaps this estimate of “panel-to-panel” variability could be made by repeating the process with different panels.

4.6. Basin Effects

The site is near the center of the shallow Pasco Basin. A brief summary of recent studies on basin effects on strong ground motion is presented below.

The evidence for differences in ground motion between sediment-filled basins and flat-layered structure includes variation of the recorded ground motion across basins, and model simulations of elastic waves for shallow basin structures. As described by Somerville (1998), ground motion within a basin can be affected by seismic waves that become trapped within a sedimentary layer of lower seismic wave velocity than the underlying rock. The conventional approach of assuming a horizontally stratified medium for ground motion prediction can sometimes underestimate the amplitude and duration of strong ground motion within basins. The difference is most significant for long-period ground motions exceeding about one second. Ground motion at the edges of shallow fault-controlled basins can also be affected by the constructive interference of direct seismic waves and by waves diffracted by the basin edge. The effect is to create a large amplification of the ground motion at the basin edge. Basin-edge effects on ground motion have been indicated for the 1995 January 17, Hyogo-ken Nanbu (Kobe) earthquake and the 1994 Northridge earthquake (Pitarka et al., 1998; Graves, et al., 1998).

Published studies have evaluated ground motion effects in basins of various sizes and shapes, with a range of layer properties, and differing earthquake sources. Different basin parameters have been indicated to be significant by various authors. These parameters include velocity contrast between sediments and underlying rock, average interface angle for sediment and rock, extent of interface angle within the basin, source location relative to the basin and resulting incidence angle.

Three-dimensional simulations of ground motions in the San Bernardino valley produced synthetic response spectral values that “were two to three times as large as those from the flat layered models, for periods of 1 to 4 sec” (Frankel, 1993). The three-dimensional simulations also showed significant differences with two-dimensional simulations. The modeling demonstrated body-wave to surface-wave conversion at the basin edge, and indicated that the largest ground velocities would occur where surface waves reflected from the basin edge interfere constructively with trapped waves. The three-dimensional grid for the San Bernardino valley simulation had dimensions of 37 km X 16 km X 7 km depth. The alluvium layer thickness varied from zero to 1,000 m. The San Andreas fault was used for the grid boundary on one side. Two hypothetical earthquakes on the San Andreas fault were simulated: a point source with a moment magnitude of M5, and a 30-km long fault-segment rupture of M6.5. As explained by Frankel, the trapping of the S wave within the alluvium results from the dip of the alluvium-bedrock interface away from the source. The dipping geometry of the interface causes the surface wave to be multiply reflected and to have higher amplitude than the direct S wave. Frankel shows the increase in velocity and duration in synthetic seismograms for the three-dimensional simulation, compared to two-dimensional and one-dimensional simulations.

Following are brief summaries of other studies for which ground motion effects in basins were evaluated:

- Santa Monica area, Los Angeles Basin, California (Graves, et al., 1998) – examined strong-motion records for 1994 Northridge earthquake; used two-dimensional finite-difference ground-motion simulations, with three subevent point sources, to evaluate the large amplification adjacent to the Santa Monica fault, located at the basin edge; “large amplification results from constructive interference of direct waves with the basin-edge-generated surface waves”.

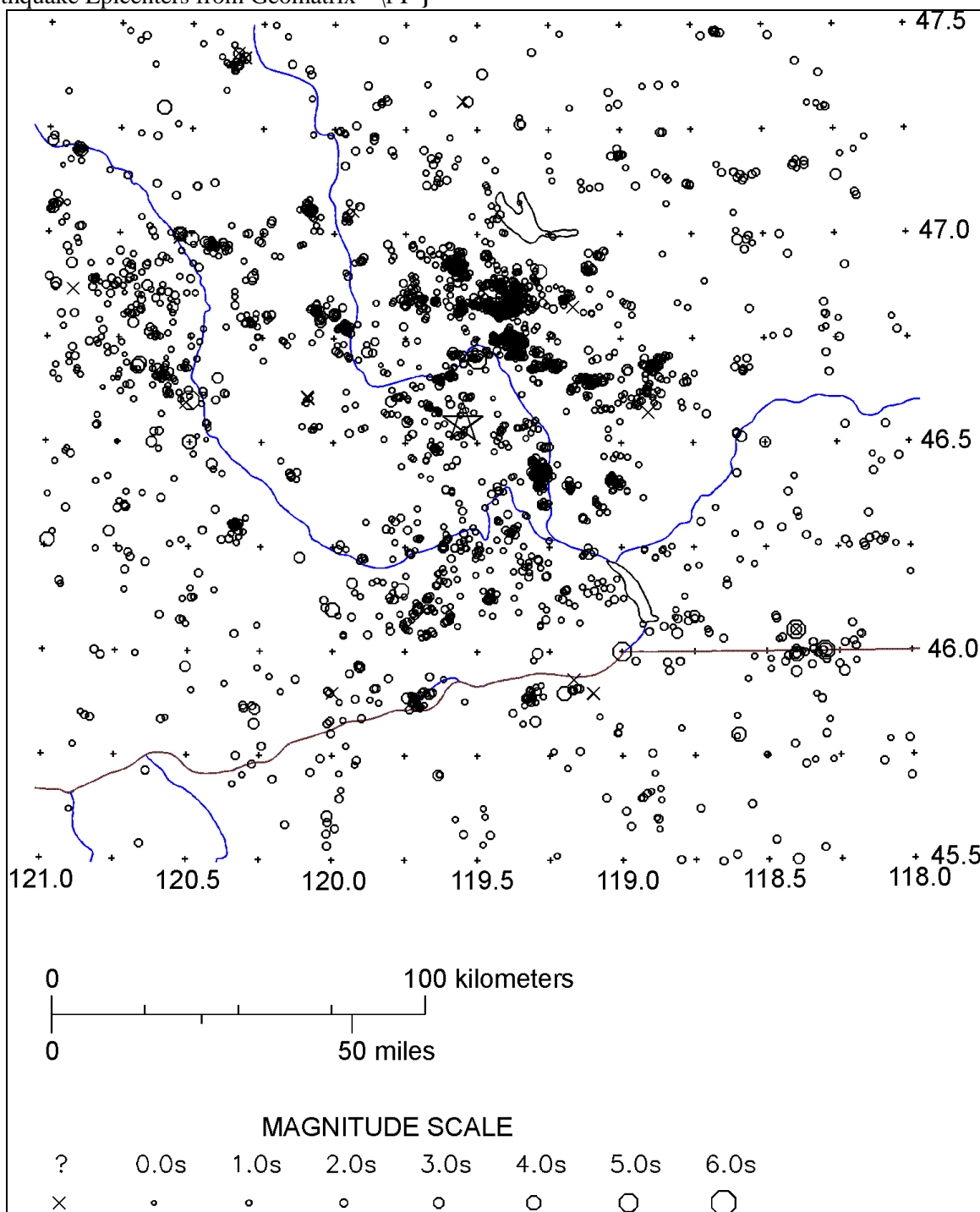
- Las Vegas, Nevada (Su, et al., 1998) – examined strong-motion records for 1992 June 29, Little Skull Mountain earthquake; prepared synthetic seismograms for Death Valley fault system earthquakes; “possible that the long durations are caused by basin-induced surface waves”.
- Taipei Basin, Taiwan (Loh, et al., 1998) – examined strong-motion records for 1994 June 5, shallow earthquake with long rupture, and 1995 June 25, deep earthquake with short rupture; “energy from the [shallow] source can easily be trapped by the basin and convert to surface waves”.
- Ubaye Valley, France (Jongmans and Campillo, 1993) – examined ground motion records for narrow river valley from local shallow earthquakes and earthquakes at further distances; computed synthetic seismograms using boundary integral equation method with steep interface, for two-dimensional modeling, and stacked horizontal layers with vertical incidence for one-dimensional modeling; large amplification and increased duration is indicated where sedimentary layers are thick.
- Salt Lake Valley, Utah (Hill, et al., 1990) – computed synthetic seismograms for four basin models: one-dimensional flat-layered model, symmetrical two-dimensional sediment-filled basin, wedge basin, and three-layer wedge basin; modeling was validated using recordings of NTS explosions; the large impedance contrast between the semi-consolidated sediments and consolidated sediments “tended to trap seismic energy within the basin” model using the three-layer wedge.
- Theoretical basins (Bard and Bouchon, 1985) – semi-numerical study using Aki-Larner technique to evaluate two-dimensional resonance in sediment-filled sine-shaped valleys; shows the “existence in relatively deep two-dimensional sediment-filled valleys of specific two-dimensional resonance patterns,” “controlled by the valley shape ratio and by its velocity contrast.”
- Chusal Valley, Russia (King and Tucker, 1984) – examined weak-motion records from a narrow valley for local earthquakes and distant earthquakes; the amplification “depends strongly on frequency and the location of the valley site, and weakly on azimuth and incidence of the input signal”; a one-dimensional flat-layer model satisfactorily predicts the middle valley response but fails to predict the fundamental frequency mode near the valley edge.
- Chusal, Yasman, and Runo Valleys, Russia (Tucker and King, 1984) – examined weak-motion records from three narrow valleys, and strong-motion records from one valley; “weak-motion measurements can be used to predict site response for ground accelerations at least as large as 0.2 g” for sediment-filled basins.
- Theoretical basins (Bard and Bouchon, 1980) – semi-numerical study using Aki-Larner technique to analyze elastic response of two-dimensional alluvial valleys; sediment boundary curvature focuses seismic rays, generates Love waves on the dipping interfaces, and traps them inside the valley; in the presence of high velocity contrast, “local surface waves can be reflected several times at the edges of the basin, resulting in a long duration of the ground shaking inside the basin.”

The velocity contrast for the Pasco basin of 5 (basalt shear wave velocity of 10,000 ft/sec to sediment shear wave velocity of 2,000 ft/sec) is comparable to the velocity contrasts of 2 to 10 for other basins with ground motion effects. A characteristic of the Pasco basin that is beyond the range evaluated in the above literature is the ratio of sediment thickness to basin half-width. The Pasco basin (see Figure 3-1 of this report) has a value of approximately 0.01 (approximately 500-foot sediment thickness and 15-km basin width), whereas values for basins evaluated within the literature are typically 0.1 to 0.3. This parameter for the Pasco basin is an order of magnitude lower than is typical for basins where ground motion effects

have been studied. Therefore, the conclusions within the literature regarding ground motion amplification and increased duration within basins may not be applicable to the Pasco basin. In the absence of sufficient ground motion records across the Pasco basin, additional evaluation with two- or three-dimensional models would be necessary to indicate the significance of ground motion effects, particularly at the basin edge.

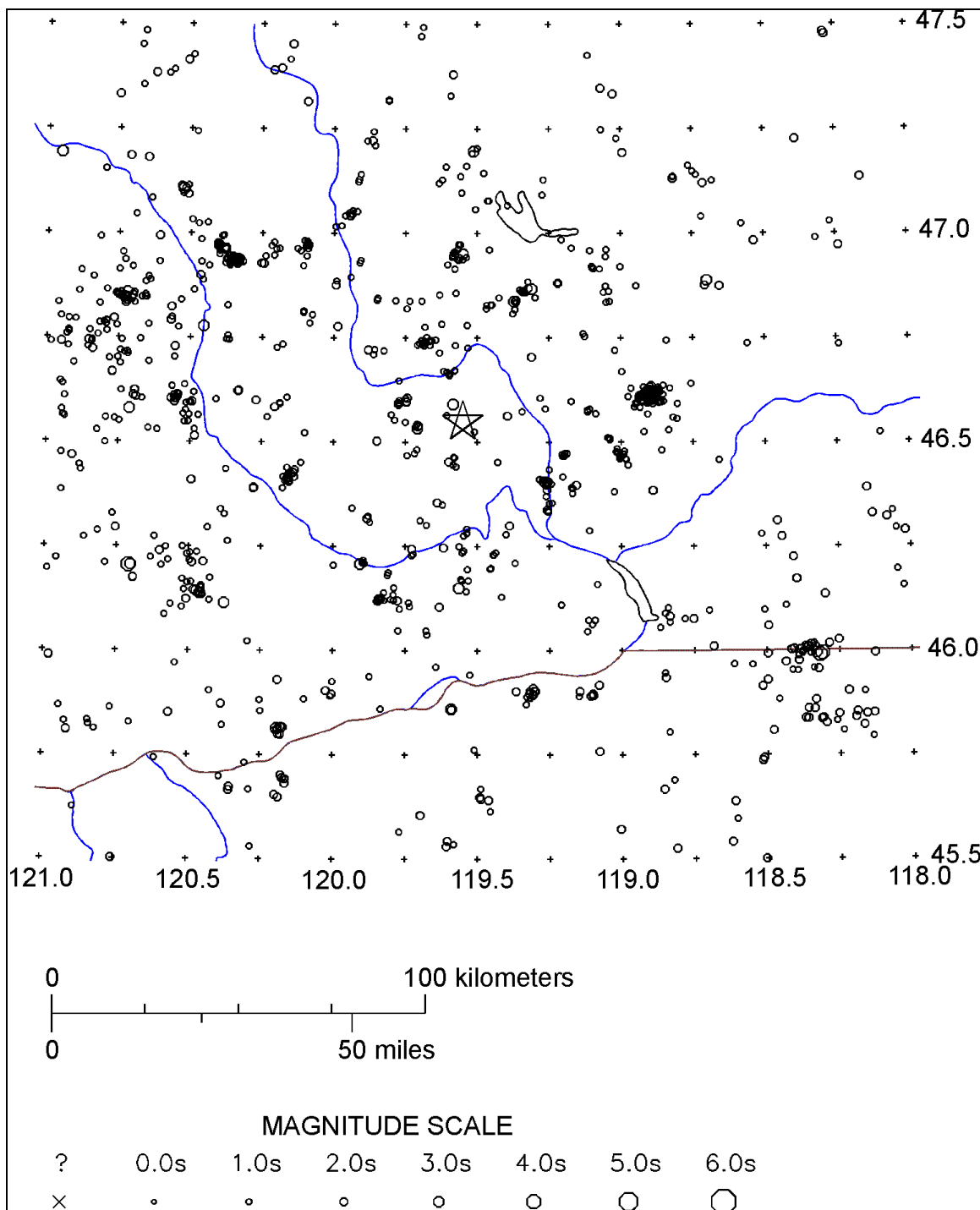
Because of its location is near the center of the Pasco Basin and because the Pasco Basin is very shallow, we believe that specific modifications by the Pasco Basin to the ground motions predicted in the Geomatrix (1996b) report will not be significant.

Figure 4-1. Plot of Earthquake Epicenters from Geomatrix (1996b, Figure 3-1){ TC "4-1. Plot of Earthquake Epicenters from Geomatrix " \f F }



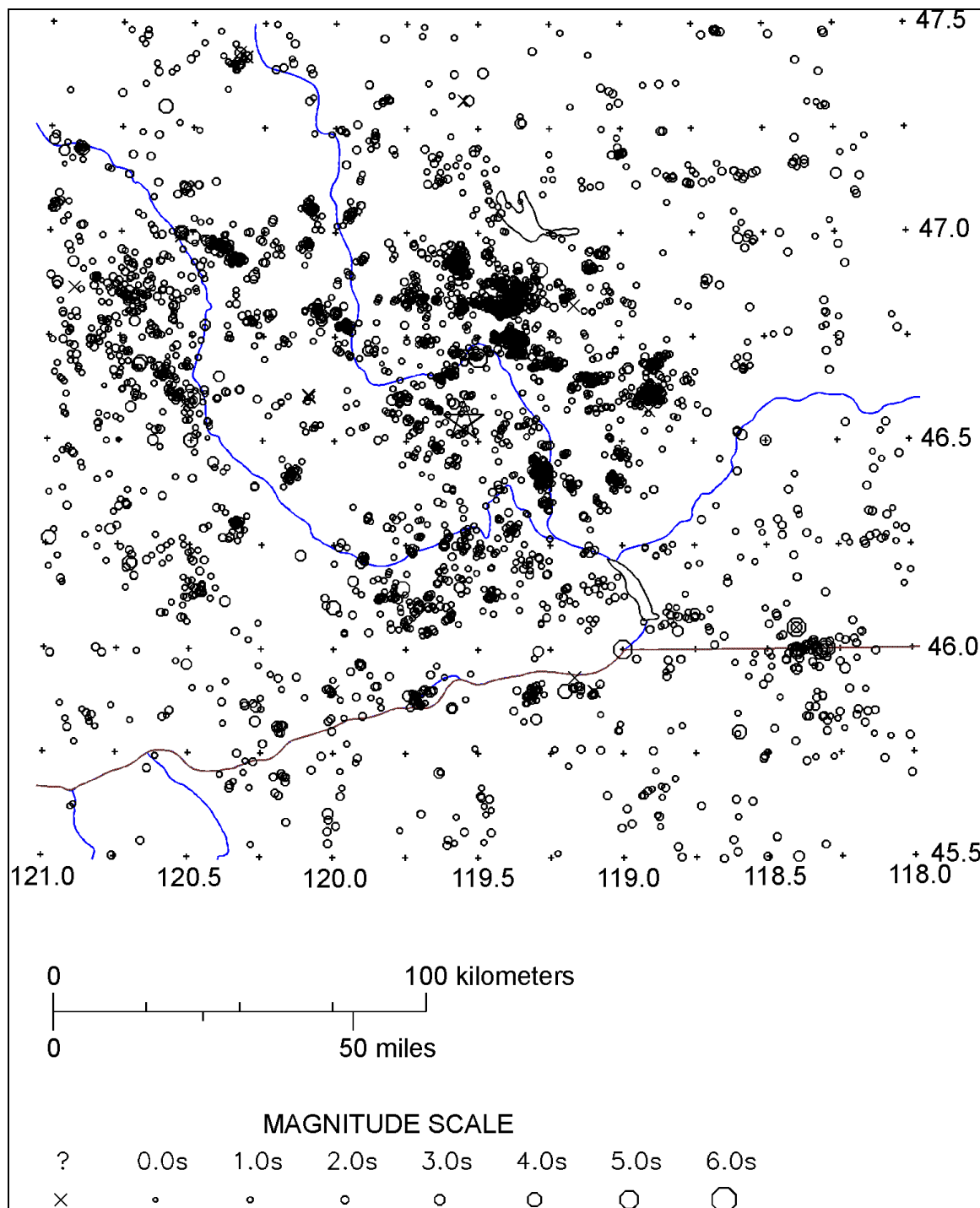
Catalog, obtained from Geomatrix (Youngs, per. comm., 1999), covers through early March 1991. Star indicates the location of 200 East Area.

Figure 4-2. Plot of Earthquake Epicenters from CNSS, Covering the Time Period of Early March 1991 to Late December 1998



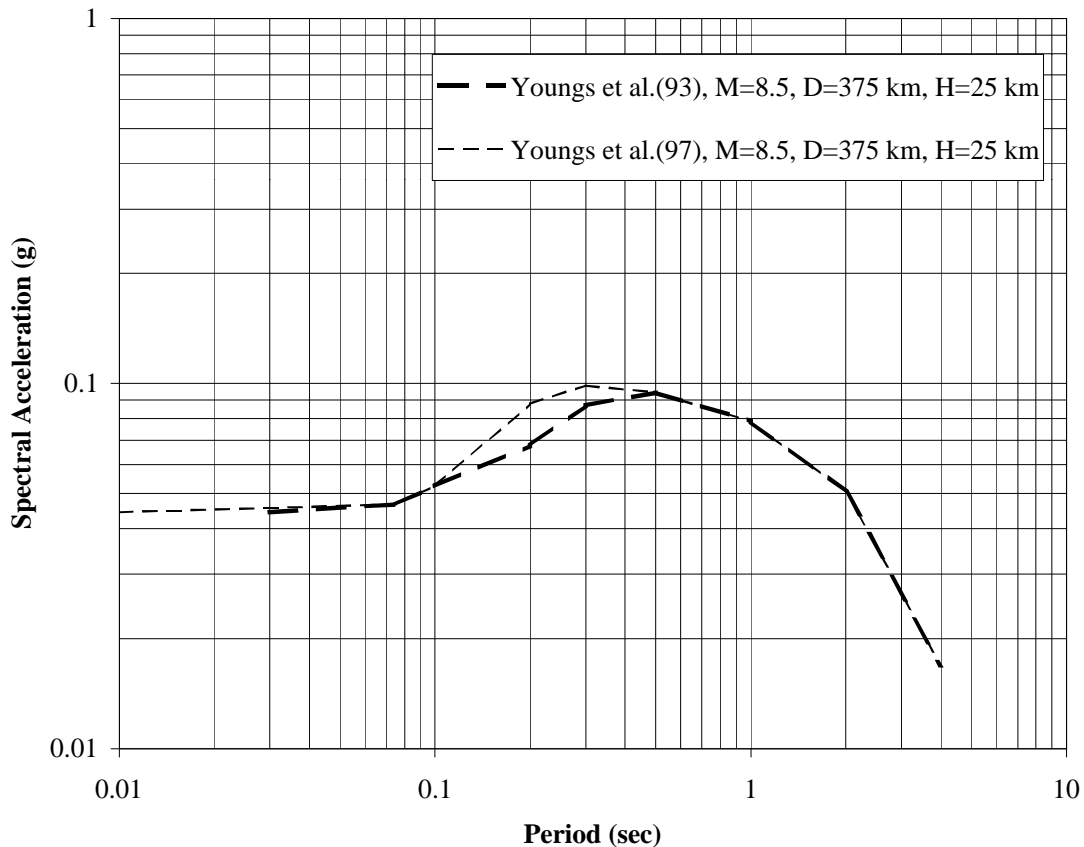
Star indicates the location of 200 East Area.

Figure 4-3. Plot of Earthquake Epicenters from 1850 to December 1998, a Composite of Figures 4-1 and 4-2{ TC "4-3. Plot of Earthquake Epicenters from 1850 to December 1998, a Composite of Figures 4-1 and 4-2" \f F }



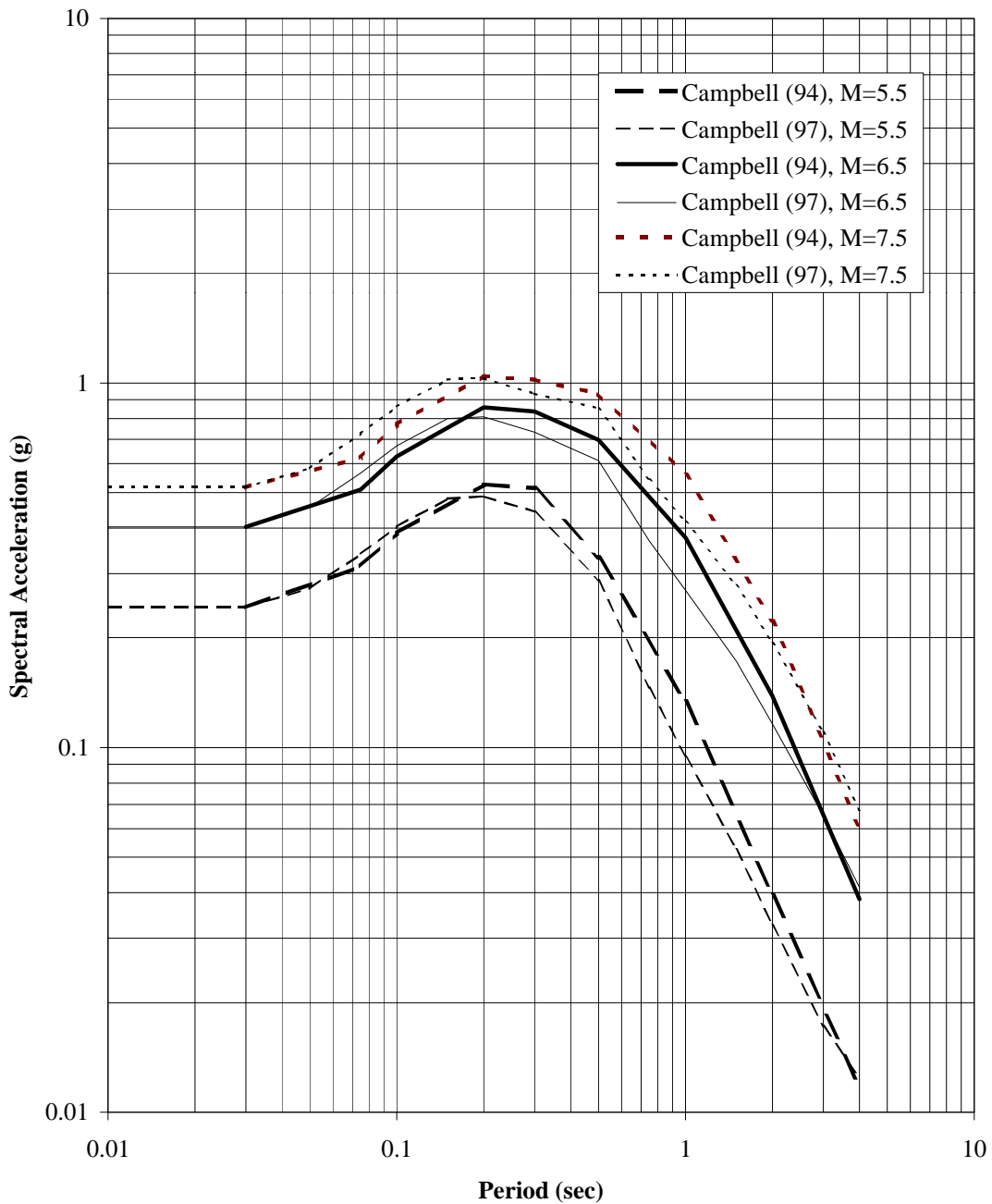
Star indicates the location of 200 East Area.

Figure 4-4. Comparison of Predicted Response Spectra Amplitudes Between Youngs et al. (1993) and Youngs et al. (1997) for a Magnitude 8.5 Earthquake on the Cascadia Subduction Zone Interface Boundary at a Distance of 375 km{ TC "4-4. Comparison of Predicted Response Spectra Amplitudes Between Youngs et al. (1993) and Youngs et al. (1997) for a Magnitude 8.5 Earthquake on the Cascadia Subduction Zone Interface Boundary at a Distance of 375 km" \f F }



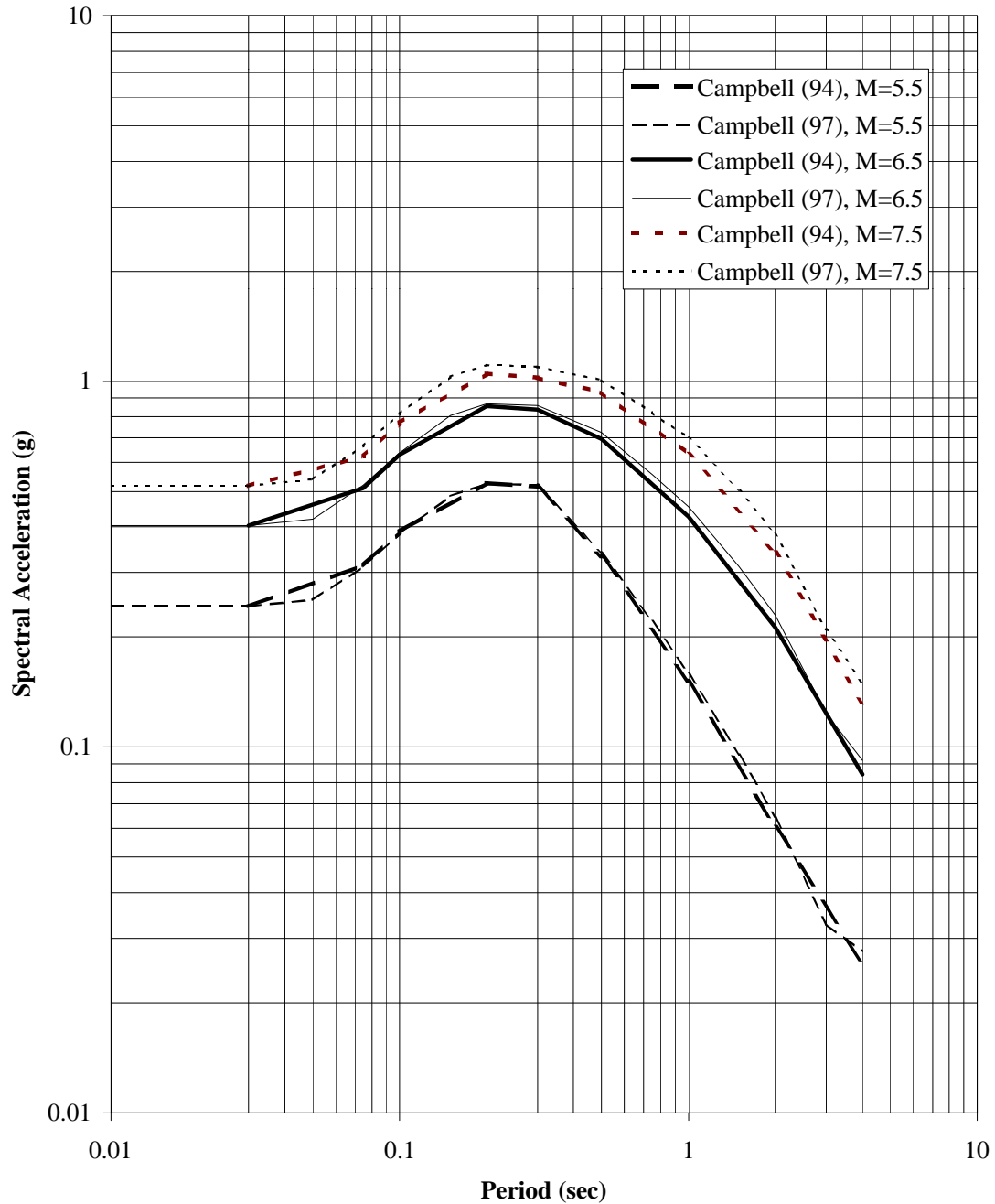
This comparison assumes depth of earthquake source of 25 km. The newer Youngs et al. values are up to about 30% higher in the 0.1-0.5 sec range, and are identical to the old Youngs et al. values outside this range. Uncertainty (sigma) values are also identical for both relationships.

Figure 4-5a. Comparison of Predicted Response Spectra Amplitudes Between Campbell (1994) and Campbell (1997)
TC "4-5. Comparison of Predicted Response Spectra Amplitudes Between Campbell (1994) and Campbell (1997)"



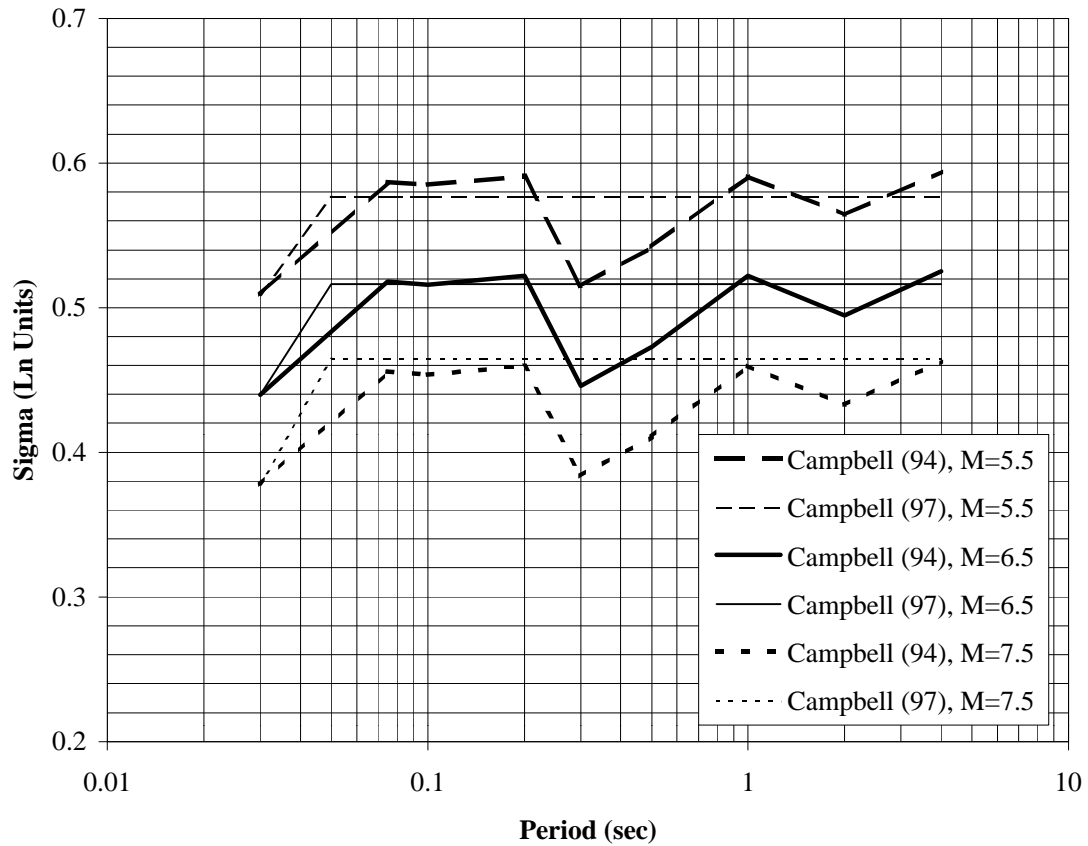
This comparison assumes distance to earthquake source of 10 km, a depth to basement of 0.6 km, and three magnitudes, 5.5, 6.5, and 7.5. The newer Campbell values are very similar to the old.

Figure 4-5b. Comparison of Predicted Response Spectra Amplitudes Between Campbell (1994) and Campbell (1997)



This comparison assumes distance to earthquake source of 10 km, a depth to basement of 8.0 km, and three magnitudes, 5.5, 6.5, and 7.5. The newer Campbell values are very similar to the old.

Figure 4-6. Comparison of Predicted Attenuation Uncertainties Between Campbell (1994) and Campbell (1997)
 TC "4-6. Comparison of Predicted Attenuation
 Uncertainties Between Campbell (1994) and Campbell (1997)" {f F }



This comparison assumes distance to earthquake source of 10 km, a depth to basement of 0.6 km, and three magnitudes, 5.5, 6.5, and 7.5. The newer Campbell values generally envelope the older uncertainties with uniform values for periods longer than 0.05 s.

5. Confirmatory Analyses

The Geomatrix (1996b) analysis of earthquake ground motion hazard for the Hanford Site is detailed and complex, and many of the Geomatrix computational algorithms are internal and proprietary. The hazard estimates derived by Geomatrix are the weighted sums of many thousands of hazard curves computed from many hundreds of input assumptions. No attempt has been made to reproduce the entire computational content of the report. Nevertheless, detailed analysis within the Geomatrix report of the relative contribution to total hazard from various sources shows that substantial portions of seismic hazard come from a relatively few modeled sources. For these selected sources, we have attempted to reproduce the Geomatrix results using a completely independent analytical algorithm to test our ability to reproduce the outcome for the model input adopted. Along the way, we have gained a fuller understanding of the mechanics of the Geomatrix hazard model and of the place within these mechanics of many of the input parameters used. The results of our confirmatory analyses are summarized in this chapter.

5.1. Site Soil Column Amplification

As discussed in Chapter 3.0, earthquake ground motions at the Department of Energy Hanford Site were computed by Geomatrix (1996b) using generally accepted, well known and still current empirical attenuation relationships. These relationships were formulated using available earthquake records substantially from California alluvial sites.

In the review of the Revision 0 of Geomatrix report (Geomatrix, 1993) a question was raised (Bandyopadhyay, 1994) about the applicability of the soils data typical of California sites to the Hanford Site. In response to this question, a comprehensive site response analyses was performed by Geomatrix. A summary of the results and the conclusions of that study are presented in Appendix A of the Geomatrix Revision 1A report (Geomatrix, 1996b). The study concludes that the empirical strong motion data from firm alluvial sites in California were appropriate for use at Hanford. In the follow up review of the Geomatrix report the review board (Costantino, 1994) concluded that there is no significant concern with the Geomatrix conclusion on the use of generic deep soil empirical attenuation relationships based on California data and that the average California model is appropriate for comparison with the Hanford Site.

In spite of the resolution reached on the applicability of the empirical relationships to Hanford sites, as part of this independent validation study, a task was identified to review the calculations supporting Appendix A and to make the following assessments:

- Assess the approach and the methodology for site response analysis adopted in the Geomatrix report for the purpose of comparison of ground motion amplification.
- Validate independently the accuracy of the computations performed in the report
- Review the supporting calculation in detail and evaluate the soil column properties in the models used for 200 East Area in terms of dynamic soil properties, soil column natural frequencies before and during earthquakes and adherence to DOE standards particularly in terms of limitation of soil material damping.

5.1.1. Approach / Methodology

The approach used in Appendix A of Geomatrix, 1996b, is to compute and compare the soil column amplification at the Hanford sites to those of typical California alluvial sites in terms of spectral acceleration ratios for a wide range of frequencies. The soil column amplifications were obtained by Geomatrix using a Geomatrix-modified version of the original computer program SHAKE, which is widely used for ground response analysis. Detail of the analysis follows.

5.1.1.1. Selection of Representative Earthquake Records

Geomatrix selected a total of eight rock acceleration time histories recorded at epicentral distances up to 14 km from earthquakes with magnitude 6 were selected (Geomatrix, 1996b, Appendix A, Table A-2). Earthquakes of this size and distance contribute most to the seismic hazard on the Hanford Site in the short to intermediate period range of ground motion. The records were uniformly scaled to peak rock accelerations of 0.25g and 0.35g, the expected peak rock acceleration at the Hanford site for motions with the return periods in the range of 1000 to 10,000 years. For the subduction zone events, a total of four rock acceleration time histories from the earthquake magnitudes in the range of 8 to 8.5 were selected (Geomatrix, 1996b, Appendix A, Table A-2). Recognizing the long distance from the Cascadia subduction zone to the Hanford Site, the rock acceleration time histories were uniformly scaled such that the acceleration spectral values at long periods (the period in the range of 1 to 2 sec) matched those expected at Hanford using the empirical attenuation relationships for subduction zone events (Geomatrix, 1996b, Appendix A, Figure A-14). Such scaling of the subduction zone records resulted in peak rock acceleration values in the range of 0.15g to 0.20g depending on the record.

5.1.1.2. Deconvolution Analysis Through California Rock Profiles

Two rock profiles were selected by Geomatrix to represent California shallow crustal conditions for Northern and Southern California from the suite of rock velocity profiles reported in the literature. For Northern California, the rock velocity profile reported by Wald et al. (1991) for the Loma Prieta study was used. For Southern California, the profile used by Magistrale et al. (1992) for the Los Angeles basin was adopted. The two rock velocity profiles were compared with the average rock velocity profile for the Hanford Site reported by Glover (1985) (see Geomatrix, 1996b, Appendix A, Figure A-11). All three profiles approach a common shear wave velocity of about 3 km/sec at a depth of approximately 3 km. Based on this observation the twelve scaled rock acceleration time histories described above were deconvolved through the two California rock profiles to a depth of 3 km using SHAKE. The rock properties were modeled as linear elastic materials with the shear wave velocities shown in Geomatrix Figure A-11. The results of these analyses in terms of outcrop response acceleration time histories at the depth of 3 km were saved for subsequent soil column analysis to assess soil column amplification for both the Hanford and California sites. Use of the outcrop response motions at the depth of 3 km was considered appropriate as input to the subsequent soil column amplification analysis due to the common velocity of rock profiles at this depth.

5.1.1.3. Soil Amplification Analysis for Hanford Sites

Based on the available information and reported velocity profiles for various projects at the Hanford Site, two composite soil-rock velocity profiles were selected for the 200 East Area. The first profile was designated "H1 + basalt" (see Geomatrix, 1996b, Appendix A, Figure A-6). The velocity profile at the depth of 4000 ft is extended uniformly to the depth of 3 km (2 mi) so that the outcrop response motions at the depth of 3 km could be used as input in the composite soil-rock profile. The second composite profile

is similar to the “H1 + basalt” profile except that the velocity in the upper 100 ft was modified using the most recent velocity measurement by Shannon & Wilson (1994). All combined, the two composite soil-rock profiles for 200 East Area were each subjected to twenty-four outcrop response motions at the depth of 3 km resulting in total of 48 response motions at the ground surface level. For the purpose of this validation report, the results corresponding to the composite “H1 + basalt” profile are discussed and the intermediate solutions are presented below.

5.1.1.4. Soil Amplification Analysis for California Deep Soil Profiles

Two velocity profiles to a depth of 500 ft were selected by Geomatrix to represent typical California deep alluvial sites. The two velocity profiles were developed based on the available information at the sites of the recording stations whose records were used to formulate the attenuation relationships and the follow up study by Pacific Engineering to characterize California alluvial site conditions. The two velocity profiles (labeled as generic S2 and generic deep soil) are compared with the H1 velocity profiles for the 200 East Area in Geomatrix (1996b) Figure A-9 indicating a stiffer site condition at Hanford. The two California soil profiles were combined with the two California crustal rock profiles (described above) resulting in four composite soil-rock profiles which were used in the soil amplification analysis.

The input motion for each soil column analysis was the outcrop response motion obtained from the respective deconvolution analysis through the California rock profiles as described above. Consistent with the deconvolution analysis, the input motion was specified as outcrop motion at the depth of 3 km in the composite soil-rock profiles. The response motions obtained from deconvolution analysis of Northern California rock profile (total of twelve response motions) were subsequently used in the site amplification analysis of the two composite profiles with the Northern California rock resulting in a set of twenty-four response motions at the ground surface level. Similarly, the composite profiles with the Southern California crustal rock were analyzed resulting in the second set of twenty-four response motions at the ground surface level.

5.1.1.5. Calculation of Acceleration Response Spectra and Spectral Ratios

Acceleration response spectra (ARS) for all ground surface time histories (both Hanford and California sites) were calculated by Geomatrix at 5% damping value. At each frequency, a spectral ratio (SR) was calculated by dividing the respective spectral value obtained from the analysis of the Hanford profile by that of the California profile. The spectral ratios were grouped together to show the effect of a variation on a specific soil property and to have common input motion. The geometric mean of each group was calculated and compared with those of other groups. For example, Figure A-18 in Appendix A (Geomatrix, 1996b) shows the average spectral ratios between the responses of “H1 + basalt” profile in 200 East Area to the composite “generic soil + Northern California rock” profile. The effects of crustal versus subduction earthquakes and the intensity of the input peak rock acceleration (0.25g versus 0.35g) on the response ratios are depicted in this figure.

5.1.2. Validation of Calculations

The SHAKE runs performed for the Geomatrix report were carried out using a Geomatrix-modified version of the original SHAKE program. To provide an independent validation of the results, we requested and obtained the original SHAKE input files, acceleration time histories, and output files, as well as the corresponding calculated ARS and SR files from Geomatrix. Selected cases in the response analyses for the 200 East Area (H1 + basalt) and for the generic deep soil for California were randomly chosen and analyzed independently using the Bechtel/BNFL in-house validated version of SHAKE (Idriss

and Sun, 1992). The results were then compared with the original SHAKE output provided by Geomatrix. Comparison of the two sets of results indicates that the differences in the output are negligible. All results differ only in the third or fourth significant digit in all cases. It can be concluded that the soil column analysis results reported by Geomatrix are consistent with the results we obtained using the most recent and validated version of SHAKE.

In the original Geomatrix report, the calculation of the response spectra for all SHAKE response motions was carried out by an in-house developed code. The spectral calculation was also validated using the Bechtel/BNFL Computer Program MICROSPEC, which is the Bechtel validated computer program for use in nuclear projects. The spectral values from the Geomatrix report were compared with the spectral values calculated by MICROSPEC at the same 91 frequency points. It was found that the two sets of spectral values were practically identical.

5.1.3. Assessment of the Results

In order to validate the consistency of the SHAKE models with the DOE requirements applicable to soil column analysis, intermediate solutions obtained from the Geomatrix SHAKE analyses were examined. The results shown correspond to the “H1 + basalt” composite profile for the 200 East Area.

Figure 5-1 shows the lower bound, average and upper bound of G/G_{\max} distributions in the soil profile for the crustal and subduction earthquakes, respectively, where G_{\max} is the initial shear modulus of the soil layer before earthquake shaking, and G is the strain-compatible shear modulus of the layer during shaking. The distributions for the crustal earthquakes are summarized from sixteen cases (composite “H1 + basalt” profile using sixteen time histories from rock deconvolution analyses), and the distributions for the subduction earthquakes are summarized from eight cases (composite “H1 + basalt” using eight time histories from rock deconvolution analyses). It can be seen from this figure that degradation of soil shear modulus is moderate in the profile in all cases. Maximum modulus degradation is only about 35% for the crustal earthquakes, and 30% for the subduction earthquakes. As expected, the effect of soil nonlinearity is small. This observation can be confirmed by examining the effective shear strain as shown in Figure 5-2. The maximum effective shear strain amplitude is 0.05% for crustal earthquakes and 0.03% for subduction earthquakes.

To examine the soil column frequencies, the initial and the strain-compatible shear wave velocity (V_s) profiles were obtained as depicted in Figure 5-3. For this plot, all strain-compatible shear wave velocity profiles for crustal earthquakes are grouped together (total of sixteen runs) and the average velocity profile is obtained. The average shear wave velocity profile from the subduction earthquakes (total of eight runs) is computed similarly. As shown in Figure 5-3, the strain-compatible velocity profile for the crustal earthquakes is slightly smaller than the one obtained from the subduction earthquakes. However, both profiles remain close to the initial profile due to small soil nonlinear effects. Using the strain-compatible velocity profiles, the predominant period of the site was computed. The site period prior to earthquake shaking is approximately 0.95 sec for the initial velocity profile, 1.03 sec for the profile during subduction earthquakes, and 1.06 sec for the profile during crustal earthquakes.

The results in terms of damping ratios were also grouped and the lower bound, average, and the upper bound of each group are shown in Figure 5-4. The maximum soil damping ratio is about 0.06 (or 6%) which is much less than the bounding value of 15% specified in the DOE standards.

In addition to the cases described above, the Geomatrix study includes parametric and sensitivity studies for various soil and rock properties including damping ratio in the rock, density of the rock, and the

intensity of the input motion. The studies confirmed that, within the expected range of soil and rock properties and intensity of the input motion, the spectral ratios between the Hanford sites and the California sites do not change significantly and are not sensitive to a specific parameter.

Appendix A of the Geomatrix report concludes that the range of variation in the ground motions between the Hanford and California sites are within the range of variation of the ground motion predicted by the adopted empirical attenuation relationships. Therefore, use of the California-based attenuation relationships is considered appropriate to develop ground motion at the Hanford sites.

Our independent evaluation of the study confirms that the approach used in Appendix A of Geomatrix (1996b) is valid and the methodology employed remains as the current industry practice for ground response analysis. Moreover, our independent validation of selected cases confirms the accuracy of the computations performed as part of the Geomatrix study. Based on these evaluations and reasonableness of the intermediate responses of the ground response analyses and compliance with the current DOE standards for such analyses, results of Appendix A study is considered valid.

5.2. Hazard from Selected Sources

To validate the computational methodology used in the Geomatrix (1996b) report and to broaden our understanding of how each earthquake source model parameter had been specified, we undertook to perform independent calculations of the Geomatrix results for selected sources using an independent, commercially available earthquake hazard analysis computer code - EZ-Frisk™ (Risk Engineering Inc. 1998).

The elements of any probabilistic characterization of earthquake strong ground motion shaking hazard are the same for any analysis methodology. These elements are the specification of expected future seismicity by using a combination of seismic, geologic, and tectonic information.

EZ-Frisk™ is an evolutionary descendant of a methodology first popularized by the work of Cornell (see for example, Cornell, 1968; Cornell and Van Marcke, 1969; McGuire, 1976). In this methodology, earthquake sources are specified that are reasonable geometric models of faults or areas with fairly consistent and definable earthquake recurrence and maximum magnitude properties. A seismic source is most often considered a homogenous group of point sources, where earthquakes are assumed to occur with equal likelihood at any location. For each source zone, a recurrence relation is defined that is the expected frequency distribution of different size earthquakes over some length of time. Most commonly (Gutenberg and Richter, 1944) the frequency distribution is defined by a log-linear function of the cumulative annual number of earthquakes, N , as a function of magnitude, M . Cataloged historical and instrumental seismicity, as well as geologic and geodetic data, are generally used to establish the maximum magnitude that a source zone is capable of attaining, as well as an estimate of a representative focal depth of the seismic activity. Earthquake sources may also be treated as faults on which rupture occurs over a finite planar surface. Because many strong ground motion attenuation relations are defined in terms of distance to zone of energy release, the treatment of a source as a plane rather than a point will increase the hazard estimate of locations near faults.

It is clear from even the summary discussion of Chapter 3.0 of this report that the Geomatrix (1996b) model is complex in order to comprehensively incorporate all identified sources of uncertainty. This complexity is manifested both in the variety of alternative input parameters considered (for example, the Umtanum-Gable Mountain crustal source has 1,224 different branches to its logic tree) and in the forms required for various input parameters (for example, nonstandard characterization of earthquake recurrence

statistics and source geometries). Many of the second type of complexity required us to improvise unconventional work-arounds to EZ-Frisk™ input values (these are specified as appropriate below).

5.2.1. Yakima Fold Belt Faults

Two Yakima Fold Belt seismic sources were selected for confirmation analysis based on their relative contributions to the total Yakima Folds seismic hazard (see Geomatrix, 1996b Figure 5-4b). For shorter period ground motions (peak ground acceleration and $T=0.3$ sec) the Umtanum-Gable Mountain fold source is the major contributing Yakima Fold source. For $T=2.0$ sec both the Umtanum-Gable Mountain and Saddle Mountains fold sources contribute about the same amount to the total Yakima Fold hazard over the return period range of interest. Hazard curves for both sources were computed for peak ground acceleration and spectral acceleration periods of 0.3 and 2.0 sec.

The seismic hazard curves were computed using EZ-Frisk™ (Risk Engineering Inc., 1998) a commercially available software program for computing seismic hazard curves. Individual fault files, each corresponding to a single branch of the logic tree shown in Figure 3-10 (Geomatrix, 1996), were generated for use with EZ-Frisk™. The corresponding weight for each hazard fault run (that is, branch of the logic tree) was applied as a post-process procedure outside of EZ-Frisk™. There are a total of 1,224 individual branches of the logic tree for the Umtanum-Gable Mountain case and 900 branches for the Saddle Mountains case.

The fault geometries and segmentations were provided by Geomatrix (Youngs, 1999 personnel communication) for the Saddle Mountains and Umtanum-Gable Mountain fault sources. The probability of activity for the Umtanum-Gable Mountain and Saddle Mountains sources were 0.25 and 0.5, respectively, and the probability of coupling was 0.15 and 0.60, respectively. Each source had a probability of segmentation of 0.6. Three dip angles of 30, 45, and 60 degrees were modeled with weights of 0.2, 0.4, and 0.4 (Umtanum-Gable Mountain) or 0.1, 0.3, and 0.6 (Saddle Mountains). The corresponding maximum magnitudes and slip rates for each case were taken from Tables 3-2, 3-3, and 3-4 of the Geomatrix (1996b) report. Three b-values of 0.82, 0.99, and 1.16 were used in the hazard analysis with weights of 0.2, 0.6, and 0.2, respectively.

The Geomatrix (1996b) hazard analysis used both the characteristic and modified exponential magnitude recurrence distribution models for the Yakima Fold sources. Unfortunately, EZ-Frisk™ is not able to use directly the modified exponential magnitude recurrence model. A close approximation to the modified exponential recurrence model was developed (Youngs, 1999 personnel communication) by estimating the activity rate based on the exponential recurrence model of Youngs and Coppersmith (1985) and then increasing the maximum magnitude by 0.25 magnitude units. A comparison between the modified exponential and the exponential magnitude recurrence relationships is shown in Figure 2-2 of the Geomatrix (1996b) report. For the characteristic model faults, the assigned slip rates were converted to activity rates based on the Youngs and Coppersmith (1985) characteristic earthquake recurrence model. The characteristic model was assigned a weight of 0.8 (that is, modified exponential model assigned a weight of 0.2) for the coupled cases, and 0.5 (that is, modified exponential model assigned a weight of 0.5) for the uncoupled cases.

The four crustal attenuation relationships for soil site conditions that were used in the Geomatrix (1996b) analysis (see Section 3.1) were used in the EZ-Frisk™ hazard analysis for both the Umtanum-Gable Mountain and Saddle Mountains cases. The two Campbell and Bozorgnia (1994) attenuation models (depth to basement rock of 0.6 and 8.0 km) were given a weight of 0.125 each as was done in Geomatrix (1996b). The other three attenuation relationships were each assigned a weight of 0.25. The sigma value

for each attenuation relationship was truncated at a value of three sigma (Geomatrix, 1996b). For both the Geomatrix (1996b) and EZ-Frisk™ hazard runs the lower magnitude limit was 5.0 for both cases with a magnitude integration step size of 0.25 magnitude units.

One difference between the Geomatrix (1996b) analysis and the current EZ-Frisk™ analysis is in the way the area magnitude relationship is modeled. For the Geomatrix (1996b) hazard curves the following area magnitude relationship was used:

$$\ln (\text{Area}) = -7.119 + 2 M$$

where Area is the area of the fault plane that is assumed to rupture in an earthquake of moment magnitude M. The area of the fault plane is further constrained to have an aspect ratio (defined as the fault length divided by the fault width) of one for a magnitude 4 and 2 for a magnitude 7. For magnitudes between 4 and 7 the aspect ratio increases linearly between values of 1 and 2. For magnitudes greater than 7, the aspect ratio function increases with the same slope (Youngs, 1999 personnel communication).

EZ-Frisk™ assumes a square rupture area (fault length equals fault width) until the minimum fault dimension (either fault width or length for a particular fault segment) is reached and thus does not allow for a completely equivalent modeling of the Geomatrix parameters. The corresponding fault length magnitude relationship used in EZ-Frisk™ can be developed from the Geomatrix equation above by setting the rupture length equal to the rupture width,

$$\text{Log}_{10}(L) = \text{Log}_{10}(W) = -1.5459 + 0.434M$$

and converting from natural log units to log base 10 units. For both the Geomatrix (1996b) and EZ-Frisk™ computations, the single mean estimate of rupture area and fault length was used (that is, sigma is zero for both equations above).

Both the Umtanum-Gable Mountain and Saddle Mountains fold fault sources contain five separate fault segments (see Table 3-2 and 3-3 of the Geomatrix, 1996b report). However, two source models for the Umtanum East were used in the Geomatrix (1996b) analysis. Estimate A was assigned a weight of 0.7 and estimate B was assigned a weight of 0.3. All of the other segments were assigned a weight of unity because the fault is either modeled as a segmented fault with all of the segments rupturing or an unsegmented fault (see the logic tree from Figure 3-10 of the Geomatrix, 1996b report).

The total hazard curve for the Umtanum-Gable Mountain fold source consists of 1,224 individual fault sources. A comparison between the EZ-Frisk™ validation and Geomatrix (1996b) hazard curves is shown in Figure 5-5. The Geomatrix (1996b) curves are shown in heavy lines while the EZ-Frisk™ hazard curves are plotted with thin lines. The agreement between the suites of hazard curves is reasonable but not perfect.

The ground motion values and per cent match between the EZ-Frisk™ and Geomatrix hazard curves are listed in Table 5-1. In this table the “hazard level” of the “Geomatrix Target” columns is the annual probability of exceedance contributed by the source to the total probability of exceedance from all sources at the specified “Accel. (g)” level. That is for example, although the total annual probability of exceedance for the 2,000-year acceleration of 0.237 g is, by definition, 5.0×10^{-4} (1/2,000), the contributions from the Umtanum-Gable Mountain and Saddle Mountains sources are 1.32×10^{-4} and 4.92×10^{-5} , respectively. Comparisons of “BNFL” fits are made both with respect to predicted annual probability for the 0.237 acceleration and with respect to acceleration for the 1.32×10^{-4} hazard.

For PGA the EZ-Frisk™ curves are slightly higher than the Geomatrix curves (by 2-5% at the 2,000 and 10,000 year return period). For the T=0.3 and T=2.0 sec, the EZ-Frisk™ curves are lower than the Geomatrix curves by approximately 7-17% at the 2,000 and 10,000 year return period. The ground motion levels and percentage level of agreement between the hazard curves are summarized in Table 5-1. A possible explanation for the differences between the two sets of hazard curves could be in the inability of EZ-Frisk™ to model the aspect ratio relationship. This difference would affect the longer period hazard curves more than the PGA and T=0.3 sec as will be discussed below for the Saddle Mountains case.

A total of 900 individual faults (logic tree branches) were generated for the Saddle Mountains fold source hazard analysis. Figure 5-6 shows a summary of the six hazard curves for the Saddle Mountains fold source. For both the PGA and T=0.3 sec case, the two sets of hazard curves are nearly identical. However, for the longer period, T=2.0 sec case, the EZ-Frisk™ hazard curve is approximately 20-35% lower than the Geomatrix (1996b) hazard curve. A possible explanation of the lower hazard curve for the EZ-Frisk™ case is, again, the failure of the program to accurately model the aspect ratio relationship for the magnitude fault length model that was used in the Geomatrix (1996b) analysis. The contribution to the T=2.0 sec hazard curve is from larger magnitude events, relative to the contribution to the hazard for the shorter period T=0.3 and PGA hazard curves (as an example see Figure 5-2b of the Geomatrix 1996b report). The inability of EZ-Frisk™ program to model the Geomatrix report's aspect ratio relationship will have the greatest effect on hazard curves that are controlled by larger magnitude events (that is, $M > 6$). For larger magnitude events, the inclusion of the aspect ratio relationship will generally result in longer shallow rupture segments whose closest approach to a site within the Yakima Fold Belt will generally be less than shorter, wider fault segments. The hazard curves estimated using these generally closer faults would be greater because the median ground motion would be greater based on the closer distance. For the Saddle Mountains case, the PGA and T=0.3 sec curves are controlled by the smaller magnitude 5 to 6 range events and show good agreement, while the T=2.0 sec case is controlled by larger magnitude range events and is lower than the Geomatrix (1996b) hazard curve. The ground motion levels and percentage level of agreement between the hazard curves are listed in Table 5-1 for the Saddle Mountains source.

5.2.2. Deep Crystalline Crust

Three tectonic fault sources were developed by Geomatrix to model the deeper seismicity (depths between 5 and 21 km) in the region: failed rift model, basement block model, and random basement model (see Section 3.2.2 above). Both the failed rift and basement block models are given low weights (0.1 each) because they do not explain the spatial pattern of the observed seismicity. A schematic logic tree indicating the input parameters for the hazard computations is shown on Figure 3-20 of the 1996b Geomatrix report.

The failed rift model is defined by either a narrow or wide rift geometry. The characteristic and modified exponential magnitude recurrence relationships were assigned weights of 0.8 and 0.2, respectively. The region located outside the narrow and wide rift models (see Figure 3-23 of the 1996b Geomatrix report) is modeled as an adjacent basement zone. This areal seismic source zone is modeled by a series of equally spaced linear faults. Each fault is assigned a dip of 60 degrees and is also used in the block tectonic and random tectonic models. The Faults A and B source model also have a dip of 60 degrees. The random tectonic model was assigned the highest weight because it models the observed seismicity which appears randomly distributed.

The four crustal attenuation relationships that were used for the Yakima Fold sources were used for the basement sources. In a similar fashion, the magnitude length relationship dependent on a linearly varying aspect ratio was used for the Geomatrix (1996b) hazard estimates. The contribution to the total hazard from the basement sources is shown in Figure 5-3b from the Geomatrix 1996 report. A sensitivity of the weighting associated with the three tectonic models is presented in the next Chapter. No independent validation of the Geomatrix computations was done for these sources.

5.2.3. Cascadia Interplate Source

The total hazard contribution for the Hanford site is shown in Figure 5-2b (Geomatrix, 1996b) for the crustal, interface, and intra-slab sources. The last two sources are associated with the Cascadia subduction zone. For peak ground acceleration and spectral response acceleration for a period of 0.3 sec, the crustal sources control the total hazard. However, for spectral response acceleration for a period of 2.0 sec, the Cascadia interface source controls the total hazard. The logic tree for the Cascadia interface hazard estimation is shown in Figure 3-28 of the 1996b Geomatrix report. The discussion of the formulation of the four individual fault models is given in Section 3.2.3 of the current report.

Each of the four fault models has a maximum length of 1,100 km. However, for the determination of activity rates and maximum magnitudes, the maximum rupture length was limited to four values of 1,100, 450, 250, and 150 km. For maximum rupture lengths of less than 1,100 km, the Cascadia interface fault source was subdivided into an Oregon segment and a Washington segment (Youngs, 1999 personnel communication). This segmentation of the fault was used to better model the changes in fault axis between the Oregon and Washington section of the subducting Juan de Fuca Plate. For the segmented cases, the activity rate of earthquakes was partitioned based on the relative lengths of each segment to the total length of 1,100 km. The Washington segment was assigned 43 percent of the activity, while the Oregon segment was assigned 57 per cent. The activity rate for the Cascadia interface source was based on a complete rupture of the entire 1,100 km fault every 450 years (Geomatrix, 1996b). The Geomatrix (1996b) report also estimates the return period for the 450 km maximum rupture length case to be 225 years. However, assuming that 2.44 events with a maximum length of 450 km is needed to completely rupture the 1,100 km long fault, the corresponding return period would be 184 years. The return periods for the shorter 250 and 150 km maximum rupture length cases are not presented in the report. An examination of the input files (Youngs, 1999 personnel communication) used in Geomatrix hazard estimation indicates that a distribution of return periods was assumed for each case in the Cascadia interface model.

Three maximum magnitude approaches (equally weighted) were used to determine the maximum magnitude for each case as listed in the logic tree for the Cascadia interface source. However, only the deformation front thermal transition zone model uses all three maximum magnitude models. For the other three geometrical models, two of the three maximum magnitude models predict similar values and have been combined into one model with a weight of 2/3 (Youngs, 1999 personnel communication). The magnitude length relationship used in the Geomatrix 1996b hazard analysis for the Cascadia interface sources is different than the relationship used for the crustal fault sources, being

$$\ln (\text{Area}) = -9.210 + 2.303 M$$

where Area is the area of the fault plane that is assumed to rupture in an earthquake of moment magnitude M. The area of the fault plane is further constrained to have an aspect ratio of one for a magnitude 4 and 2 for a magnitude 7. For magnitudes between 4 and 7 the aspect ratio increases linearly. For magnitudes greater than 7, the aspect ratio increases with the same slope (Youngs, 1999 personnel communication).

EZ-Frisk™ assumes a square rupture area (fault length equals fault width) for the earthquake and thus does not allow for the modeling of the increasing aspect ratio. The corresponding fault length magnitude relationship used in EZ-Frisk™ can be developed from the above equation by setting the rupture length equal to the rupture width, and converting from natural log units to log base 10 units yielding.

$$\text{Log}_{10}(L) = \text{Log}_{10}(W) = -2 + 0.5 M$$

For both the Geomatrix (1996b) and EZ-Frisk™ computations, the single mean estimate of rupture area and fault length was used (sigma of zero for both above equations).

Two magnitude recurrence relationship models were used for the Cascadia interface seismic source in the Geomatrix (1996b) report. The characteristic relationship was assigned a weight of 0.5. The second magnitude recurrence relationship model was based on the observed aspect ratio (that is, fault length divided by fault width) of interface earthquakes and assigned a weight of 0.5. A comparison of the characteristic and aspect ratio magnitude recurrence functions is shown in Figure 3-32 of the Geomatrix report. EZ-Frisk™ cannot easily model the aspect ratio magnitude recurrence relationship.

Three subduction based attenuation relationships were used for the Cascadia interface source (see Section 3.1 of the current report). Each attenuation relationship is truncated at three sigma. Three b-values were used in the Geomatrix 1996b hazard: 0.5, 0.6, and 0.7. The assigned weights for the three b-values listed in the logic tree (0.2, 0.6, and 0.2) for the Cascadia interface source (see Figure 3-28 of the Geomatrix 1996b report) represent rounded values. The actual values used in the hazard estimates are 0.185, 0.630, and 0.185. As was discussed earlier, the horizontal integration step was 2 km for distances of less than 200 km and 3 km for distance less than 300 km. The vertical integration step, however, was not uniformly distributed over depth as was the case for the Yakima Fold sources. A higher distribution weighting was given to the deeper portion of the fault plane model (Youngs, 1999 personnel communication). This unequal vertical integration step cannot be modeled using EZ-Frisk™.

One of the four Geomatrix geometrical models was selected to confirm the hazard curves from the Geomatrix 1996b report for the Cascadia interface source. The deformation front thermal transition zone fault model was selected as an average representation of the four Cascadia source models (see Figure 3-29 of the Geomatrix 1996b report). The weighted mean hazard curve was computed using EZ-Frisk™. Only the characteristic magnitude distribution case was computed with EZ-Frisk™. The activity rate for each fault was determined using the characteristic magnitude recurrence model of Youngs and Coppersmith (1985). The Cascadia interface source contributes to total site hazard for longer period motions. A comparison of the EZ-Frisk™ and Geomatrix hazard curves is shown in Figure 5-7 for spectral acceleration at 2.0 sec period. To make our comparison as simple as possible we asked Geomatrix to compute the equivalent hazard curve. Thus, the Geomatrix curve plotted in Figure 5-7 is for the characteristic magnitude recurrence model for the deformation front thermal transition zone fault model (Youngs, 1999 personnel communication), one of four constituent branches of the full Cascadia model logic tree in the original Geomatrix report. This model for the Cascadia fault source produces a mean hazard curve which is greater than the mean hazard curve from all four fault models. This result is expected based on the geometry of the four fault models. For the thermal boundary fault cases, the Washington segment of the fault source extends further to the east (i.e., closer to the site) than the zero isobase fault models (see Figure 3-29 of the Geomatrix, 1996b report). The ground motion values are listed in Table 5-2 for peak ground acceleration and response spectral accelerations at periods of 0.3 and 2.0 sec.

From Figure 5-7 it is seen that the EZ-Frisk™ hazard curve is slightly lower than the Geomatrix curve. The under-prediction of the EZ-Frisk™ hazard curve relative to the Geomatrix curve for the T=2.0 second spectral acceleration is similar to the under-prediction for the Saddle Mountain case for T=2.0 seconds (i.e., see Figure 5-6). A possible explanation for the lower EZ-Frisk™ hazard curve is the lack of the hazard code to model the aspect ratio relationship used in the Geomatrix (1996b) analysis.

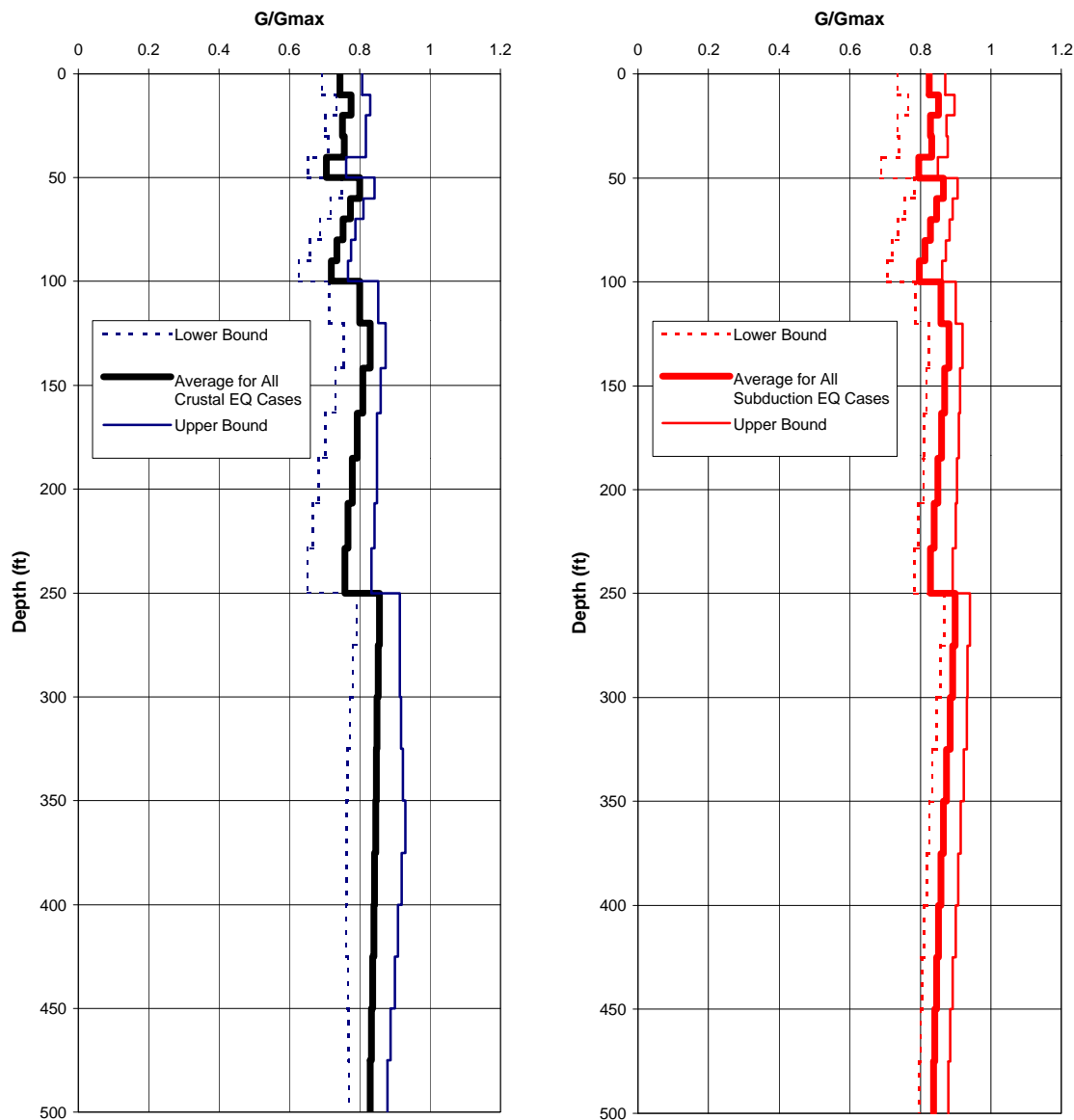
**Table 5-1. Summary of Degree-of-Fit to Geomatrix Hazard Curves{ TC "5-1.
Summary of Degree-of-Fit to Geomatrix Hazard Curves" \f T }**

Source: Umtanum-Gable Mtn.						
	2,000-year					
	Geomatrix Target		BNFL			
Ground Motion	Hazard Level	Accel.(g)	Hazard Level @ Accel.	%	Accel.(g) @ Hazard Level	%
PGA	1.32x10 ⁻⁴	0.237	1.39x10 ⁻⁴	104.8	0.216	103.7
0.3s	1.27x10 ⁻⁴	0.502	1.16x10 ⁻⁴	91.4	0.466	92.8
2.0s	4.20x10 ⁻⁵	0.127	3.51x10 ⁻⁵	83.4	0.114	89.9
	10,000-year					
	Geomatrix Target		BNFL			
Ground Motion	Hazard Level	Accel.(g)	Hazard Level @ Accel.	%	Accel.(g) @ Hazard Level	%
PGA	4.97x10 ⁻⁵	0.440	5.15x10 ⁻⁵	103.6	0.448	101.7
0.3s	4.65x10 ⁻⁵	0.974	4.11x10 ⁻⁵	88.3	0.907	93.0
2.0s	1.25x10 ⁻⁵	0.243	1.05x10 ⁻⁵	84.3	0.225	92.6
Source: Saddle Mtns.						
	2,000-year					
	Geomatrix Target		BNFL			
Ground Motion	Hazard Level	Accel.(g)	Hazard Level @ Accel.	%	Accel.(g) @ Hazard Level	%
PGA	4.92x10 ⁻⁵	0.237	4.98x10 ⁻⁵	101.3	0.238	100.5
0.3s	5.35x10 ⁻⁵	0.502	5.32x10 ⁻⁵	99.4	0.501	99.8
2.0s	2.77x10 ⁻⁵	0.127	2.05x10 ⁻⁵	73.9	0.110	86.8
	10,000-year					
	Geomatrix Target		BNFL			
Ground Motion	Hazard Level	Accel.(g)	Hazard Level @ Accel.	%	Accel.(g) @ Hazard Level	%
PGA	6.56x10 ⁻⁶	0.440	6.66x10 ⁻⁶	101.5	0.442	100.4
0.3s	8.60x10 ⁻⁶	0.974	7.82x10 ⁻⁶	90.9	0.945	97.0
2.0s	7.45x10 ⁻⁶	0.243	4.85x10 ⁻⁶	65.1	0.204	83.9

**Table 5-2. Summary of Degree-of-Fit to Geomatrix Hazard Curves{ TC "5-2.
Summary of Degree-of-Fit to Geomatrix Hazard Curves" \f T }**

Source: Cascadia Interface						
	2,000-year					
	Geomatrix Target		<u>BNFL</u>			
Ground Motion	Hazard Level	Accel.(g)	Hazard Level @ Accel.	%	Accel.(g) @ Hazard Level	%
<u>PGA</u>	9.02x10 ⁻⁵	0.237	5.02x10 ⁻⁵	55.7	0.200	84.4
0.3s	9.63x10 ⁻⁵	0.502	6.23x10 ⁻⁵	64.8	0.433	86.4
2.0s	5.05x10 ⁻⁴	0.127	3.85x10 ⁻⁴	76.4	0.113	88.6
	10,000-year					
	Geomatrix Target		<u>BNFL</u>			
Ground Motion	Hazard Level	Accel.(g)	Hazard Level @ Accel.	%	Accel.(g) @ Hazard Level	%
<u>PGA</u>	8.38x10 ⁻⁶	0.440	4.29x10 ⁻⁶	51.1	0.379	86.2
0.3s	8.65x10 ⁻⁶	0.974	5.55x10 ⁻⁶	64.1	0.870	89.3
2.0s	1.15x10 ⁻⁴	0.243	8.11x10 ⁻⁵	70.6	0.215	88.4

Figure 5-1. G/G_{max} vs. Depth Relationship during Earthquake Shaking for Hanford 200 East Area Soil Profile: "H1 + Basalt"
TC "5-1. G/G_{max} vs. Depth Relationship during Earthquake Shaking for Hanford 200 East Area Soil Profile: "H1 + Basalt"
\f F }



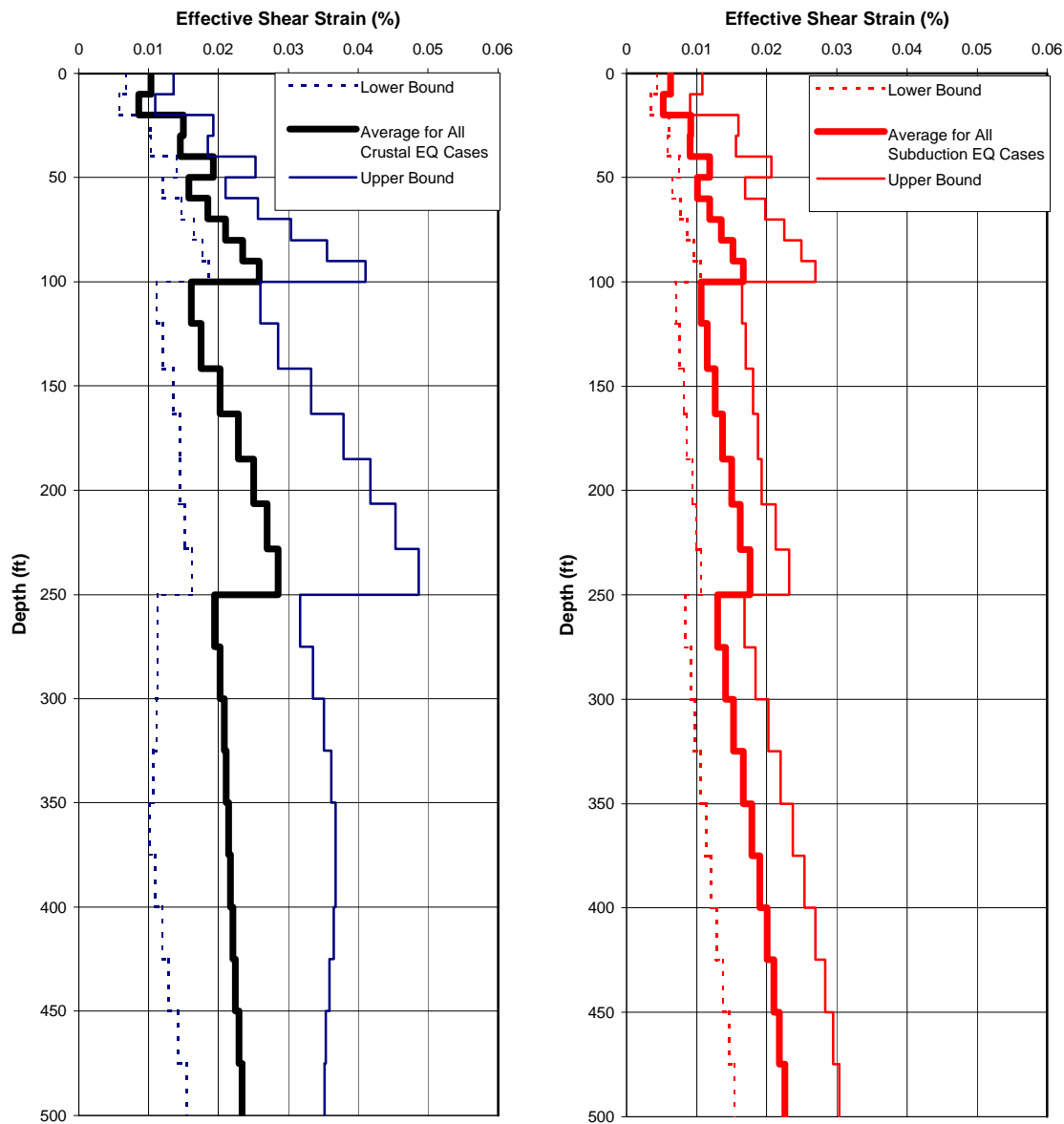
(a) For all crustal earthquake cases -
Average of sixteen runs.

(b) For all subduction earthquake cases -
Average of eight runs.

All crustal and subduction earthquake events are treated separately.

Figure 5-2. Effective Shear Strain Distribution during Earthquake Shaking for Hanford 200 East Area Soil Profile: "H1 + Basalt"
TC "5-2. Effective Shear Strain

**Distribution during Earthquake Shaking for Hanford 200 East Area Soil Profile:
'H1 + Basalt' \f F }**



(a) For all crustal earthquake cases -
Average of sixteen runs.

(b) For all subduction earthquake cases -
Average of eight runs.

All crustal and subduction earthquake events are treated separately.

**Figure 5-3. Initial and Strain-Compatible Shear-Wave Velocity Profiles for
 Hanford 200 East Area Soil Profile: "H1 + Basalt" TC "5-3. Initial and
 Strain-Compatible Shear-Wave Velocity Profiles for Hanford 200 East Area Soil
 Profile: 'H1 + Basalt'" \f F }**

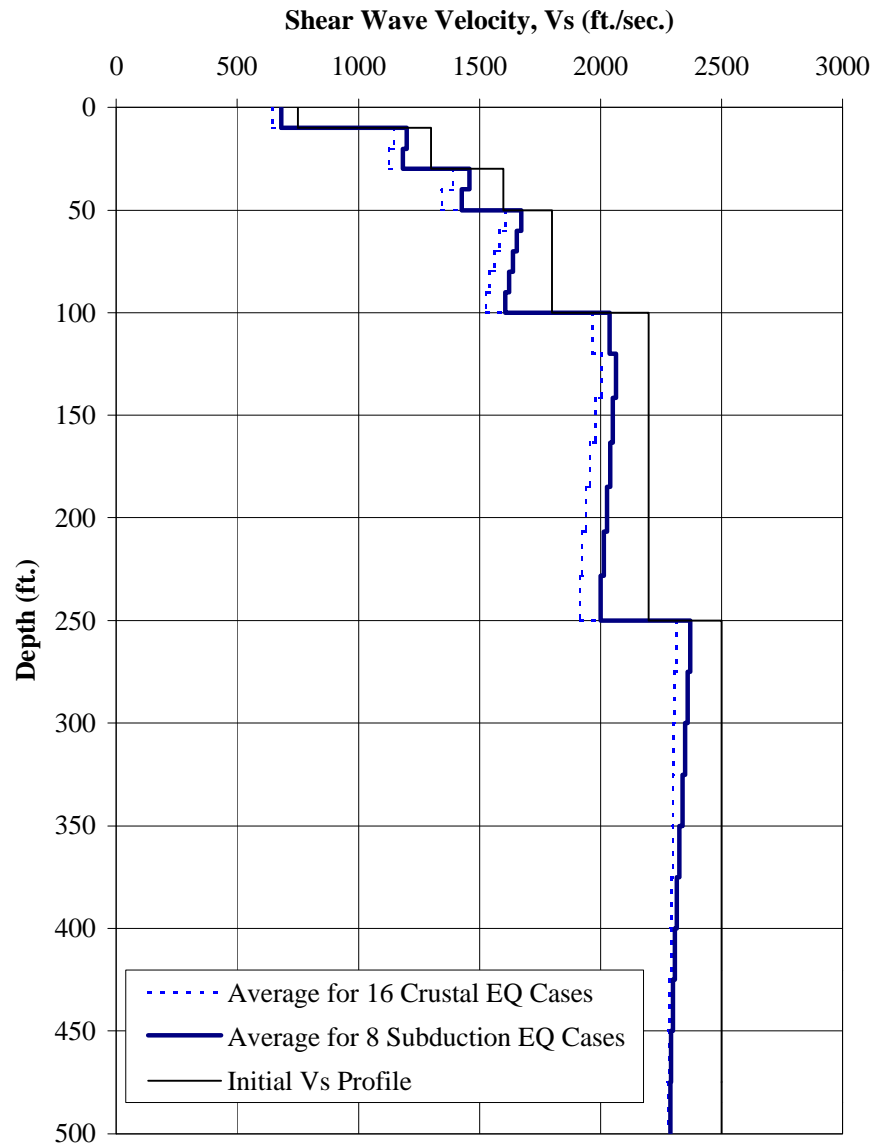
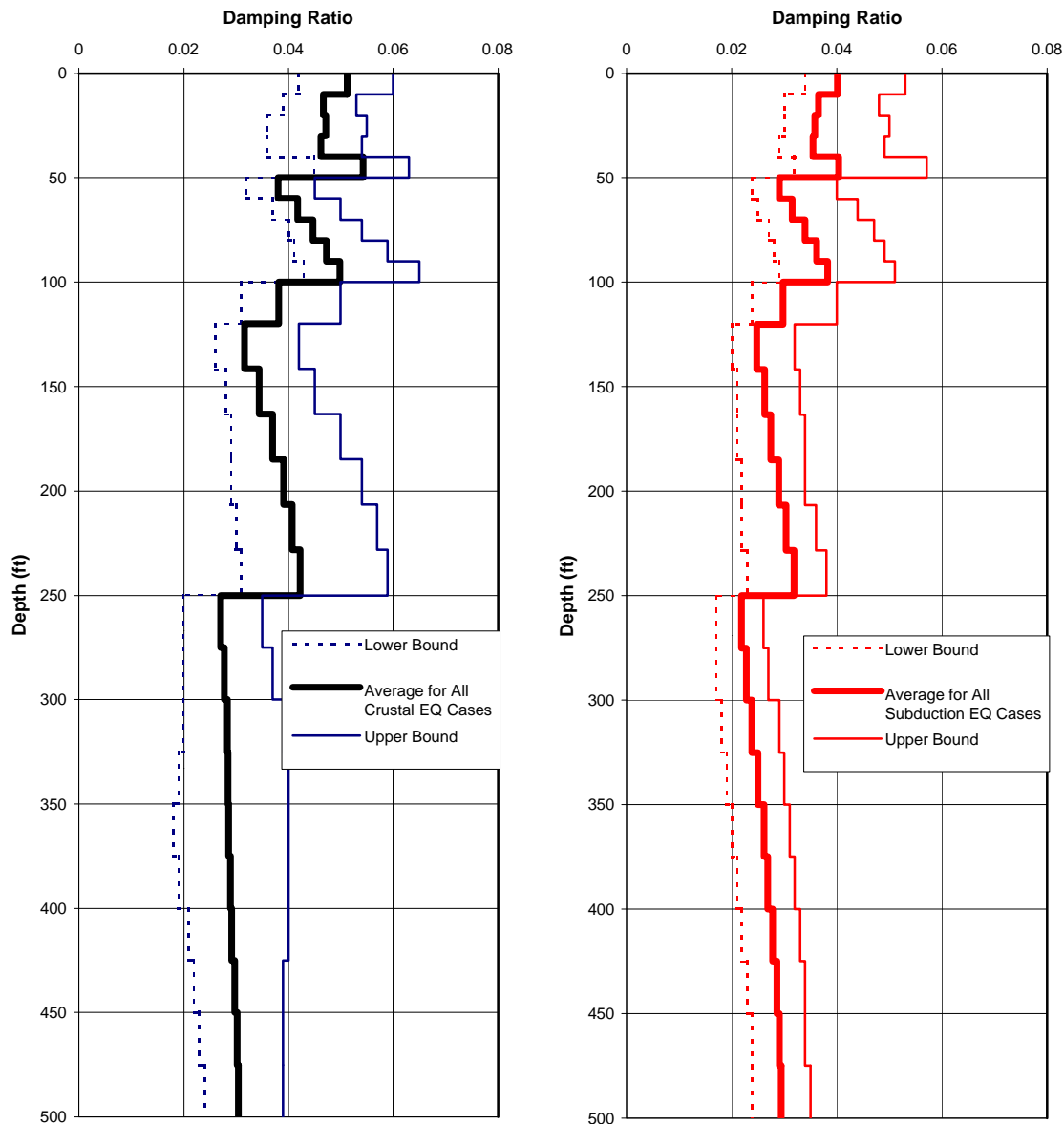


Figure 5-4. Strain-Compatible Damping Ratios for Hanford 200 East Area Soil Profile: "H1 + Basalt" { TC "5-4. Strain-Compatible Damping Ratios for Hanford 200 East Area Soil Profile: "H1 + Basalt" } { F }



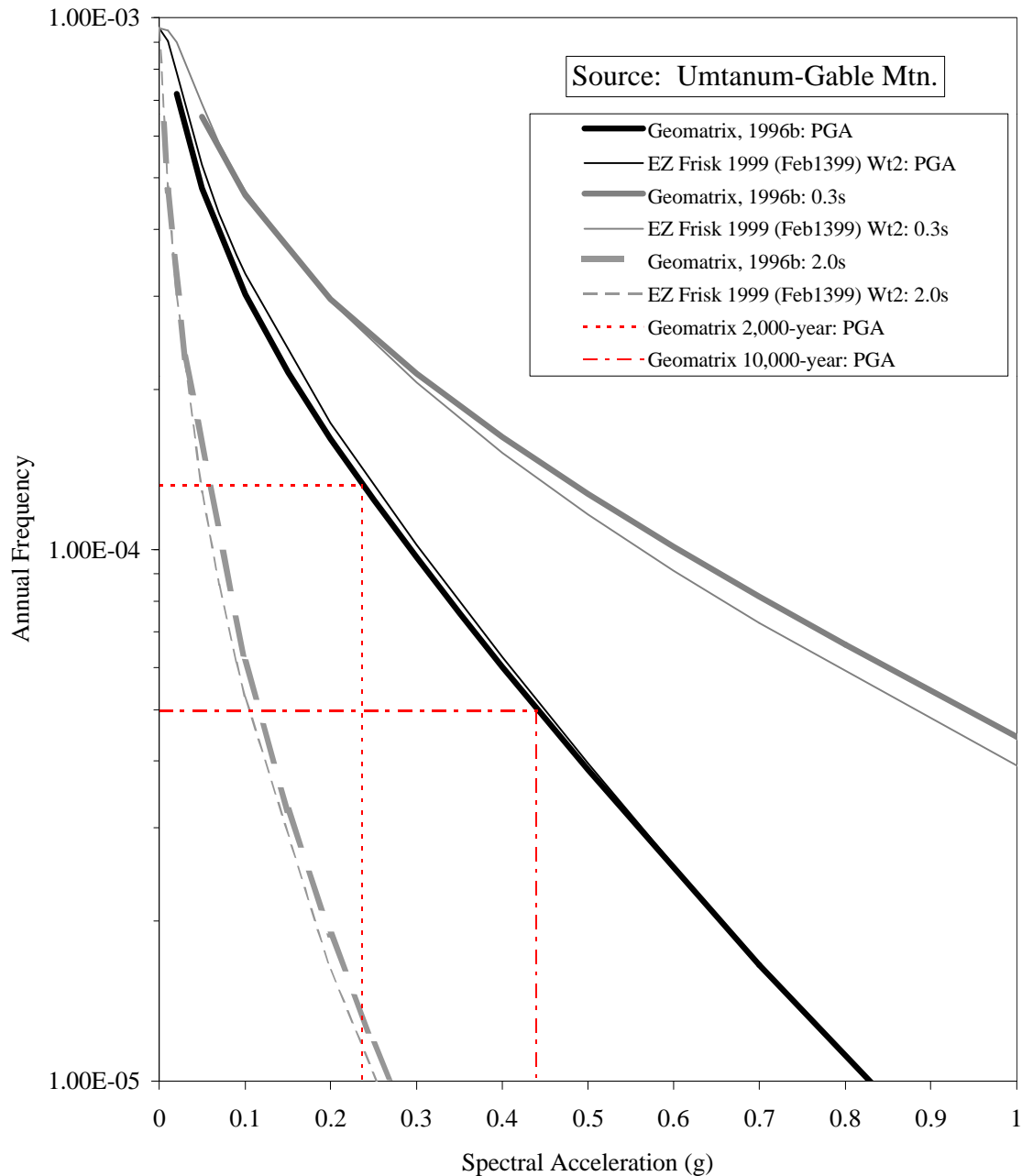
(a) For all crustal earthquake cases -
Average of sixteen runs.

(b) For all subduction earthquake cases -
Average of eight runs.

All crustal and subduction earthquake events are treated separately.

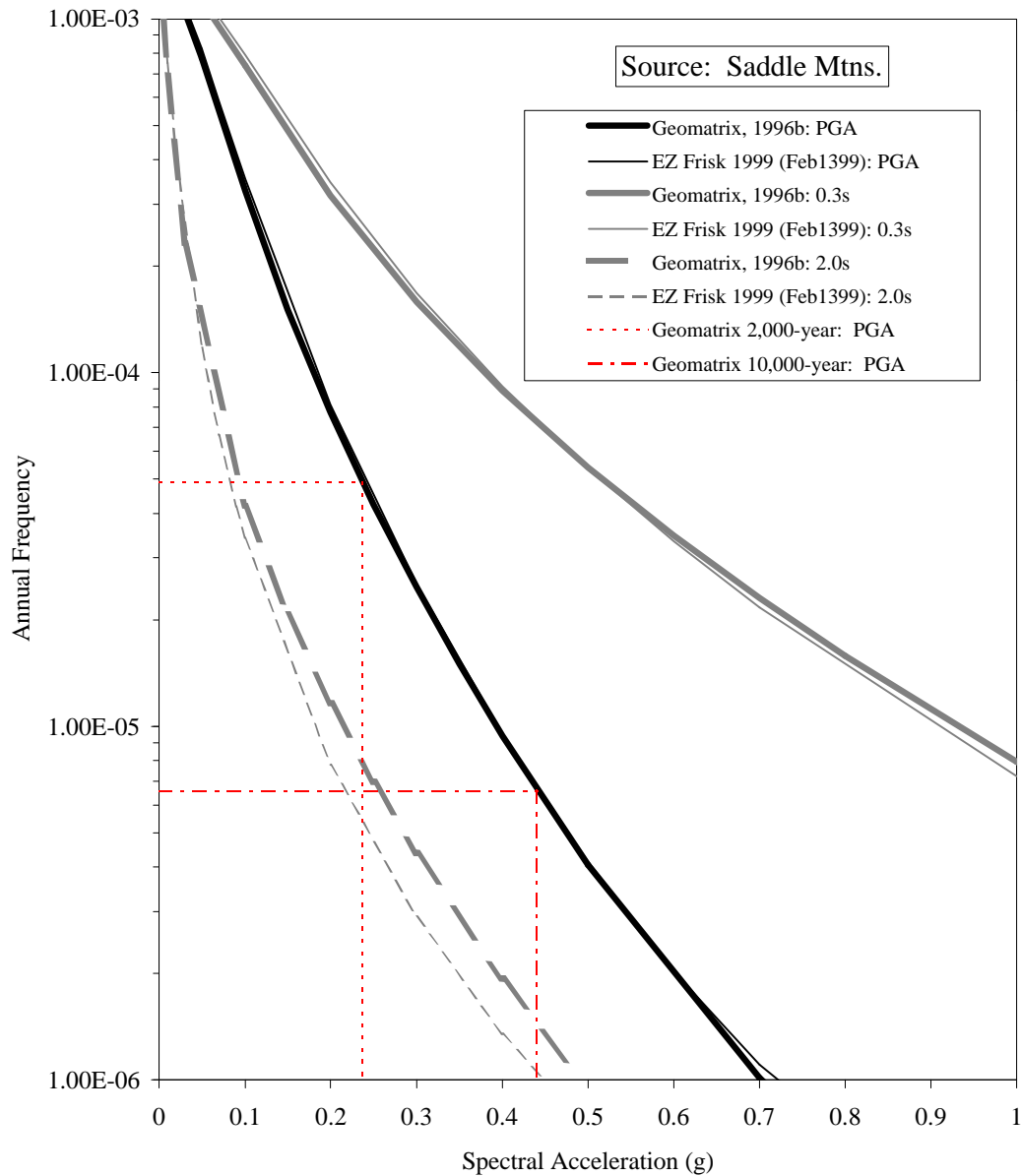
Figure 5-5. Comparison of Hazard Curves (Annual Frequency of Exceedance) at 200 East Area from the Umtanum – Gable Mtn. Seismic Source { TC "5-5.

**Comparison of Hazard Curves (Annual Frequency of Exceedance) at 200 East Area
from the Umtanum – Gable Mtn. Seismic Source " \f F }**



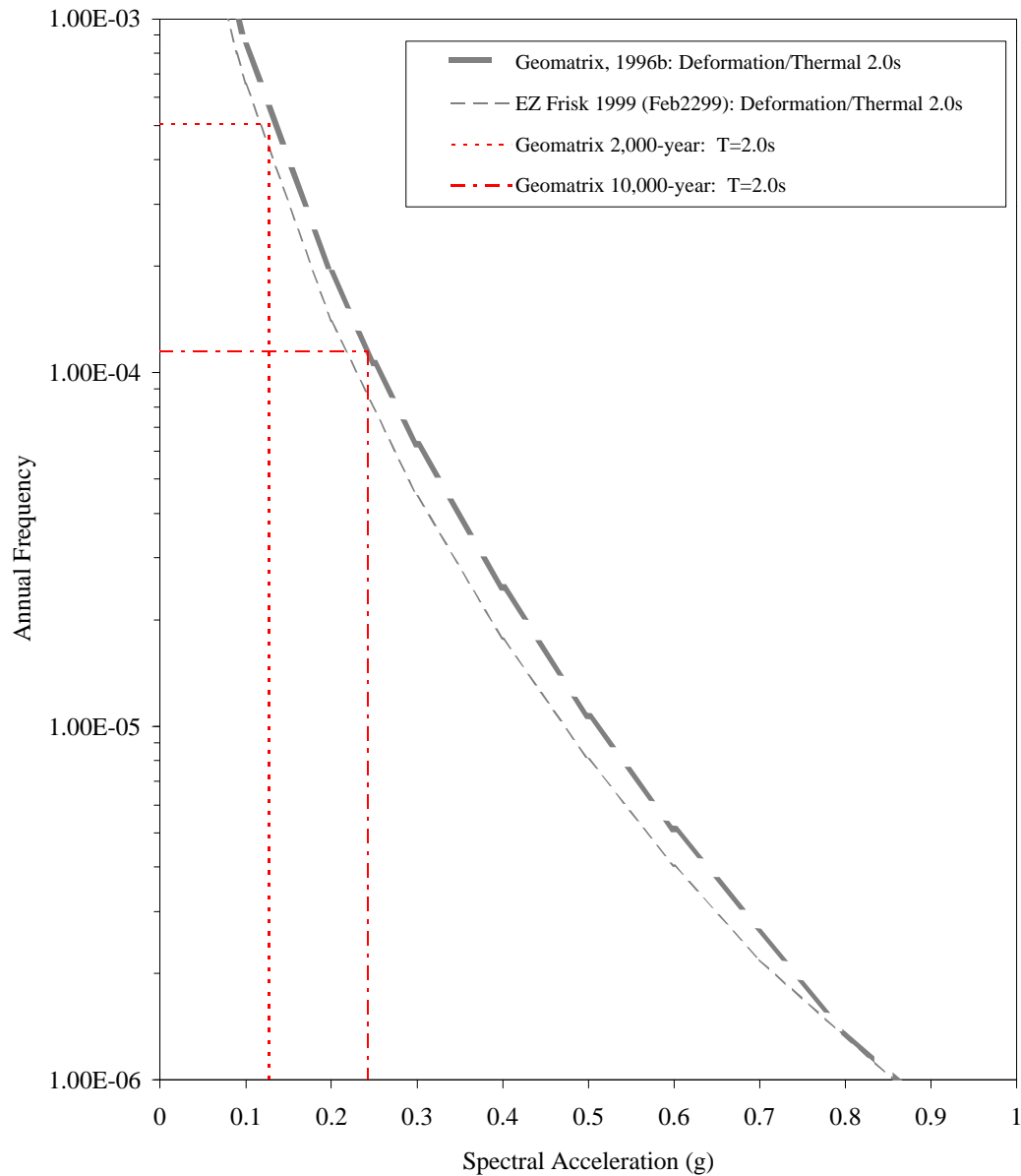
As given by Geomatrix (1996b) and current verification using the program EZ-FRISK. Hazard curves are shown for peak acceleration (PGA) and spectral ordinates (5% critical damping) at 0.3 sec and 2.0 sec. Comparisons between curves should be made at the ground motions given by the hazard curves for all sources ("total" hazard) at the hazard levels of interest (e.g., 2,000-year or 10,000-year return period). For example, Geomatrix (1996b) gives the total hazard PGA of about 0.24 g and 0.44 g for the 2,000-year (5×10^{-4}) and 10,000-year (1×10^{-4}) return periods (hazards), respectively.

Figure 5-6. Comparison of Hazard Curves (Annual Frequency of Exceedance) at 200 East Area from the Saddle Mtns. Seismic Source{ TC "5-6. Comparison of Hazard Curves (Annual Frequency of Exceedance) at 200 East Area from the Saddle Mtns. Seismic Source }



As given by Geomatrix (1996b) and current verification using the program EZ-FRISK. Hazard curves are shown for peak acceleration (PGA) and spectral ordinates (5% critical damping) at 0.3 sec and 2.0 sec. Comparisons between curves should be made at the ground motions given by the hazard curves for all sources ("total" hazard) at the hazard levels of interest (e.g., 2,000-year or 10,000-year return period). For example, Geomatrix (1996b) gives the total hazard PGA of about 0.24 g and 0.44 g for the 2,000-year and 10,000-year return periods, respectively.

Figure 5-7. Comparison of Hazard Curves (Annual Frequency of Exceedance) at 200 East Area from the Cascadia Interface Seismic Source{ TC "5-7. Comparison of Hazard Curves (Annual Frequency of Exceedance) at 200 East Area from the Cascadia Interface Seismic Source" \f F }



As given by Geomatrix (1996b) and current verification using the program EZ-FRISK. Hazard curves are shown for 2.0 sec spectral acceleration for characteristic magnitude recurrence and the deformation front thermal fault model. Comparisons between curves should be made at the ground motions given by the hazard curves for all sources ("total" hazard) at the hazard levels of interest (that is, 2,000-year and 10,000-year return periods). Specifically, Geomatrix (1996b) gives the total hazard for the 2.0 sec

spectral acceleration of about 0.13 g and 0.24 g for the 2,000-year and 10,000-year return periods, respectively.

6. Hazard Sensitivity Results

Several specific model input parameters were identified in Chapter 4.0 as being of interest for additional examination. These were: 1) the effect of alternative weighting schemes for two input variables (coupled/uncoupled characterization for Yakima Fold Belt features and the credibility of the Deep Crystalline Basement Rift source), 2) possible variation of several model attenuation relationships, 3) consideration of the effect of inclusion in the model of a May Junction fault source, and 4) inclusion of alternative slip rates on two segments of the Saddle Mountains Fold fault system. This chapter assesses the sensitivity of variation of these specific elements of a regional earthquake source model.

To aid the sensitivity assessments made below, we obtained the digital data for specific hazard curves plotted in Chapter 5 of the Geomatrix report. These plots are for three specific spectral ordinates: peak acceleration, 5%-damped spectral acceleration at 0.3 sec period, and 5%-damped spectral acceleration at 2.0 sec period. In this chapter we use these available hazard curves for the given spectral ordinates to assess the impact on the overall equal hazard spectrum for both the 2,000-year and 10,000-year return periods.

Figure 5-1b of the Geomatrix report shows the mean and several percentile (5th%, 15th%, 50th%, 85th%, and 95th%) hazard curves for the three spectral ordinates at the 200 East Area. Figures 6-1 and 6-2 of this report show the full equal hazard spectra for 2,000-year and 10,000-year return periods, respectively, from Table 5.1 of the Geomatrix report, and the corresponding percentile values for the spectral ordinates determined from the digital data of Figure 5-1b. In Figures 6-1 and 6-2 smoothed curves have been drawn through the 5th% and 95th% values for illustration only, as data from Figure 5-1b are available only for the three spectral ordinates, as discussed above.

Several observations are made regarding Figures 6-1 and 6-2. First, in each of these figures the solid line is the mean equal hazard spectrum as given in Table 5-1 of the Geomatrix report, identified in the legend as “Geomatrix (1996b)”. The circle symbols, labeled “Interpolated” are our log-log interpolation of the Figure 5-1b digital data for the mean curve. The purpose of obtaining the “Interpolated” spectral ordinates was to verify that we could duplicate the return period interpolations of the primary hazard curves from which the Geomatrix Table 5-1 was derived. While we used simple log-log interpolation of the hazard curve data, Geomatrix used a log-log spline fitting routine, intended to better capture the gentle curvature between hazard curve values plotted in a log-log fashion. Figures 6-1 and 6-2 show good agreement between these two interpolation methods, except for the 2.0 sec (0.5 Hz) spectral ordinate for the 2,000-year return period. Table 5-1 indicates the 2,000-year spectral acceleration at 2.0 sec to be 0.121g, while the corresponding “Interpolated” value is slightly higher at 0.127g. Upon subsequent review, Geomatrix has determined that their log-log spline interpolation function for the 2.0 sec hazard curve was “too loose” in the immediate portion of the curve from which the 2,000-year motion was estimated. The remainder of the 2.0 sec hazard curve appears well-behaved. For the sensitivity plots given in this section, when displaying the total equal hazard spectra of Figure 5-1b, the “Interpolated” values will also be shown. We prefer the “Interpolated” values when considering the sensitivity assessments, particularly for the 2,000-year spectral ordinate at 2.0 sec.

Figures 6-1 and 6-2 indicate that the mean equal hazard spectra are more conservative (higher) than the median, as indicated by the 50th% spectral ordinate values. For both the 2,000-year and 10,000-year spectra, the spread of the 5th% to 95th% spectra is about a factor of 3. For the 2,000-year spectrum the 5th% to 95th% PGA spread is 0.131g to 0.373g, with a median of 0.211g, compared to the mean of 0.237g. For the 10,000-year spectrum the 5th% to 95th% PGA spread is 0.228g to 0.710g, with a median of 0.362g, compared to the mean of 0.440g.

6.1. Coupled/Uncoupled Yakima Fold Belt Fault Models

The Geomatrix source modeling of the Yakima Fold Belt allows associated faults to be either shallow structures (4 km or less in depth) confined to the basalts of the CRBG (“uncoupled” model) or to extend deeper (21 km deep) into the crystalline basement (“coupled” model). Table 3-1 of the Geomatrix report, which gives the assessed “Probability of Coupling” for each Yakima Folds seismic source, reflects the discussion in the text that the degree to which it is believed that the geological and seismological data suggest continuity of the Yakima Fold structures to the crystalline basement varies for the different proposed fold structures. The assessment of the weights to give to either model for each fold is based on subjective professional judgement (see, for example, Sections 3.2.1.2 and 3.2.1.3 of this report). The DOE RU expressed interest in the effect of the choices made for these weights on the hazard results. In this section we examine the sensitivity of analysis results to these subjective weights.

Figure 5-10b of the Geomatrix report indicates one perspective of the sensitivity of the effect of coupling on the hazard curve contribution from the Yakima Folds. Mean hazard curves for each of the spectral ordinates for the composite of the Yakima Folds sources, as incorporated in the final total hazard assessment, is shown along with confidence intervals of 5th% and 95th%. Also shown, are mean Yakima Folds hazard curves that would have resulted if all Yakima Fold faults were modeled as coupled (the weight on the “coupled” limb of the logic tree were 1 and the weight on the “uncoupled” limb of the logic tree were 0 for every YFB seismic source) or as uncoupled (the weight on the “coupled” limb of the logic tree were 0 and the weight on the “uncoupled” limb of the logic tree were 1 for every YFB seismic source). The 100% coupled curves and 100% uncoupled curves (Geomatrix, 1999b, Figure 5-10b) cannot be simply weighted to obtain the final mean Yakima Folds mean because each is a composite of several source hazard curves that have different Probabilities of Coupling, as discussed above. Nevertheless, some assessment of sensitivity of this modeling can be made.

Figure 5-10b was used to create the equal hazard spectral plots of Figures 6-3 and 6-4 for 2,000-year and 10,000-year return periods, respectively. These figures show the final total Geomatrix equal hazard spectra, as given in Table 5-1, compared to the total equal hazard spectral ordinates (PGA, Sa at 0.3 sec, and Sa at 2.0 sec) that would have resulted if the Yakima Fold sources had been considered 100% coupled or 100% uncoupled. For reference, our-interpolated values for the total equal hazard spectra are shown (“Interpolated”).

Figures 6-3 and 6-4 show that there is very little dependency within the Geomatrix model in the total hazard contribution from YFB sources whether they are completely coupled or completely uncoupled. Close inspection of the spectral ordinates indicates that, in all cases except for the 2.0 sec spectral ordinate for 100% coupled, the spectral values are lower than the values obtained from the total using the actual coupled/uncoupled weights of the Geomatrix report. In initially considering this sensitivity assessment of the coupling factor, we thought that we might see some systematic exceedance of the final spectral values given one type of coupling extreme, and non-exceedance given the opposite coupling extreme. We thought that consideration of the extreme coupling conditions might define bounds in which the final hazard curve would be contained. In fact, the effect of the coupling models is more complex.

Most simply, as given in Table 3-1 of the Geomatrix report, the coupled/uncoupled weights vary significantly for the different Yakima Fold sources. In addition, however, whether a YFB source is coupled or uncoupled fundamentally affects source size, in turn fundamentally affecting maximum magnitude and, with a slip rate independent of source size, fundamentally affecting moment rate, which, in turn, is complexly distributed on both empirical (“b-value”) and theoretical (“exponential/characteristic”) grounds.

The results of our assessment show that the final equal hazard spectrum is not bounded by the extreme cases of the single coupled/uncoupled variable, as defined here, suggesting that higher final equal hazard spectral values could be obtained with some other combination of the coupled/uncoupled weights. Two conclusions are suggested here, however. First, systematically finding the combination of coupled/uncoupled weights to lead to a particular spectral bound – high or low – would be a very complex and difficult process. Second, it is still considered that the assessment performed here suggests that the ultimate high value bound from alternative weighting on coupling would not greatly exceed the final Geomatrix spectra for either the 2,000-year or 10,000-year return period.

Both sets of figures – the panels of Figure 5-10b of the Geomatrix report and the Figures 6-3 and 6-4 presented here – reveal some significant elements of source contribution as it relates to the coupling parameter. First, the primary effect of the coupling parameter is to affect the downdip width of the modeled source. For a given source and maintaining many of the source parameters constant (for example, slip-rate, b-value, rupture length) one effect of increasing the downdip width (considering the coupled case over the uncoupled) is to cause a higher moment rate and a larger maximum magnitude (in the models where magnitude is a function of downdip width or rupture area). Specifically, and for conventional relations between fault area, moment rate, maximum magnitude, and maximum moment, the moment rate increases more slowly than the moment of the largest events, resulting in a net decrease in the number of earthquakes (see Youngs and Coppersmith, 1984). In addition, with a larger and deeper rupture area, the smaller magnitude events with their smaller rupture areas are allowed to occur at deeper, more distant locations, thereby generally “pushing” some of the small magnitude events away (down) from the site, resulting in smaller site intensities. Figure 5-6b of the Geomatrix report shows the relative contribution to the Yakima Folds seismic hazard as a function of magnitude. This figure shows a common feature that the high frequency ground motions are dominated by the more frequent small magnitude earthquakes, and that with longer period ground motions the larger magnitude events become more important. This effect is accentuated for longer return periods. Figure 5-10b of the Geomatrix report and Figures 6-3 and 6-4 show that the 100% uncoupled scenario gives a higher hazard from the peak acceleration and 0.3 sec motions than the 100% coupled scenario. This trend is reversed for the longer period 2.0 sec motions. The interplay of various source parameters in the coupled/uncoupled cases is complex.

6.2. Weighting Scheme for Crustal Crystalline Basement Source

Chapter 3 of the Geomatrix report discusses seismic sources within the crystalline basement beneath the low-velocity sub-basalt sediments of the Columbia Plateau. Additional discussion is presented in Section 3.2.2 of this report.

The occurrence of seismicity within the basement confirms that it is seismogenic, although, as discussed by Geomatrix and in Chapter 3.0 of this report, the causative structures giving rise to the seismicity are not at all well known. Three models have been considered for the crystalline basement. The failed rift and basement block models represent interpretations of the crustal structure of the Columbia Plateau in the vicinity of the Yakima Folds. The Geomatrix report argues that, although these two models are

reasonable interpretations of the evolution of the crust, neither appears to explain the present-day spatial pattern of seismicity (see also discussion in Sections 3.2.2.1 and 3.2.2.2 of this report). The failed rift and basement block models are assigned “relatively low weight (0.1 each) that they represent models explaining the occurrence of present-day seismicity.” The remaining weight (0.8) is assigned to the random basement model, an areal source zone wherein the seismicity is assumed to occur randomly -- distributed uniformly -- throughout the source zone since the causative sources are unknown. The seismicity recurrence rate for the random basement model is derived directly from the observed rate of historical seismicity.

Figure 5-3b of the Geomatrix report indicates that for the higher frequency hazard at 200 East Area -- represented by peak acceleration and 0.3 sec spectral acceleration -- the Yakima Folds sources comprise the dominate group of contributing sources among the three groups of Crustal sources. At the 2,000-year return period ground motions (0.237g for peak acceleration and 0.502g for the 0.3 sec spectral acceleration) the contribution from basement sources is about half of that from the Yakima Folds sources. At the 10,000-year return period the relative contribution of the Basement sources is even less. Figure 5-3b also indicates that for the lower frequency ground motion hazard -- represented by the 2.0 sec spectral acceleration -- the Yakima Folds sources and Basement sources are closer in contribution, though the Yakima Folds sources are still the greater contributor.

Figure 5-13b shows the effect on the composite hazard curves of the Basement model only considering alternative extreme weighting of the three Basement models. In this figure the “Basement” mean is where the preferred weighting is applied, as reviewed above. Alternatively, hazard curves are shown where each of the three sources are considered in turn as the only Basement source. Figure 5-13b indicates, for example, that if the Rift model were considered the only acceptable Basement model, the resultant Basement hazard curve would be considerably higher than that presented by Geomatrix.

To further examine the effect on the total 2,000-year and 10,000-year equal hazard spectra of the Basement modeling hazard curve sensitivities presented in Figure 5-13b, we constructed Figures 6-5 and 6-6. These are plots of the total 2,000-year and 10,000-year Geomatrix spectra, respectively, with the corresponding spectral values resulting from considering the alternative extreme weighting schemes of Figure 5-13b. The spectral values for 100% weighting for each of the Basement model alternatives are interpolated directly from the hazard curves of Figure 5-13b and combined with the hazard of Figure 5-3b and Figure 5-2b to obtain the total hazard curves shown in Figures 6-5 and 6-6. The “Equal Weighting” values, representing the spectral mean assuming equal weighting (0.333 each) for the three Basement models, have been processed similarly to present the effect on the total hazard spectrum. Table 6-1 below lists the explicit spectral ordinate values plotted in Figures 6-5 and 6-6 for the three representative periods.

From these figures and table, as well as the panels of Figure 5-13b, it can be seen that the equal hazard spectrum would have been lower for both return periods at all period motions if the crystalline basement had been modeled only with the uniform distribution of randomly located earthquakes (“100% Uniform”). The total 2,000-year and 10,000-year peak accelerations would have been 0.227g and 0.429g, respectively, or about 2 to 5% lower. Similar reductions are observed for the other spectral ordinates.

At the other extreme, if the crystalline basement had been modeled only with the Rift model (100% Rift), the total 2,000-year and 10,000-year peak accelerations would have been 0.288g and 0.500g, respectively, or about 14 to 22% higher. In this case the other spectral ordinates show even higher increases of 19 to 34%.

Unlike the case of coupled/uncoupled alternatives for the Yakima Fold Belt sources, the effect of varying relative weights for sources of the crystalline basement is straight-forward. This exercise quantifies the obvious: that, while the basement seismicity could have been simply modeled using an areal source zone based on the observed seismicity (100% Uniform), Geomatrix has considered a model that results in a more conservative approach (that is, one that yields higher ground motions) by incorporating the possibilities of active basement structures as modeled by the Rift and Block models. It is apparent that even higher ground motions would have resulted if the weighting of the Rift and Block models had been assessed to have greater credibility.

6.3. Effect of Alternative Attenuation Relationships

Two modifications of attenuation relationships used in the 1996b Geomatrix report are noted and specified in Section 4.2 of this report. In addition, a question about the accuracy, at relevant distances and for relevant magnitudes, of long period attenuation relationships adopted for the Cascadia interface subduction zone has been raised by DOE RU during meetings on TWRS-P Facility seismic design (see Appendix A). These issues are examined in this section.

6.3.1. Cascadia Interface Subduction Zone

Figure 5-2b Geomatrix report indicates that the Cascadia subduction interface source is the dominant hazard source over the Intralab source and the composite of all crustal sources for the spectral ordinate at 2.0. Figure 5-5b indicates that the large magnitude (7.5 to 9) events modeled for this source are the most significant earthquakes.

Figure 4-4 of the current report compares the Youngs et al. (1993) relationship used as one of several to model attenuation from the Cascadia subduction zone with a slightly updated version (Youngs et al., 1997). For a spectral acceleration period of 0.3 sec, the Youngs et al. (1997) empirical attenuation relationship predicts higher (up to 30% higher) spectral accelerations for a magnitude 8.5 earthquake at a distance of 375 km. Therefore, its use to calculate earthquake shaking hazard at the Hanford Site rather than the Youngs et al. (1993) relationship would lead to slightly higher hazard values for this ground motion period. However, the total hazard for the Hanford site at this spectral period would not be expected to change significantly based on the limited contribution to the total hazard from the Cascadia Interface source at this spectral period (see Figure 5-2b of the Geomatrix 1996b report). The peak ground acceleration and 2.0 sec spectral response hazard curves would not change if the Youngs et al. (1997) attenuation relationship was used because the Youngs et al. (1993) and Youngs et al. (1997) relationships are identical for PGA and spectral accelerations for periods greater than 0.5 sec. (see Figure 4-4).

In Chapter 4 of the Geomatrix (1996b) report, ground motion attenuation relations are presented that are used in the seismic hazard evaluation. In presenting the attenuation relations appropriate for the Cascadia subduction interface earthquakes, Geomatrix presents Figure 4-10 showing the available subduction interface data for peak ground acceleration for events of about magnitude 7 and 8, and plotting the attenuation relations used in the report for this seismic source. In this figure the attenuation relations generally show a good fit to the data, although goodness of fit in the specific distance range relevant to the Hanford Site – namely, about 300 to 400 kilometers – has been questioned (see Appendix A of this report).

Figure 6-7 is a modified plot of the peak acceleration data of the Geomatrix Figure 4-10. Figure 6-7 differs from Figure 4-10 in that the distance scale has been increased from 500 kilometers to 700 kilometers. For the magnitude 8 data plot this has brought into view two more data points at the far

distances. In the original Figure 4-10 it could have been argued that for the magnitude 7 peak acceleration data the Cascadia Subduction Interface attenuation relations plot below the visual center of the data, and that for the magnitude 8 data the relations may be attenuated too rapidly – that is, the attenuation relations should angle upwards slightly (higher motions) in the 300 to 400 kilometers distance range. On inspection of the magnitude 7 data of Figure 6-7 (or the original Figure 4-10), indeed the several data points lying above the attenuation relations in the 100 to 200 kilometer distance range could suggest underestimation of ground motions by the relations, but the relations appear to be very centered in the important 300 to 400 kilometer distance range. With regard to the magnitude 8 peak acceleration data of Figure 6-7, the additional data points at about 500 kilometers suggest that angling the attenuation relations upward would be inappropriate.

More importantly for the seismic hazard at the Hanford Site, Figures 6-8 and 6-9 are plots of the Cascadia subduction interface attenuation relations for magnitude 7 and 8 for spectral accelerations at periods of 1.0 sec and 2.0 sec, respectively. The available data are fewer for these spectral ordinates than for peak ground acceleration, all data being for distances less than 300 kilometers. Both figures indicate that, while there is more variability in the trends of the attenuation relations themselves for these spectral ordinates, they all fit well through the visual centroid of the available data.

We conclude that the attenuation relations used by Geomatrix for the Cascadia subduction interface source are appropriate and adequate for estimating ground motions at the Hanford Site.

6.3.2. Campbell Attenuation Relationships

Campbell (1997) represents an update to the Campbell (1994) crustal attenuation model that was used in the Geomatrix (1996b) report. The differences between the two attenuation relationships have been discussed in Section 4.2.2 and shown in Figure 4-5a and 4-5b. The peak ground acceleration hazard curve for the crustal fault sources would not change if Campbell (1997) was used in place of the Campbell (1994) relationships because the median estimate and standard error for PGA ground motion are the same for the two relationships. For a spectral period of 0.3 sec, the hazard curve would be expected to be similar. Figures 4-5a and 4-5b of this report indicate a lower median ground motion for $T=0.3$ sec when comparing Campbell (1997) and Campbell (1994). However, the standard error for Campbell (1997) is larger at $T=0.3$ sec (see Figure 4-6). This tradeoff between lower median ground motion estimates and higher standard error should result in a similar hazard curve for the crustal sources. For $T=2.0$ sec, the Campbell (1997) curves are also lower in median ground motion and higher in standard error. Thus, an updated hazard computation using the Campbell (1997) attenuation relationship in place of the Campbell (1994) relationship would be expected to produce a similar hazard curve.

Because the Campbell attenuation relationships apply to local crustal sources, which comprise the sources most important to earthquake ground motion hazard estimates for the Hanford Site particularly for higher frequency ground motions, we reran the hazard from the Umtanum-Gable Mountain using the updated Campbell attenuation relations. The peak ground acceleration hazard curve is not modified because, again, the Campbell (1994) and Campbell (1997) attenuation relationships are identical for PGA (see section 4.2.2). For $T=0.3$ and 2.0 sec, the inclusion of Campbell (1997) instead of Campbell (1994) produces slightly higher hazard curves which are shown in Figure 6-10. The source of the increased hazard curve is attributable to the increase in sigma between the Campbell 1994 and Campbell 1997 attenuation relationship. The sigma values are shown in Figure 4-6 for three representative magnitudes. The $T=0.3$ and 2.0 sec sigma values show the largest increase between the two attenuation relationships.

6.4. Effect of May Junction Fault

As discussed in Section 4.3 of this report, the panel of regional experts suggested that we consider the May Junction fault as a new seismic source, one not considered in the Geomatrix (1996b) report. Although of low assessed likelihood of activity (see discussion of Section 4.3) it is close to the 200 East Area and, therefore, of interest. With advice from the panel of experts, and in a way conformable to the logic tree for the Yakima Folds seismic sources (Geomatrix, 1996b, Figure 3-10), we adopted the following seismic source parameters for the May Junction:

<u>Logic Tree Branch</u>	<u>Element</u>	<u>Weight(s)</u>
Activity:	Active	0.1
Coupling:	Uncoupled	1.0
Segmentation:	Unsegmented	1.0
Length:	6 km	1.0
Dip:	80° to the east	1.0
Seismogenic depth:	4 km	1.0
Maximum magnitude:	5.5	1.0
b-values:	0.82, 0.99, 1.16	0.2, 0.6, 0.2
Magnitude distribution:	Characteristic, Exponential	0.5, 0.5
Slip rate:	0.009 mm/year	1.0

Again in analogy to the Geomatrix (1996b) report, the effective maximum magnitude is $5.5 + 0.25 = 5.75$. The minimum magnitude used is 5.0. There are six branches for this hazard evaluation, differentiated by the b-value and the magnitude distribution. Youngs and Coppersmith (1985) was used with these parameters to determine the activity rates (N5: annual number of magnitude 5 and greater earthquakes) for the six branches:

<u>b-value</u>	<u>Characteristic</u>	<u>Exponential</u>
0.82	$N5 = 2.662 \times 10^{-5}$	$N5 = 3.206 \times 10^{-5}$
0.99	$N5 = 2.612 \times 10^{-5}$	$N5 = 2.889 \times 10^{-5}$
1.16	$N5 = 2.561 \times 10^{-5}$	$N5 = 2.329 \times 10^{-5}$

The same crustal attenuation relations and magnitude-length relation as used by Geomatrix (1996b) were used for evaluating the seismic hazard contribution from the proposed May Junction fault.

The results of our calculation are shown in Figure 6-11 in which the May Junction contribution (light dashed line) is compared to the contributions of the individual Yakima Fold Belt (light solid lines, undifferentiated) and to the sum of the YFB hazards (heavy gray line). The May Junction fault under this model (heavy dashed line) does not add measurably to site hazard.

6.5. Effect of Higher Slip Rate on Saddle Mountains Fault Segments

As discussed in Section 4.4 of this report, field studies on the Saddle Mountains fold fault system (West and Shaffer, 1989; West et al., 1996) suggested a re-evaluation of the slip rates on the Saddle Mountains fold source. We confirmed that the geology experts still favor the slip rates used in the Geomatrix (1996b) report, but that they recommended that double this slip rate could be used for sensitivity analyses of hazard contributions of the Saddle Gap and Smyrna Bench segments. The slip rates for the other segments and for the unsegmented case were not modified. We computed the hazard for the Saddle

Mountains fold source keeping all other parameters fixed to the values used in the sample confirmatory analysis (see Section 5.2.1).

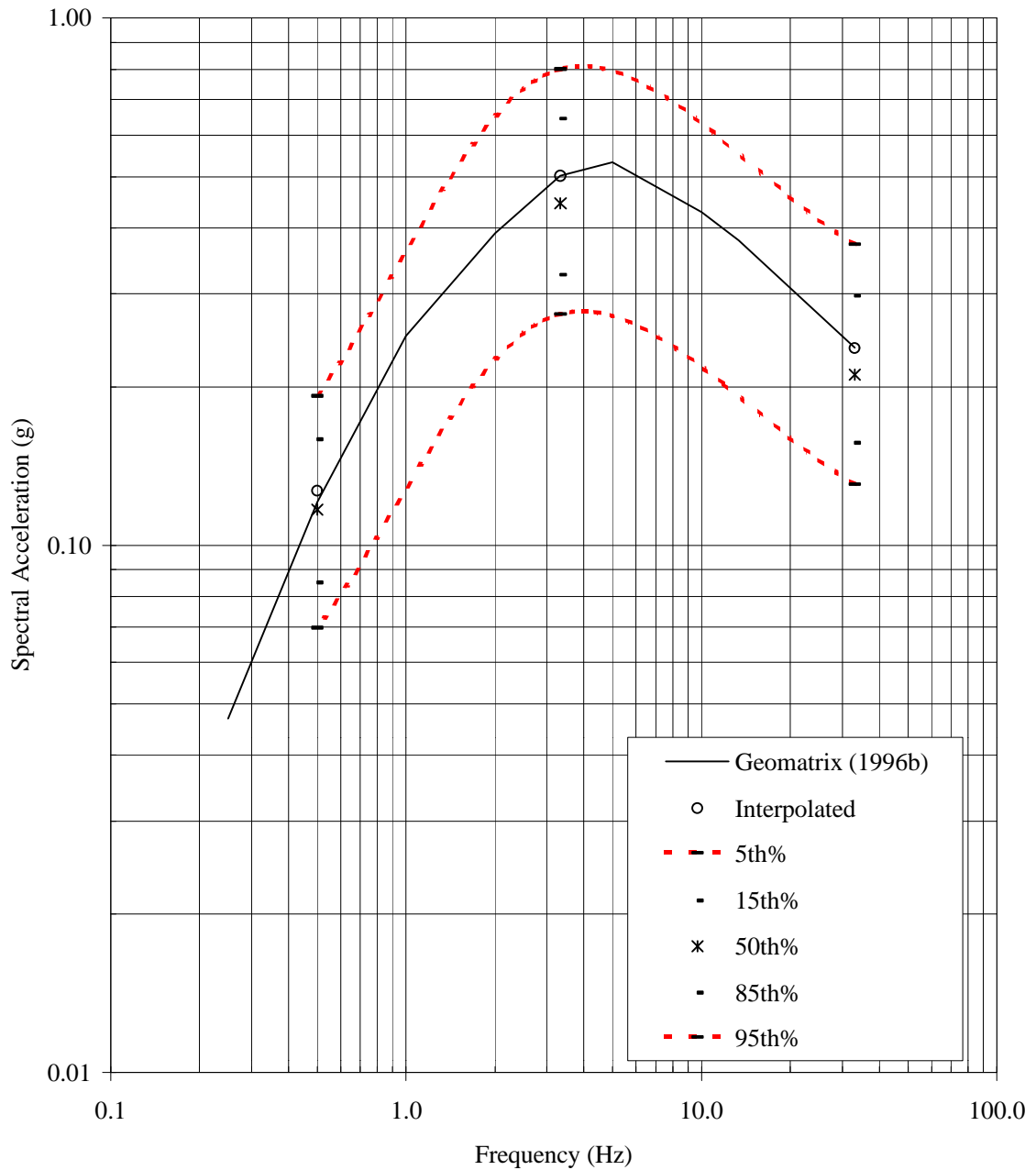
The increase in slip rate leads to an increase in the hazard curves for the Saddle Mountains case as would be expected. To investigate the effect on the total Yakima Fold hazard curve, the ratios between the original base case Saddle Mountains curve and the new double slip rate Saddle Mountains curves from the EZ-Frisk™ runs were computed for peak ground acceleration, and spectral acceleration at periods of 0.3 and 2.0 sec. This ratio was then applied to the Geomatrix (1996b) hazard curves to estimate the corresponding Geomatrix hazard curves associated with the increase in slip rate for the Saddle Gap and Smyrna Bench segments. This modified Geomatrix Saddle Mountains hazard curve was then combined with the original Geomatrix hazard curves for the other Yakima Fold sources to see the overall effect on the total Yakima Fold hazard curves. The curves are plotted in Figures 6-12a, b, and c for PGA, T=0.3, and T=2.0 sec, respectively. As is evident from the figures, the doubling of the slip rate for the Saddle Gap and Smyrna Bench segment causes a very small increase in the total hazard associated with the Yakima fold sources and would not significantly add to the site hazard.

**Table 6-1. Spectral Ordinates for Alternate Weighting of Basement Models{ TC
"6-1. Spectral Ordinates for Alternate Weighting of Basement Models" \f T }**

2,000-Year Return Period					
	Geomatrix "Interpolated"	100% Uniform	100% Rift	100% Block	Equal Wt.
Period(s)	Sa (g)	Sa (g)	Sa (g)	Sa (g)	Sa (g)
PGA (0.03)	0.237	0.227	0.288	0.246	0.257
0.30	0.502	0.476	0.648	0.520	0.555
2.00	0.127	0.122	0.170	0.125	0.140

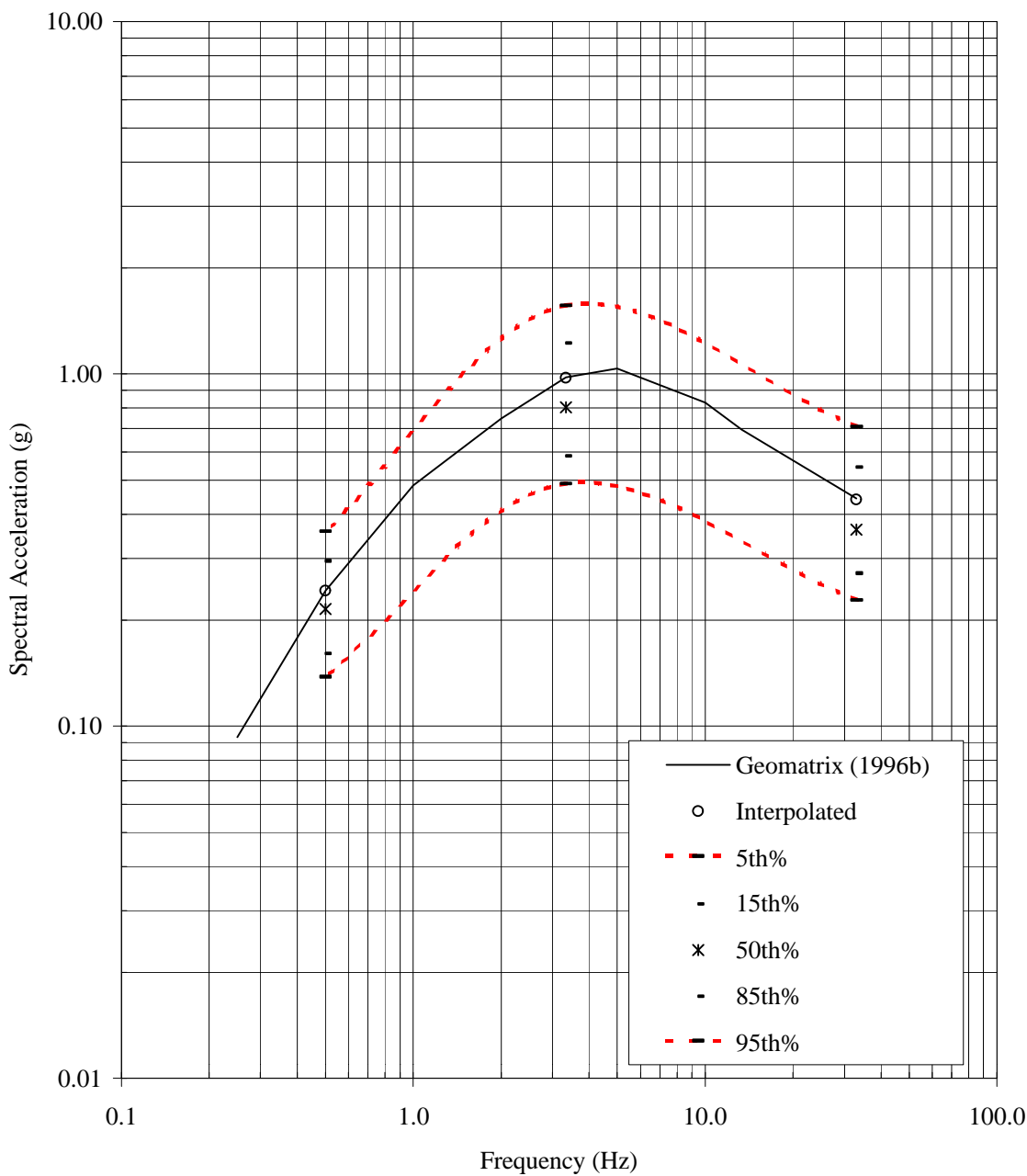
10,000-Year Return Period					
	Geomatrix "Interpolated"	100% Uniform	100% Rift	100% Block	Equal Wt.
Period(s)	Sa (g)	Sa (g)	Sa (g)	Sa (g)	Sa (g)
PGA (0.03)	0.440	0.429	0.500	0.452	0.463
0.30	0.974	0.937	1.158	0.996	1.045
2.00	0.244	0.231	0.324	0.237	0.269

Figure 6-1. Geomatrix (1996b) Mean Equal Hazard Spectrum at 200 East Area for 2,000-Year Return Period (Solid Line) with Confidence Intervals for Spectral Ordinates at PGA (Shown Here at 33 Hz), 0.3 sec (3.3 Hz), and 2.0 sec (0.5 Hz) { TC
"6-1. Geomatrix (1996b) Mean Equal Hazard Spectrum at 200 East Area for 2,000-Year Return Period (Solid Line) with Confidence Intervals for Spectral Ordinates at PGA (Shown Here at 33 Hz), 0.3 sec (3.3 Hz), and 2.0 sec (0.5 Hz)" \f F
}



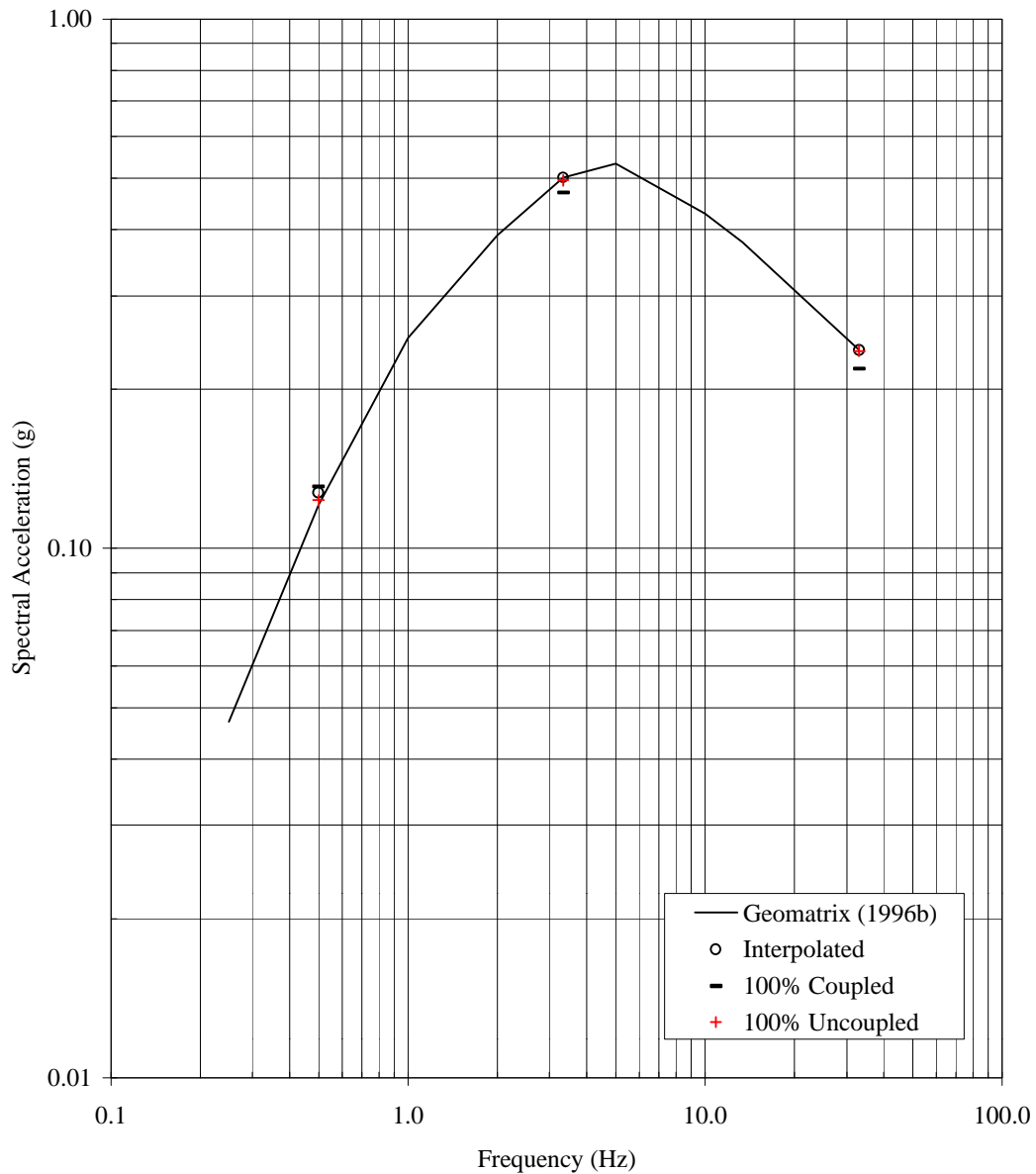
As given in Figure 5-1b of Geomatrix (1996b). “Interpolated” values should replicate mean curve values – cause of variance is discussed in the text. Dashed curves through the three available 5th% and 95th% spectral ordinates are illustrative only, as they are “smoothed” curves defined by MS EXCEL through these points.

Figure 6-2. Geomatrix (1996b) Mean Equal Hazard Spectrum at 200 East Area for 10,000-Year Return Period (Solid Line) with Confidence Intervals for Spectral Ordinates at PGA (Shown Here at 33 Hz), 0.3 sec (3.3 Hz), and 2.0 sec (0.5 Hz) { TC
"6-2. Geomatrix (1996b) Mean Equal Hazard Spectrum at 200 East Area for 10,000-Year Return Period (Solid Line) with Confidence Intervals for Spectral Ordinates at PGA (Shown Here at 33 Hz), 0.3 sec (3.3 Hz), and 2.0 sec (0.5 Hz)" \f F
}



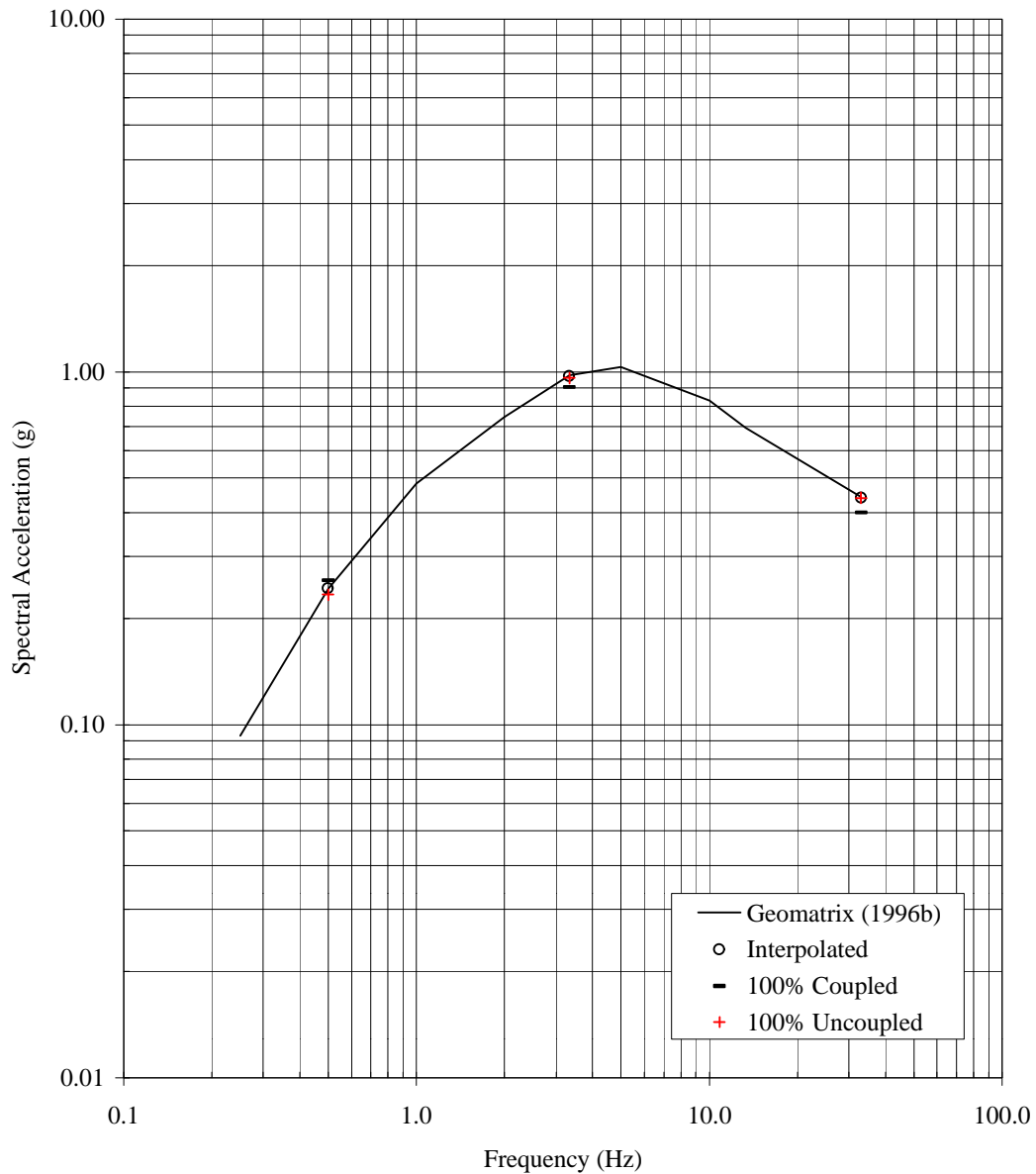
As given in Figure 5-1b of Geomatrix (1996b). “Interpolated” values should replicate mean curve values – cause of variance is discussed in the text. Dashed curves through the three available 5th% and 95th% spectral ordinates are illustrative only, as they are “smoothed” curves defined by MS EXCEL through these points.

Figure 6-3. Sensitivity of Coupled/Uncoupled Weighting of Yakima Folds Seismic Sources on the Total 2,000-Year Mean Equal Hazard Spectrum at 200 East Area
(Solid Line) { TC "6-3. Sensitivity of Coupled/Uncoupled Weighting of Yakima Folds Seismic Sources on the Total 2,000-Year Mean Equal Hazard Spectrum at 200 East Area" \f F }



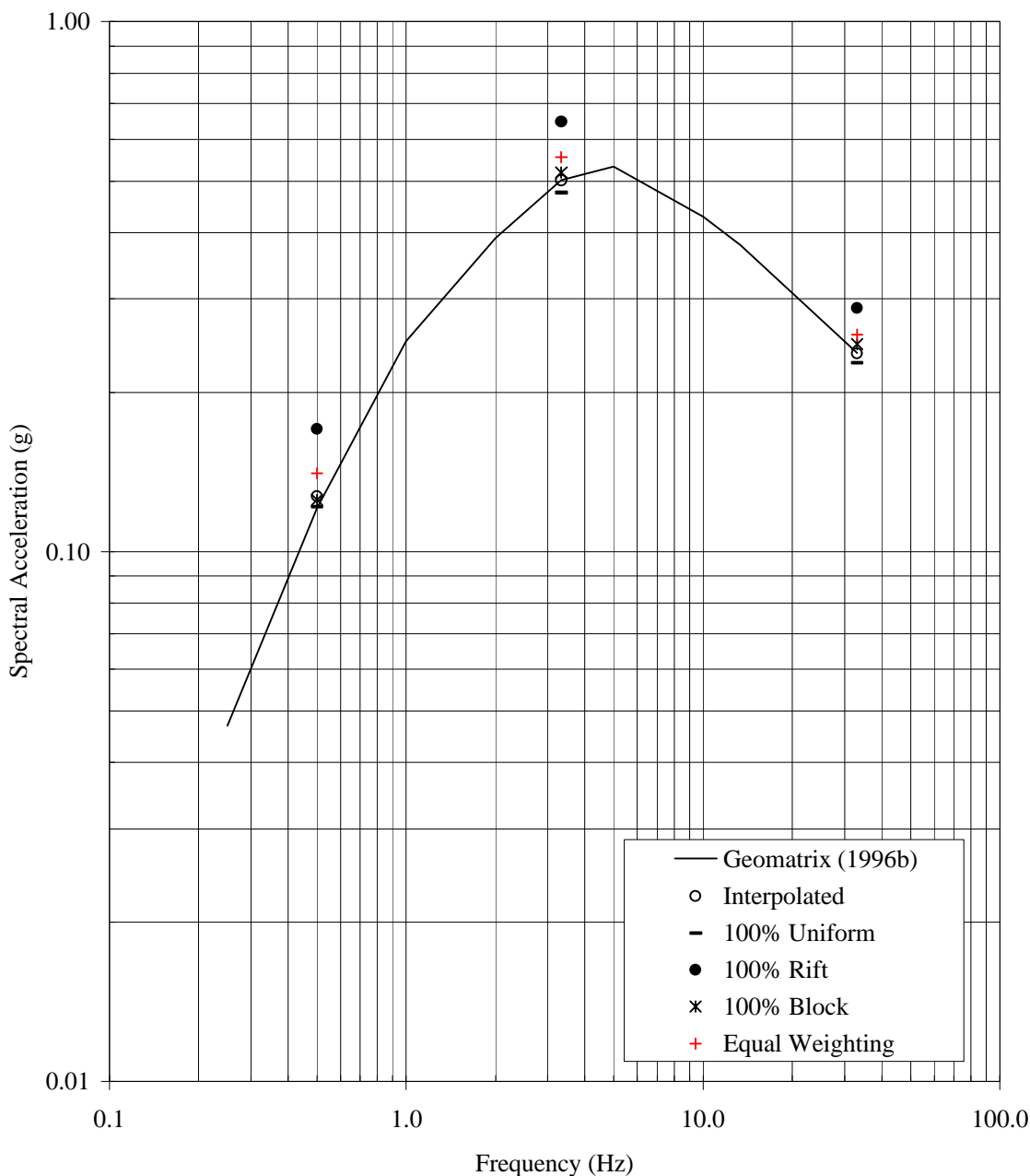
From hazard curves given in Figure 5-10b of Geomatrix (1996b) the ‘-’ and ‘+’ symbols indicate the resultant mean equal hazard spectral ordinate values from all sources for PGA (shown at 33 Hz), 0.3 sec (3.33 Hz), and 2.0 sec (0.5 Hz) considering all Yakima Fold seismic sources are either fully coupled only or uncoupled only, respectively. As discussed in the text, comparisons to the “Interpolated” values are preferred.

Figure 6-4. Sensitivity of Coupled/Uncoupled Weighting of Yakima Folds Seismic Sources on the Total 10,000-Year Mean Equal Hazard Spectrum at 200 East Area
(Solid Line) TC "6-4. Sensitivity of Coupled/Uncoupled Weighting of Yakima Folds Seismic Sources on the Total 10,000-Year Mean Equal Hazard Spectrum at 200 East Area" \f F }



From hazard curves given in Figure 5-10b of Geomatrix (1996b) the ‘-’ and ‘+’ symbols indicate the resultant mean equal hazard spectral ordinate values from all sources for PGA (shown at 33 Hz), 0.3 sec (3.33 Hz), and 2.0 sec (0.5 Hz) considering all Yakima Fold seismic sources are either fully coupled only or uncoupled only, respectively. As discussed in the text, comparisons to the “Interpolated” values are preferred.

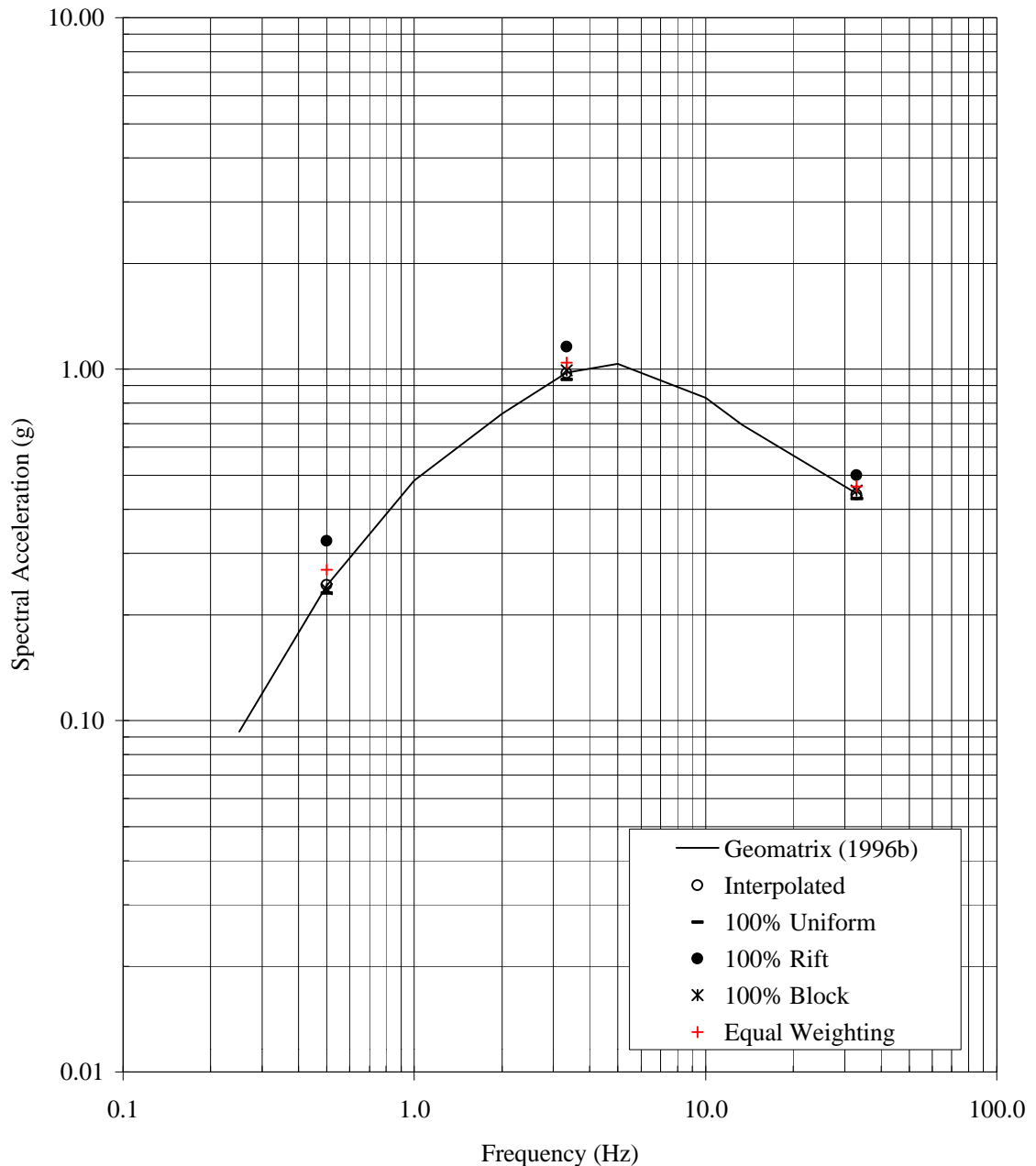
Figure 6-5. Sensitivity of Various Weighting Schemes of the Crystalline Basement Source Models on the Total 2,000-Year Mean Equal Hazard Spectrum at 200 East Area (Solid Line)
TC "6-5. Sensitivity of Various Weighting Schemes of the Crystalline Basement Source Models on the Total 2,000-Year Mean Equal Hazard Spectrum at 200 East Area" {f F }



From hazard curves given in Figure 5-13b of Geomatrix (1996b) the identified symbols indicate the resultant mean equal hazard spectral ordinate values from all sources for PGA (shown at 33 Hz), 0.3 sec

(3.33 Hz), and 2.0 sec (0.5 Hz), considering various weightings of the basement models. As discussed in the text, comparisons to the “Interpolated” values are preferred.

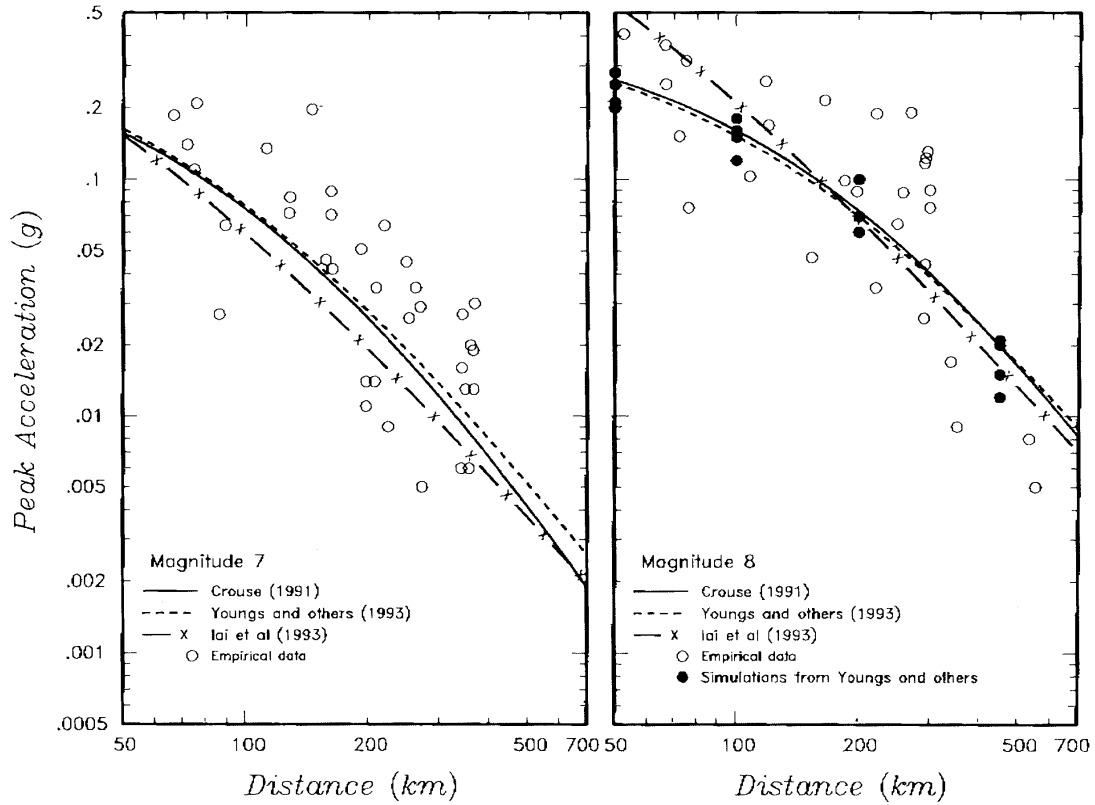
Figure 6-6. Sensitivity of Various Weighting Schemes of the Crystalline Basement Source Models on the Total 10,000-Year Mean Equal Hazard Spectrum at 200 East Area (Solid Line)
TC "6-6. Sensitivity of Various Weighting Schemes of the Crystalline Basement Source Models on the Total 10,000-Year Mean Equal Hazard Spectrum at 200 East Area" {f F }



From hazard curves given in Figure 5-13b of Geomatrix (1996b) the identified symbols indicate the resultant mean equal hazard spectral ordinate values from all sources for PGA (shown at 33 Hz), 0.3 sec

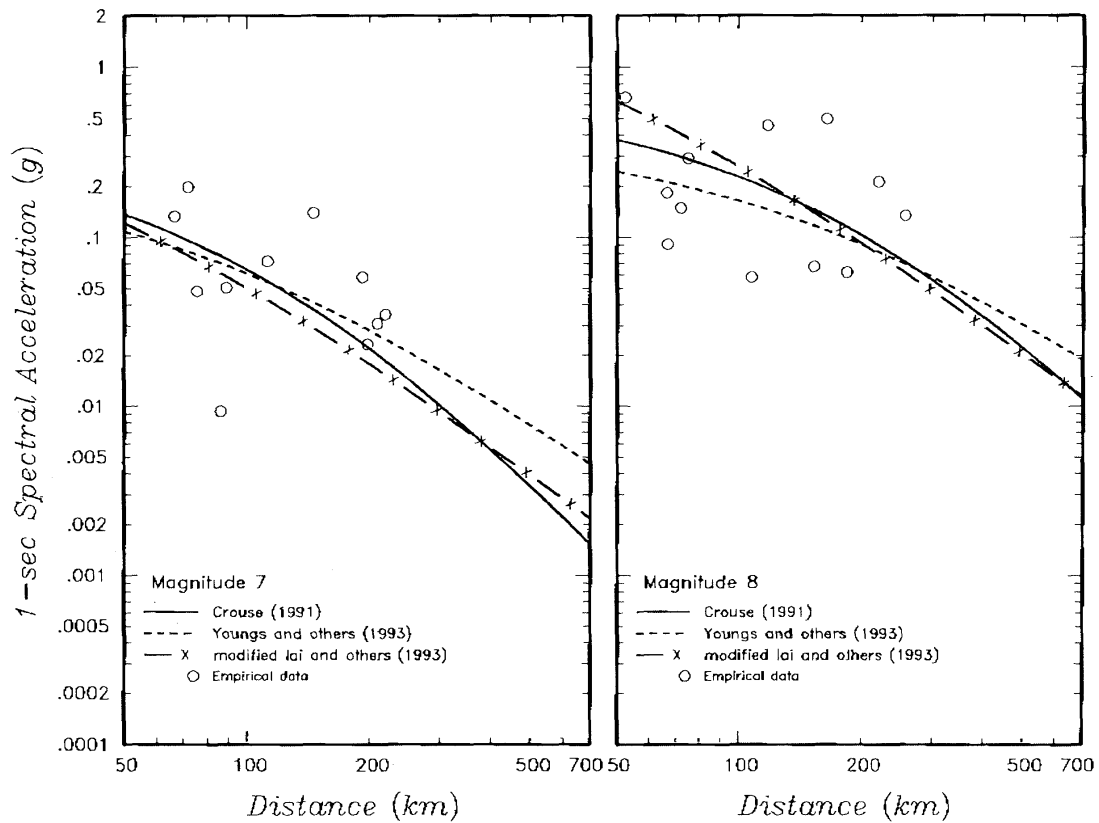
(3.33 Hz), and 2.0 sec (0.5 Hz), considering various weightings of the basement models. As discussed in the text, comparisons to the “Interpolated” values are preferred.

**Figure 6-7. Modified Version of Figure 4-10 of Geomatrix (1996b){ TC "6-7.
 Modified Version of Figure 4-10 of Geomatrix (1996b)" \f F }**



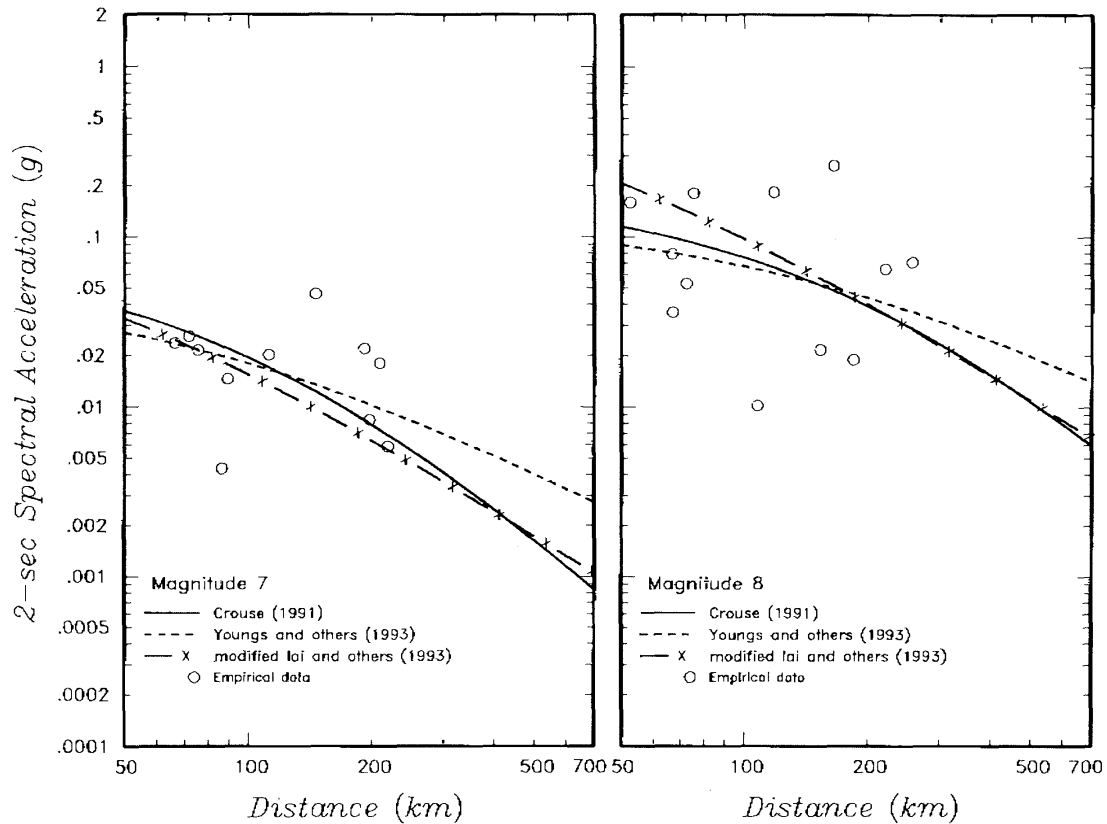
Plot indicates available peak acceleration data for subduction interface earthquakes of about magnitude 7 (left panel) and magnitude 8 (right panel) as compared to attenuation relations used by Geomatrix for the Cascadia subduction interface seismic source.

**Figure 6-8. Variation of Figure 4-10 of Geomatrix (1996b) { TC "6-8. Variation of
 Figure 4-10 of Geomatrix (1996b)" \f F }**



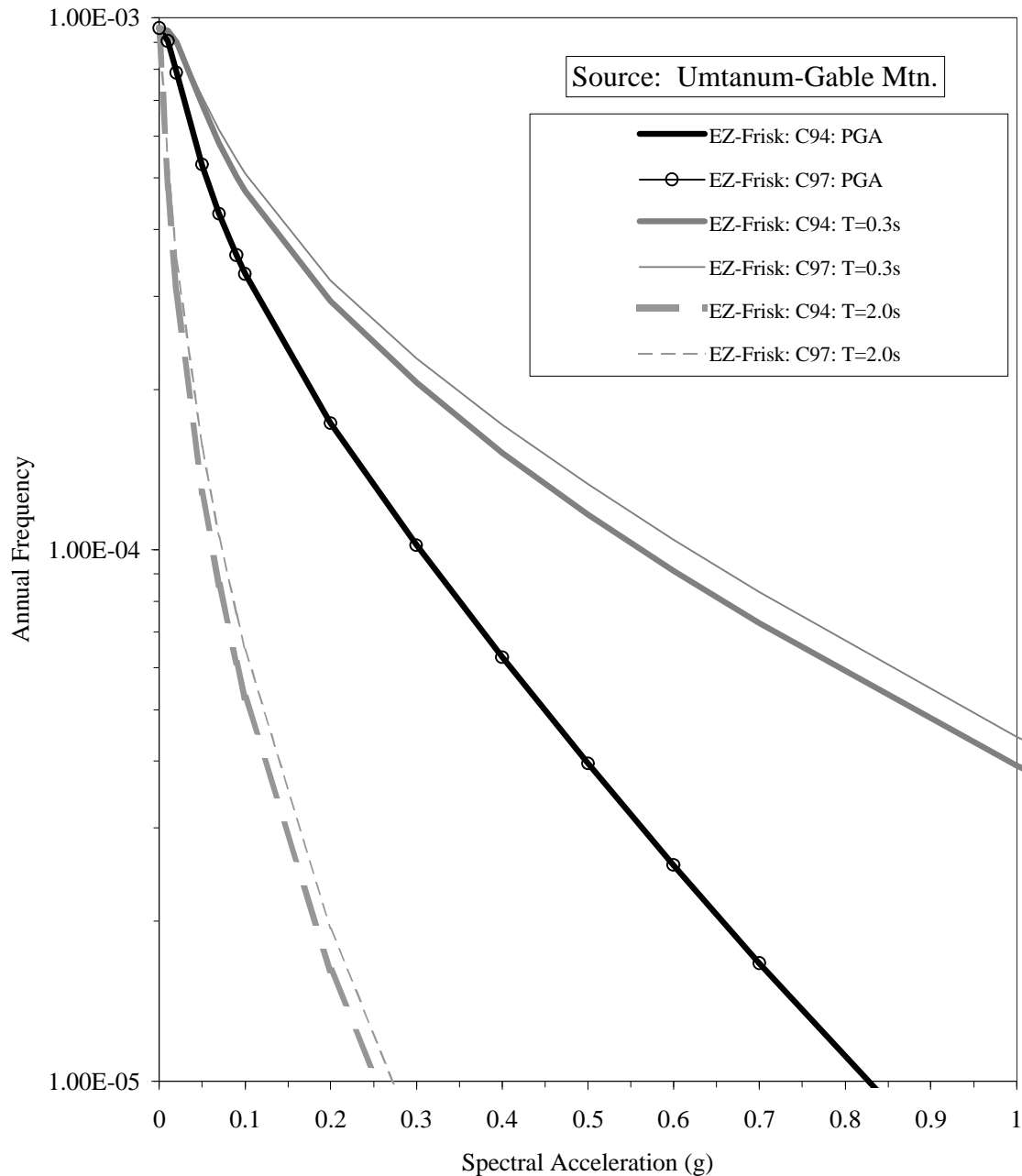
Plot indicates 1.0 sec spectral ordinate data (5% critical damping) for subduction interface earthquakes of about magnitude 7 (left panel) and magnitude 8 (right panel) as compared to attenuation relations used by Geomatrix for the Cascadia subduction interface seismic source.

**Figure 6-9. Variation of Figure 4-10 of Geomatrix (1996b) { TC "6-9. Variation of
 Figure 4-10 of Geomatrix (1996b)" \f F }**



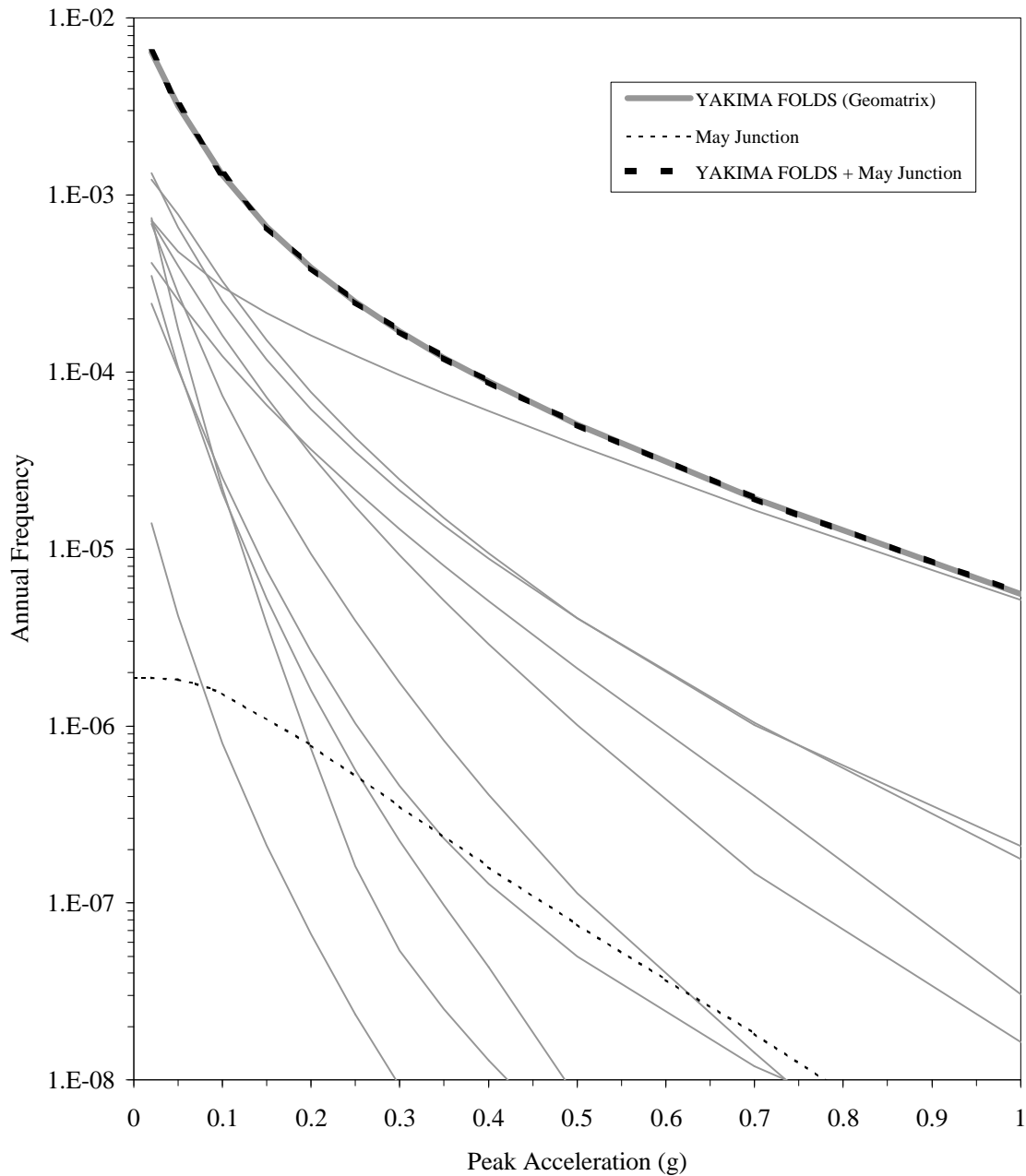
Plot indicates 2.0 sec spectral ordinate data (5% critical damping) for subduction interface earthquakes of about magnitude 7 (left panel) and magnitude 8 (right panel) as compared to attenuation relations used by Geomatrix for the Cascadia subduction interface seismic source.

Figure 6-10. Geomatrix Figure 5-4b Supplemented and Extended to Lower Annual Hazard Values to Include the Sensitivity Results for Campbell 1994 (C94) and Campbell 1997 (C97)
TC "6-10. Geomatrix Figure 5-4b Supplemented and Extended to Lower Annual Hazard Values to Include the Sensitivity Results for Campbell 1994 (C94) and Campbell 1997 (C97)"



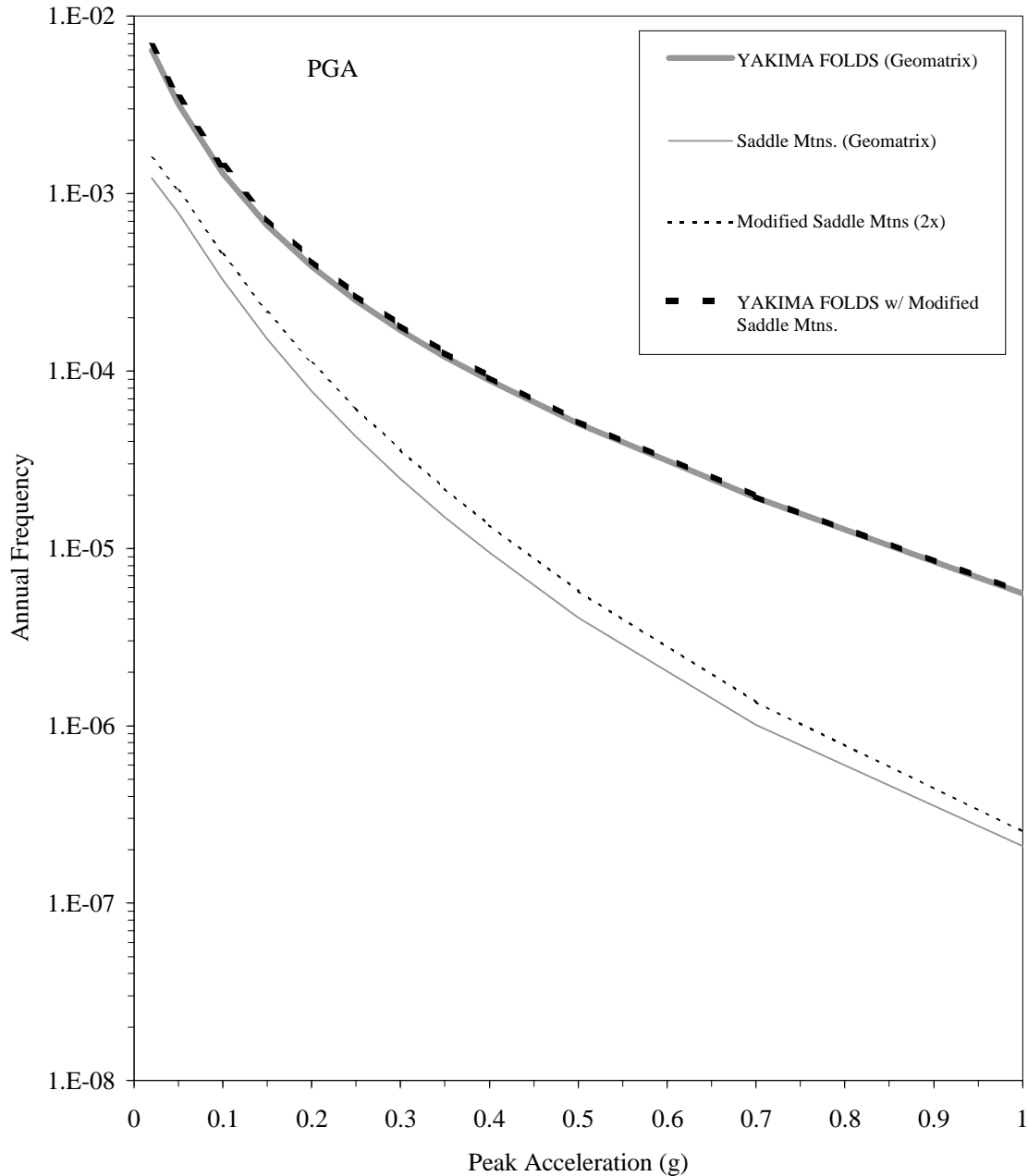
The hazard curves using the C94 attenuation relationship are shown as heavy lines and the C97 curves are shown as thin lines. The PGA hazard is unaffected while the T=0.3 and 2.0 second hazard curves show an increase for the C97 attenuation relationship.

Figure 6-11. Geomatrix Figure 5-4b Supplemented and Extended to Lower Annual Hazard Values to Include the Contribution of the May Junction Fault{ TC "6-11. Geomatrix Figure 5-4b Supplemented and Extended to Lower Annual Hazard Values to Include the Contribution of the May Junction Fault" \f F }



The peak ground accelerations from faults associated with Yakima Folds are shown in light gray (undifferentiated) while the contribution from the May Junction fault is represented by the light dashed line. The total hazard is essentially unaffected. Specific model parameters for the May Junction fault are described in the text.

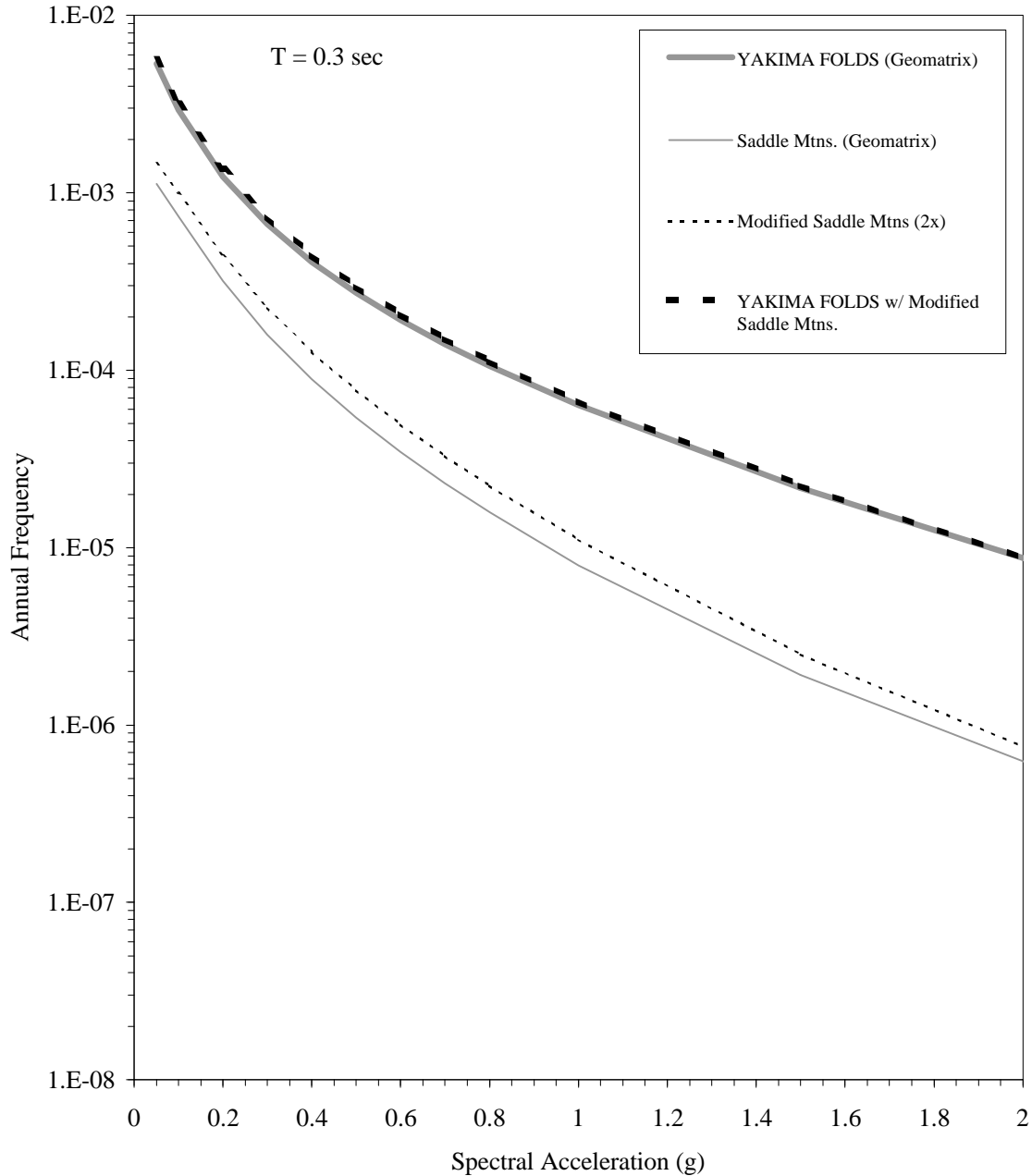
Figure 6-12a. Geomatrix Figure 5-4b Supplemented and Extended to Lower Annual Hazard Values to Include the Contribution of the Sensitivity Analysis for the Saddle Mountain Fault{ TC "6-12. Geomatrix Figure 5-4b Supplemented and Extended to Lower Annual Hazard Values to Include the Contribution of the Sensitivity Analysis for the Saddle Mountain Fault" \f F }



The peak ground accelerations from the original Saddle Mountain source and the modified (double slip rate) Saddle Mountain fault source are shown in light lines. The corresponding total hazard for the

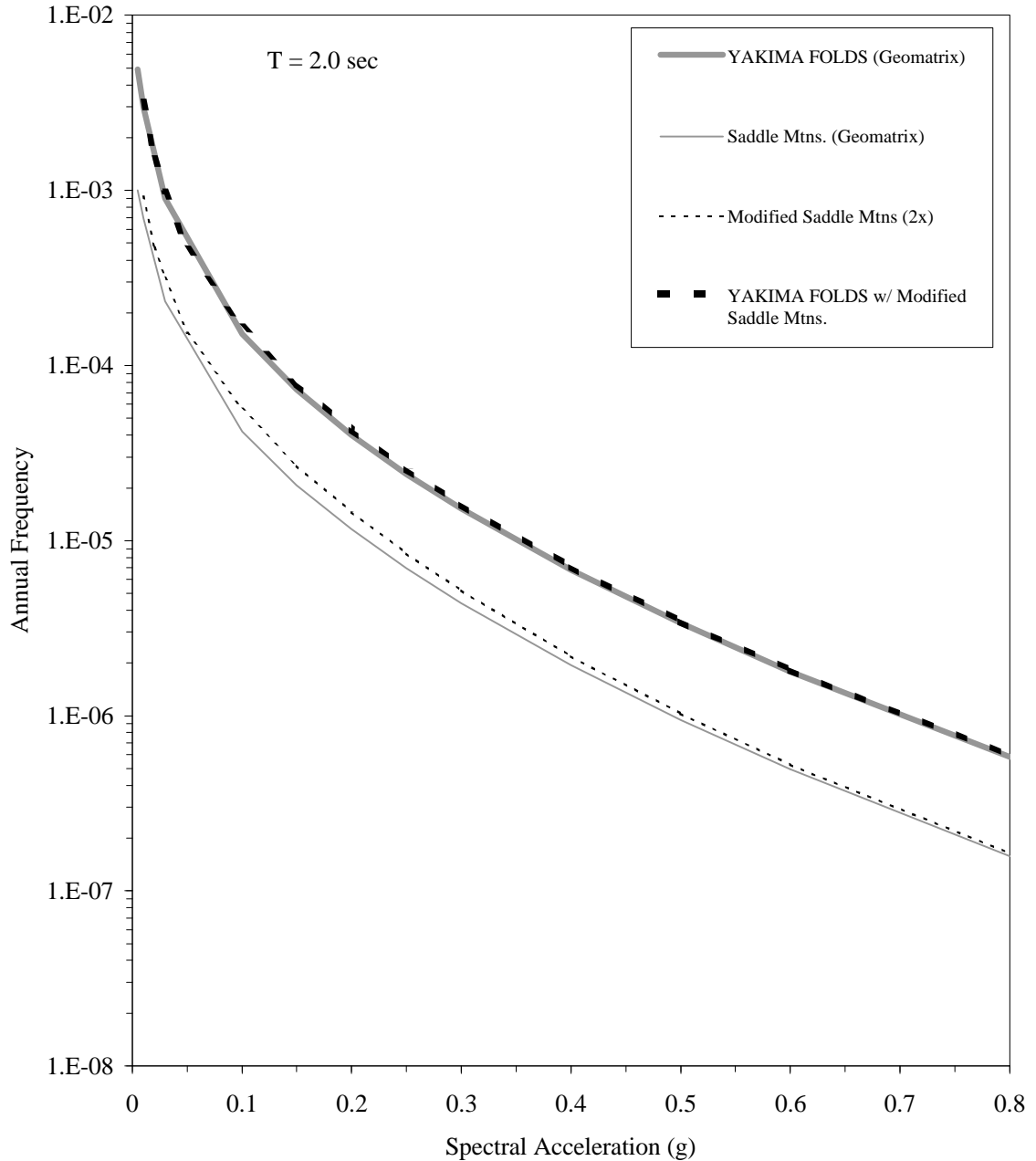
Yakima Fold sources for both cases of the Saddle Mountain models are shown as heavy lines. The total hazard for the Yakima Fold source is essentially unaffected.

Figure 6-12b. Geomatrix Figure 5-4b Supplemented and Extended to Lower Annual Hazard Values to Include the Contribution of the Sensitivity Analysis for the Saddle Mountain Fault



The spectral accelerations ($T=0.3$ second) from the original Saddle Mountain source and the modified (double slip rate) Saddle Mountain fault source are shown in light lines. The corresponding total hazard for the Yakima Fold sources for both cases of the Saddle Mountain models are shown as heavy lines. The total hazard for the Yakima Fold source is essentially unaffected.

Figure 6-12c. Geomatrix Figure 5-4b Supplemented and Extended to Lower Annual Hazard Values to Include the Contribution of the Sensitivity Analysis for the Saddle Mountain Fault



The spectral accelerations ($T=2.0$ second) from the original Saddle Mountain source and the modified (double slip rate) Saddle Mountain fault source are shown in light lines. The corresponding total hazard for the Yakima Fold sources for both cases of the Saddle Mountain models are shown as heavy lines. The total hazard for the Yakima Fold source is essentially unaffected.

7. Conclusions

In the context of applicable Natural Hazard Phenomena design criteria, the TWRS-P Facility is categorized as a PC-3 facility for which a return period of 2,000 years needs to be established for the DBE in accordance with Table 2-1 of DOE-STD-1020-94 (DOE 1996a).

Geomatrix Report (1996b) provides equal hazard spectra for 2,000 year return period suitable, pending validation, for TWRS-P Facility seismic design (BNFL, 1999). The Geomatrix report has already been extensively reviewed and accepted by DOE for use for facilities on the Hanford Site (BNFL, 1999; Wagoner, 1997).

The current report, through a review by a BNFL team of geotechnical experts, provides further validation of the Geomatrix (1996b) report for its use on the TWRS-P Project.

In developing the scope of our validation effort, we proposed a number of tasks. We read a series of comments, questions, and responses that passed between Geomatrix and the several earlier reviewers of the report. We surveyed independent estimates of seismic hazard at the Hanford Site, particularly the recent work of Frankel et al. (1996). We reviewed all elements of the fundamental regional model (such as earthquake sources specified, temporal recurrence of earthquakes as a function of magnitude, strong ground motion attenuation with distance, maximum earthquakes anticipated) to determine whether the Geomatrix report contains model parameters that information developed over the past several years might change.

The regional earthquake source model specified in the Geomatrix report is detailed and complex. The hazard estimates derived by Geomatrix are the weighted sums of many thousands of hazard curves computed from many hundreds of input assumptions. No attempt was made to reproduce the entire computational content of the report. Nevertheless, detailed analysis within the Geomatrix report of the relative contribution to total hazard from various sources shows that substantial portions of seismic hazard come from a relatively few modeled sources: several of the faults associated with Yakima Fold Belt structures and interface earthquakes from the Cascadia subduction zone. For these selected sources, we attempted to reproduce the Geomatrix results using a completely independent analytical approach to test our ability to reproduce the outcome for the model input adopted.

During the course of our validation effort we have had the benefit of several technical discussions with many of the scientists who worked on the latest (and earlier) version of the Geomatrix report and with DOE personnel and consultants. These discussions often called on us to ponder the scientific basis for particular model characteristics and on their uncertainties. To address these questions, we have performed representative sensitivity checks on selected parameters for selected models with emphasis on those parameters cited during the technical discussions.

The following can be concluded from our analyses:

- The earthquake source model of the Hanford Site region used by Geomatrix to estimate site earthquake hazard is comprehensive and up-to-date.
- The site earthquake hazard estimates developed by Geomatrix are robust and in agreement with the recent national mapping estimates.

- The treatment of strong motion attenuation and site foundation conditions is the best possible with existing data, remembering that no strong motion shaking has been recorded on the Hanford Site. Solicitation of subjective weights from regional experts for alternative geologic and seismologic model parameters and the use of conventional methodological parameters are to industry and regulatory standards.
- An update of regional seismicity data and a search for local strong motion records were performed. No information was found that would suggest revision of pertinent model assumptions used in the Geomatrix report.
- The significance of specific alternative earthquake source model parameters, known at the time of, but not incorporated into the Geomatrix report, was evaluated. It was found that these alternative parameters, if added to the scenarios of the Geomatrix report, would not significantly influence the final composite hazard result.
- The Pasco Basin is so shallow, and the 200 East Area is so centrally located within it, that significant basin effects are thought to be unlikely.
- Detailed confirmatory analyses were performed on Geomatrix's modeling of the site soil column. Our results reproduced the Geomatrix results. Earthquake hazard contributions from the Umtanum-Gable Mountain, the Saddle Mountains folds and part of the Geomatrix Cascadia source were modeled independently using a commercially available algorithm with close agreement attained.
- A number of sensitivity analyses, suggested by several discussions with DOE RU personnel, were run on various elements of the Geomatrix model. All demonstrated the stability of the Geomatrix results.
- The results of the Geomatrix report are appropriate for their application to design of important, potentially hazardous facilities at the site.

8. References

- Abrahamson, N. A. and W. J. Silva (1995). "A Consistent Set of Ground Motion Attenuation Relations Including Data from the 1994 Northridge Earthquake," Abstract, Seism. Res. Let., **66**, 23.
- Abrahamson, N. A. and W. J. Silva (1997). "Empirical Response Spectral Attenuation Relations for Shallow Crustal Earthquakes," Seism. Res. Let., **67**, 94-127.
- Abrahamson, N. A. and K. M. Shedlock (1997). "Overview," Seism. Res. Let., **67**, 9-23.
- Algermissen, S. and D. Perkins (1976). *A Probabilistic Estimate of Maximum Acceleration in Rock in the Contiguous United States*, U.S. Geological Survey Open-file Report 76-416.
- Algermissen, S., D. Perkins, P. Thenhaus, S. Hanson, and B. Bender (1982). *Probabilistic Estimates of Maximum Acceleration and Velocity in the Contiguous United States*, U. S. Geol. Survey, Open-file Report 82-1033.
- Algermissen, S., D. Perkins, P. Thenhaus, S. Hanson, and B. Bender (1990). *Probabilistic earthquake acceleration and velocity maps for the United States and Puerto Rico*. U. S. Geol. Survey, Miscellaneous Field Studies Map MF-2120, 2 sheets, 1:7,500,000.
- Algermissen, S., E. Leyendecker, G. Bollinger, N. Donovan, J. Ebel, W. Joyner, R. Luft, and J. Singh (1991). "Probabilistic Ground-Motion Hazard Maps of Response Spectral Ordinates for the United States," Proceedings of Fourth International Conference on Seismic Zonation, Stanford University, August, , 687-694.
- Applied Technology Council (1978). *Tentative Provisions for the Development of Seismic Regulations for Buildings*, NBS SP 510/ATC 3-06/NSF 78-8, U. S. Government Printing Office, Washington, D. C.
- Atwater, B. and E. Hemphill-Haley (1996). *Preliminary Estimates of Recurrence Intervals for Great Earthquakes of the Past 3500 Years at Northeastern Willapa Bay, Washington*, U.S. Geological Survey, Open-file Report 96-001.
- Atwater, B., A. Nelson, J. Clague, G. Carver, D. Yamaguchi, P. Bobrowsky, J. Bourgeois, M. Darienzo, W. Grant, S. Palmer, C. Peterson, and M. Reinhart (1995). "Summary of coastal geologic evidence for past great earthquakes at the Cascadia subduction zone, Earthquake Spectra, **11**, 1-18.
- Bandyopadhyay, K. (1994). Letter Kamal K. Bandyopadhyay, Brookhaven National Laboratory, to Dinesh Gupta, Department of Energy, "Probabilistic Seismic Hazard Analysis, DOE Hanford Site, Washington, WHC-SD-W236A-TI-002, Revision 0, Prepared by Geomatrix, dated December 1993," dated December 20, 1994.
- Bard, P.-Y., and M. Bouchon (1980). "The seismic response of sediment-filled valleys. Part 1. The case of incident waves," Bull. Seism. Soc. Am., **70**, 1263-1286.

- Bard, P.-Y., and M. Bouchon (1985). "The two-dimensional resonance of sediment-filled valleys," *Bull. Seism. Soc. Am.*, **75**, 519-541.
- Bentley, R. (1977). "Stratigraphy of the Yakima basalts and structural evolution of the Yakima Ridges in the Western Columbia Plateau," in *Geology Excursions in the Pacific Northwest*, E. H. Brown and R. C. Ellis (eds.), *Western Washington University*, 339-389.
- Bernreuter, D., J. Savy, R. Mensing, J. Chen, and B. Davis (1985). *Seismic Hazard Characterization for 69 Nuclear Power Plant Sites East of the Rocky Mountains*, U. S. Nuclear Regulatory Commission, NUREG/CR-5250.
- Bernreuter, D., J. Savy, R. Mensing, and J. Chen (1989). *Seismic Hazard Characterization of the Eastern United States, Volume 1, Methodology and Results for Ten Sites*, Lawrence Livermore National Laboratory, Report UCID-20421, Livermore, CA.
- BNFL (1999). *TWRS-P Facility Design Basis Earthquake – Peak Ground Acceleration, Seismic Response Spectra, and Seismic Design Approach*, Revision 1 (draft), February 12, 1999, British Nuclear Fuels Limited Inc., Richland, Washington.
- Boore, D. M., W. B. Joyner and T. E. Fumal (1995). *Ground Motion Estimates for Strike- and Reverse-slip Faults*, Letter Report, January 13, 1995.
- Boore, D. M., W. B. Joyner, and T. E. Fumal (1997). "Equations for estimating horizontal response spectra and peak acceleration from western North American earthquakes: A summary of recent work," *Seism. Res. Let.*, **67**, 128-153.
- Campbell, K. W. (1990). *Empirical Prediction of Near-Source Soil and Soft-Rock Ground Motion for the Diablo Canyon Power Plant Site, San Luis Obispo County, California*, Report Prepared for Lawrence Livermore National Laboratory, Dames and Moore, Evergreen, Colorado.
- Campbell, K. W. and Bozorgnia (1994). "Empirical analysis of strong ground motion from the 1992 Landers, California Earthquake," *Bull. Seism. Soc. Amer.*, **84**, 573-588.
- Campbell, K. W. (1997). "Empirical near-source attenuation relationships for horizontal and vertical components of peak ground acceleration, peak ground velocity, and pseudo-absolute acceleration response spectra," *Seism. Res. Let.*, **67**, 154-179.
- Campbell, N. (1989). "Structural and stratigraphic interpretation of the rocks under the Yakima Fold Belt based on recent surface mapping and well data," in *Volcanism and Tectonism in the Columbia River Flood-Basalt Province*, S. P. Reidel and P. R. Hooper, editors, Special Paper 239, Geological Society of America.
- Campbell, N. and R. Bentley (1981) "Late Quaternary deformation of the Toppenish Ridge uplift in South-Central Washington, *Geology*, **9**, 519-524.
- Catchings, R. and W. Mooney (1988). "Crustal structure of the Columbia Plateau - Evidence for continental rifting," *J. Geophys. Res.*, **19**, 459-474.

- Chandra, U. (1974). "Seismicity, earthquake mechanisms, and tectonics along the western coast of North America, from 42° N to 61° N," Bull. Seism. Soc. Am., **64**, 1529-1549.
- Coats, D. and R. Murray (1984). *Natural Phenomena Hazards Modeling Project: Seismic Hazard Models for Department of Energy Sites*, UCRL-53582, Lawrence Livermore Laboratory, Livermore, California.
- Cornell, C. A. (1968) "Engineering seismic risk analysis", Bull. Seism. Soc. Am., **58**, 1583-1606.
- Cornell, C. (1999). Memo, C. A. Cornell, BNFL Consultant, to J. Litehiser, Bechtel/BNFL, "Jan. 7, 1999 Meeting on the Hanford Site PSHA," dated February 9, 1999.
- Cornell, C. and E. Van Marke (1969). "The major influences on seismic risk,": Proc. Of the Third World Conf. On Earthquake Engineering, Santiago, Chile, **A-1**, 69-93.
- Costantino, C. (1994). Letter Carl J. Costantino, City College of New York, to Kamal Bandyopadhyay, Brookhaven National Laboratory, "Review 'Seismic Design Spectra, 200 West and East Areas, DOE Hanford Site, Washington," dated November 29 1994.
- Crouse, C. B. (1991). "Ground-motion attenuation equations for earthquakes on the Cascadia subduction zone," Earthquake Spectra, **7**, 210-236.
- EPRI (1986). *Seismic Hazard Methodology for the Central and Eastern United States Volume 1, Methodology*, Electric Power Research Institute, Report EPRI NP-4726, Palo Alto, CA.
- Fecht, K. (1978). *Geology of Gable Mountain-Gable Butte Area*, RHO-BWI-LD-5, Rockwell Hanford Operations, Richland, Washington.
- Fluor Daniel Hanford, Inc. (1998). *TWRS Phase 1 Privatization Site Preconstruction Characterization Report*, HNF-2067, Revision 0, prepared for the U.S. Department of Energy, March 1998.
- Frankel, A. (1993). "Three-dimensional simulations of ground motions in the San Bernardino Valley, California, for the hypothetical earthquakes on the San Andreas Fault," Bull. Seism. Soc. Am., **83**, 1020-1041.
- Frankel, A., C. Mueller, T. Barnhard, D. Perkins, E. Leyendecker, N. Dickman, S. Hanson, and M. Hopper (1996). *National Seismic-Hazard Maps: Documentation*, U.S. Geological Survey, Open-file Report 96-532.
- Fukushima, Y. and T. Tanaka (1990). "A new attenuation relation for peak horizontal acceleration of strong earthquake ground motion in Japan," Bull. Seism. Soc. Am., **80**, 757-783.
- Geomatrix Consultants (1993). *Probabilistic Seismic Hazard Analysis, DOE Hanford Site Washington*, WHC-SD-W236-TI-002, Revision 0, prepared for Westinghouse Hanford Company, Richland, Washington, December 1993.
- Geomatrix Consultants (1994a). *Probabilistic Seismic Hazard Analysis, WNP-2 Nuclear Power Plant, Hanford, Washington*, prepared for Washington Public Power Supply System, December 1994.

- Geomatrix Consultants (1994b). *Seismic Design Spectra, 200 West and East Areas, Hanford Site, Washington*, WHC-SD-W236A-TI-016, Revision 0, prepared for Westinghouse Hanford Company, Richland, Washington, November 1994.
- Geomatrix Consultants (1995). *Seismic Design Mapping, State of Oregon*, Final Report prepared for Oregon Department of Transportation, Salem, Oregon.
- Geomatrix Consultants (1996a). *Probabilistic Seismic Hazard Analysis, DOE Hanford Site Washington*, WHC-SD-W236-TI-002, Revision 1, prepared for Westinghouse Hanford Company, Richland, Washington, February 1996.
- Geomatrix Consultants (1996b). *Probabilistic Seismic Hazard Analysis, DOE Hanford Site Washington*, WHC-SD-W236-TI-002, Revision 1a, prepared for Westinghouse Hanford Company, Richland, Washington, October 1996.
- Glover, D. (1985). *Crustal Structure of the Columbia Basin, Washington, from Borehole and Refraction Data*, M.S. Thesis, University of Washington, Seattle, Washington.
- Goff, F. (1981). *Preliminary Geology of Eastern Umtanum Ridge, South-Central Washington*, RHO-BWI-C-21, Rockwell Hanford Operations, Richland, Washington.
- Golder Associates (1981a). *Gable Mountain: Structural Investigations and Analysis*, Golder Associated for Northwest Energy Services Company, Kirkland, Washington.
- Golder Associates (1981b) *Geologic Structure of Umtanum Ridge: Priest Rapids Dam to Sourdough Canyon*, Report prepared for Northwest Energy Services Company, Kirkland, Washington.
- Golder Associates (1982) in Puget Sound Power and Light Co. *Skagit/Hanford Nuclear Project, Preliminary Safety Analysis Report*, Amendment 24, Bellevue, Washington.
- Graves, R., A. Pitarka, and P. Somerville (1998). "Ground motion amplification in the Santa Monica Area: Effects of shallow basin edge structure," *Bull. Seism. Soc. Am.*, **88**, 1224-1242.
- Grolier, M. and J. Bingham (1978). *Geology of Parts of Grant, Adams, and Franklin Counties, East-Central Washington*, Bulletin 71, Washington State Department of Natural Resources, Olympia, Washington.
- Gutenberg, B. and C. F. Richter (1944) 'Frequency of earthquakes in California', *Bull. Seism. Soc. Am.*, **34**, 185-188.
- Hagood, M. (1986) *Structure and Evolution of the Horse Heaven Hills in South-Central Washington*, RHO-BWI-SA-344 P, Rockwell Hanford Operations, Richland, Washington.
- Hartshorn, D., and S. Reidel, and A. Rohay (1998). *Annual Hanford Seismic Report – Fiscal Year 1998*, Prepared by Pacific Northwest National Laboratory for the U. S. Department of Energy under Contract DE-AC06-76RLO 1830, December.
- Heaton, T. and S. Hartzell (1987). "Earthquake hazards on the Cascadia subduction zone," *Science* **236**, 162-168.

- Heaton, T. and H. Kanamori (1984). "Seismic potential associated with subduction in the northwest United States," *Null. Seism. Soc. Am.* **74**, 933-941.
- Hill, J., H. Benz, M. Murphy, and G. Schuster (1990). "Propagation and resonance of SH waves in the Salt Lake valley, Utah," *Bull. Seism. Soc. Am.*, **80**, 23-42.
- Hosler, A. (1998). E-mail W. A. Kiel, WPPSS, to Alan Hosler, SAIC/BNFL, "Strong Motion Recording at WNP-2," dated December 29, 1998.
- Hosler, A. (1999). E-mail W. A. Kiel, WPPSS, to Alan Hosler, SAIC/BNFL, "Recording of Seismic Events," dated January 20, 1999.
- Iai, S., Y. Matsunga, T. Morita, H. Sakurai, E. Kurata, and K. Mukai (1993). "Attenuation of peak ground acceleration in Japan," *Proc. International Workshop on Strong Motion Data*, Menlo Park, California, December 13-17, **2**, 3-21.
- Idriss, I. and J. Sun (1992). *User's Manual for SHAKE91*, Center for Geotechnical Modeling, Department of Civil and Environmental Engineering, University of California, Davis, California.
- International Conference of Building Officials (1997). *Uniform Building Code*, Whittier, California.
- Jongmans, D., and M. Campillo (1993). "The response of the Ubaye Valley (France) for incident SH and SV waves: Comparison between measurements and modeling," *Bull. Soc. Seism. Soc. Am.*, **83**, 907-924.
- Katsumata, A. (1996). "Comparison of magnitudes estimated by the Japan Meteorological Agency with moment magnitudes for intermediate and deep earthquake," *Bull. Seism. Soc. Am.*, **86**, 832-842.
- Keinle, C., R. Bentley, and J. Anderson (1977). "Geologic reconnaissance in the Cle Elum-Wallula Lineament and related structures," in *Washington Public Power Supply System Nuclear Project Number 2, Preliminary Safety Analysis Report*, Vol. 2A, Amendment 23, Subappendix 2RD, pp1 to 33, Washington Public Power Supply System, Richland, Washington.
- Kennedy, R. (1989). "Engineering characterization of small magnitude earthquakes," in *Proceedings: Engineering Characterization of Small-Magnitude Earthquakes*, Jack Benjamin and Associates, Inc., Mountain View, CA., Electric Power Research Institute Report, EPRI NP-6389, 2-66 to 2-95, June.
- Kennedy, R., S. Short, J. McDonald, M. McCann, Jr., R. Murray, and J. Hill (1990). *Design and Evaluation Guidelines for Department of Energy Facilities Subjected to Natural Phenomena Hazards*, UCRL-15910, Prepared for the Office of the Assistant Secretary for Environment, Safety, & Health, Office of Safety Appraisals, United States Department of Energy, June.
- Kim, K., A. Dischler, J. Aggson, and M. Hardy (1986). *The State of In-situ Stresses Determined by Hydraulic Fracturing at the Hanford Site*, RHO-BW-ST-73P, Rockwell Hanford Operations, Richland, Washington.
- King, J. and B. Tucker (1984). "Observed variations of earthquake motion across a sediment-filled valley," *Bull. Seism. Soc. Am.*, **74**, 137-151.

- Kulkarni, R., R. Youngs, and K. Coppersmith (1984). "Assessment of confidence intervals for results of seismic hazard analysis," Proc. Of the Eighth World Conference on Earthquake Engineering, San Francisco AC., **1**, 263-270.
- Leyendecker, E., D. Perkins, S. Algermissen, P. Thenhaus, and S. Hanson (1995). *USGS Spectral Response Maps and Their Relationship with Seismic Design Forces in Building Codes*, U.S. Geological Survey, Open-file Report 95-596.
- Loh, C.-H., J.-Y. Hwang, and T.-C. Shin (1998). "Observed variation of earthquake motion across a basin - Taipei City," *Earthquake Spectra*, **14**, 115-133.
- Ludwin, R., C. Weaver, and R. Crosson (1992). "Seismicity of Washington and Oregon", in Slemmons, D. B. E. R. Engdahl, M. D. Zoback, M. L. Zoback and D. Blackwell, eds., *Neotectonics of North America*, Geological Society of America, Boulder, Colorado.
- Magistrale, H., H. Kanamori, and C. Jones (1992). "Forward and inverse three-dimensional P-wave velocity models of the southern California crust," *J. Geophys. Res.*, **97**, 14,115-14,135.
- Martin, G. R. and R. Dobry (1994). "Earthquake site response and seismic code provisions," *NCEER Bulletin*, **8**, 1-6.
- McGuire, R. (1976). *Fortran Computer Program for Seismic Risk Analysis*, U. S. Geol. Surv. Open-file Report 76-67.
- Molas, G. and F. Yamazaki (1995). "Attenuation of earthquake ground motions in Japan including deep focus events," *Bull. Seism. Soc. Am.*, **85**, 1343-1358.
- National Earthquake Hazard Reduction Project (1991 and 1994 editions). *NEHRP Recommended Provisions for the Development of Seismic Regulations for New Buildings*, Building Seismic Safety Council (1992 and 1995), Federal Emergency Management Agency, Washington, D. C.
- Nishimura, C., D. Wilson, and R. Hey (1984). "Pole of rotation analysis of present-day Juan de Fuca plate motion," *J. Geophys. Res.* **89**, 10283-10290.
- Pitarka, A., K. Irikura, T. Iwata and H. Sekiguchi (1998). "Three-dimensional simulation of the near-fault ground motion for the 1995 Hyogo-ken Nanbu (Kobe), Japan, earthquake," *Bull. Seism. Soc. Am.*, **88**, 428-440.
- Power, M. S., K. J. Coppersmith, R. R. Youngs, D. P. Schwartz, and F. H. Swan III, (1981). "Seismic Exposure for the WNP-2 and WNP-1/4 Site," Appendix 2.5K, Amendment 18, *Final Safety Analysis Report*, WNP-2, Washington Public Power Supply System, Richland, Washington, September 1981.
- Price, E. (1982). *Structural Geometry, Strain Distribution, and Tectonic Evolution of Umtanum Ridge at Priest Rapids, and a Comparison with Other Selected Localities within the Yakima Fold structures, South-Central Washington*, RHO-BWI-SA-138, Rockwell Hanford Operations, Richland, Washington.
- Price, E. and A. Watkinson (1989). "Structural geometry and strain distribution within Umtanum Ridge, South-Central, Washington, and its tectonic significance," in *Volcanism and Tectonism on the*

- Columbia Plateau*, Special Paper 239, S. P. Reidel and P. R. Hooper, editors, Geological Society of America, Boulder, Colorado.
- Puget Sound Power and Light Co. (1982). *Skagit/Hanford Nuclear Project, Preliminary Safety Analysis Report*, 4, App. 20, Amendment 23, Bellevue, Washington.
- Reidel, S. (1984) "The Saddle Mountains: The Evolution of an Anticline in the Yakima Fold Belt," *American Journal of Science*, **284**, 942-978.
- Reidel, S. (1988). *Geologic Map of the Saddle Mountains, South-central Washington*, Geologic Map GM-38, Washington Division of Geology and Earth Resources, Olympia, Washington.
- Reidel, S., and N. Campbell (1989). "Structure of the Yakima Fold Belt, central Washington," in *Geologic Guidebook for Washington and Adjacent Areas*, eds., N.L. Joseph, et al., Washington Division of Geology and Earth Resources Information Circular 86.
- Reidel, S., N. Campbell, K. Fecht, and K. Lindsey (1994). "Late Cenozoic structure and stratigraphy of South-central Washington," Washington Division of Geology and Earth Resources, Bulletin 80, 159-1994.
- Reidel, S., and K. Fecht (1994). *Geologic Map of the Priest Rapids 1:100,000 Quadrangle, Washington*, Washington Division of Geology and Earth Resources, Open-file Report 94-13, September 1994.
- Reidel, S., K. Fecht, M. Hagood, and T. Tolan (1989) "The Geologic Evolution of the Central Columbia Plateau," in *Volcanism and Tectonism in the Columbia River Flood-Basalt Province*, Special Paper 239, S. P. Reidel and P. R. Hooper, editors, Geological Society of America, Boulder, Colorado.
- Reiter, L. (1990). *Earthquake Hazard Analysis – Issues and Insights*, Columbia University Press, New York.
- Riddihough, R. (1978). "The Juan de Fuca plate," EOS **59**, 836-842.
- Risk Engineering Inc. (1998). EZ-Frisk™, Version 4.2, November 1998.
- Rohay, A., D. Glover, and S. Malone (1985). *Time-Term Analysis of Upper Crustal Structure in the Columbia Basin, Washington*, RHO-BW-SA-435P, Rockwell Hanford Operations, Richland, Washington.
- Sadigh, K. (1996). "Updated attenuation relationships for soil sites developed by Sadigh and others, 1986," written communication.
- Sadigh, K., C.Y. Chang, J. A. Egan, F. Makdisi, and R. R. Youngs (1997). "Attenuation relationships for shallow crustal earthquakes based on California strong motion data," Seism. Res. Let., **67**, 154-179.
- Saltus, R. (1993). "Upper-crustal structure beneath the Columbia River Basalt Group: Gravity interpretation controlled by borehole and seismic studies," Geological Society of America Bulletin, **105**, 1247-1259.

- Schuster, J., C. Gulick, S. Reidel, K. Fecht, and S. Zurenko (1997). *Geologic Map of Washington – Southeast Quadrant*, Washington Division of Geology and Earth Resources, Geologic Map GM-45.
- Shannon & Wilson, Inc. (1994). *Geotechnical Investigation KEH W-236A, Multi-function Waste Tank Facility, Hanford Site, Richland, Washington*, Repot prepared for SCM Consultants, H-1053-05, January.
- Somerville, P. (1998). “Emerging art: Earthquake ground motion,” in *Geotechnical Earthquake Engineering and Soil Dynamics III, Volume One*, eds., P. Dakoulas, M. Yegian and R. D. Holtz, ASCE Geo-Institute Geotechnical Special Publication No. 75.
- Su, F., J.G. Anderson, S. Der Ni, and Y. Zeng (1998). “Effect of site amplification and basin response on strong motion in Las Vegas, Nevada,” *Earthquake Spectra*, **14**, 357-376.
- SSHAC (1997). *Recommendations for PSHA: Guidance on Uncertainty and Use of Experts*, NUREG/CR-6372, UCRL-ID-122160, Prepared by Senior Seismic Hazard Analysis Committee (SSHAC), April, 1997.
- Swanson, D., J. Anderson, R. Bentley, V. Camp, J. Gardner, and T. Wright, (1979) *Reconnaissance Geologic Map of the Columbia River Basalt Group in Eastern Washington and Northern Idaho*, U. S. Geological Survey Open File Report 79-1363, Washington, D. C.
- Tabor, R., R. Waite, Jr., V. Frizzell, Jr., D. Swanson, G. Byerly, and R. Bentley (1982). *Geologic Map of the Wenatchee 1:100,000 Quadrangle, Central Washington*, Miscellaneous Investigations Series Map I-1311, U.S. Geological Survey, Washington, D.C.
- Tallman, A. (1999). Email, A. M. Tallman, SAIC/BNFL, to J. Litehiser, Bechtel/BNFL, “Reference,” dated February 11, 1999.
- Tera Corporation, (1982). *Seismic Hazard Analysis for the Hanford Reservation Richland, Washington*, B-82-129, Prepared for Lawrence Livermore National Laboratory by Tera Corporation, Berkeley, California.
- Tucker, B., and J. King (1984). “Dependence of sediment-filled valley response on input amplitude and valley properties,” *Bull. Seism. Soc. Am.*, **74**, 153-165.
- U. S. Department of Energy (1975). *FFTF Final Safety Analysis Report, WHC-TI-75001*, Richland, Washington.
- U. S. Department of Energy (1988). *Site Characterization Plan Reference Repository Location, Hanford Site, Washington*, DOE/RW-0164, **2**, Washington, D.C.
- U. S. Department of Energy (1996), *Natural Phenomena Hazards Design and Evaluation Criteria for Department of Energy Facilities*, DOE-STD-1020-94, Change Notice 1, January 1996, Washington, D.C.
- U. S. Nuclear Regulatory Commission (1973). “Seismic and Geologic Siting Criteria for Nuclear Power Plants,” Appendix A to Part 100, Code of Federal Regulations.
- U. S. Nuclear Regulatory Commission (1974). *Nuclear Power Plant Instrumentation for Earthquakes*, Regulatory Guide 1.12, Revision 1, April 1974.

- U. S. Nuclear Regulatory Commission (1978) *Safety Evaluation Report Related to the Operation of the Fast Flux Test Facility, U. S. Department of Energy*, NUREG-0358.
- U. S. Nuclear Regulatory Commission (1982a). *Safety Evaluation Report Related to the Operation of WPPSS Nuclear Project No. 2, Docket No. 50-397*, NUREG-0892, Supplement No. 1, August 1982.
- U. S. Nuclear Regulatory Commission (1982b) *Safety Evaluation Report Related to the Construction of Skagit/Hanford Nuclear Project, Units 1 and 2*, NUREG-0309, Supplement No. 3, December 1982.
- Wagoner, J. D. (1997). Letter 97-PMD-026 to H. J. Hatch, FDH, "Contract No. DE-AC06-96RL13200 – Approval of Probabilistic Seismic Hazard Analysis," dated June 17, 1997.
- Wald, D., D. Helmberger, and T. Heaton (1991). "Rupture model of the 1989 Loma Prieta earthquake from the inversion of strong-motion and broadband teleseismic data," *Bull. Seism. Soc. Am.*, **81**, 1540-1572.
- Washington Public Power Supply System (1981). *Final Safety Analysis Report for Unit WNP-2 Amendment No. 18*, September.
- Washington Public Power Supply System (1985). "Site-specific response spectra for the WNP-2 Power Plant," in *Final Safety Analysis Report for Unit WNP-2*, Appendix 2.5Q, Amendment No. 36, December.
- Washington Public Power Supply System (1995). *Individual Plant Examination of External Events, Washington Nuclear Plant 2*, June.
- Washington Public Power Supply System (1996). *Technical Specifications*, 3/4 3.7, "Monitoring Instrumentation."
- Washington Public Power Supply System (1998). *Final Safety Analysis Report*, Amendment No. 53.
- Wells, D. and K. Coppersmith (1981). "Analysis of fault dip and sense of slip for historical earthquakes (abs), *Seismological Research Letters*, v. 62, p 38.
- West, M. (1998). "A continuation of a "pilot" study of Quaternary surface deformation, Saddle Mountains Anticline, northern Pasco Basin, Washington," USGS Award No.: 1434-HQ-97-GR-02999, Reston, VA, URL: <http://erp-web.er.usgs.gov/reports/vol39/pn/g2999.htm>.
- West, M., F. Ashland, A. Busacca, G. Berger and M. Shaffer (1996). "Late Quaternary deformation, Saddle Mountains Anticline, South-Central Washington, *Geology*, **24**, 1123-1126.
- West, M. and M. Shaffer (1989). "Late Quaternary tectonic deformation on the Smyrna Bench and Saddle Gap segments, Saddle Mountains anticline, Yakima Fold Belt, central Columbia Basin, Washington," *Geol. Soc. Am., Abstracts with Programs*, **21**, 157-158.
- Weston Geophysical Corporation (1981). *Geologic Models in the Columbia Plateau Constrained by Gravity Data*, report prepared for Washington Public Power Supply System, Richland, Washington.

- Woodward-Clyde Consultants, (1989). *Evaluation of Seismic Hazard for Nonreactor Facilities, Hanford Reservation, Hanford Washington*, WHC-MR-0023, prepared for Westinghouse Hanford Company, Richland, Washington.
- Youngs, R., S. Chiou, W. Silva, and J. Humphrey (1993). "Strong ground motion attenuation relationships for subduction zone earthquakes based on empirical data and numerical modeling (abs)," *Seism. Res. Let.*, **64**, 18.
- Youngs, R., S. Chiou, W. Silva, and J. Humphrey (1997). "Strong ground motion attenuation relationships for subduction zone earthquakes," *Seism. Res. Let.*, **67**, 58-73.
- Youngs, R. and K. Coppersmith (1985). "Implications of fault slip rates and earthquake recurrence models to probabilistic seismic hazard estimates," *Bull. Seism. Soc. Am.*, **75**, 939-964.
- Youngs, R., F. Swan, M. Power, D. Schwartz, and R. Green (1987). "Probabilistic analysis of earthquake ground shaking hazard along the Wasatch Front, Utah," in *Assessment of Regions Earthquake Hazards and Risk Along the Wasatch Front, Utah*, U. S. Geological Survey, Open-file Report 87-585, **V II**, M1-M110.

Appendix A – Responses to Specific DOE RU Questions/Comments

BNFL (1999, Section 5.0) provides a comprehensive list of written comments and questions received from the DOE Regulatory Unit (RU) following a Topical Meeting on seismic issues held on December 14, 1998, RU comments and questions from earlier Level 1 Meetings held on November 6, 1998 and December 3, 1998, and from a meeting with Geomatrix Consultants on January 7, 1999.

BNFL (1999) addresses each of these comments and questions either explicitly or by reference to this and other BNFL documents. Where response has been by reference to this document, the comments and questions are addressed in the tables of this appendix.

**Table A-1. Preliminary Questions Concerning the Geomatrix Report and Dynamic Analysis (sent by the RU following the 12/3/98 Level 1 Meeting){ TC
"A-1. Preliminary Questions Concerning the Geomatrix Report and Dynamic Analysis (sent by the RU following the 12/3/98 Level 1 Meeting)" {f T }**

No.	Question/Comment	Response
2	What is the range of estimated fundamental periods of the site before and during earthquake loading?	The site period prior to earthquake shaking is approximately 0.95 second for the initial velocity profile, 1.03 second for the profile during subduction earthquakes, and 1.06 second for the profile during crustal earthquakes. See Section 5.1.3 of this report for discussion.
4	How were recurrence relationships determined for magnitudes greater than the empirical databases (see Figures 3-3, 3-5, 3-14, 3-15, 3-24, and 3-26)?	Recurrence relationships are determined either from maximum likelihood fits of the truncated exponential form to the empirical data or from centroid measures of a suite of model characteristic/modified exponential fits to moment rates determined from structure slip rates.
5	Why do the two significant earthquakes (M=6.5 and M=7.0) plot above the recurrence relationship (Figure 3-35)?	Both of the earthquakes which exceed the recurrence curve have very large uncertainties which plot on and continue below the recurrence curves. That is, they are statistically consistent with the recurrence curves. The magnitude 7 Washington intraslab event is well within the uncertainty error bar. The Southern Oregon intraslab magnitude 6.5 event is more of an outlier. Note, however, that intraslab earthquakes as a group contribute almost nothing to hazard at Hanford (see Fig. 5-2b of the Geomatrix report) and that almost none of the little hazard they do contribute is likely to come from the Southern Oregon segment because of its great distance (> 200 km, Fig. 3-34 of the Geomatrix report).
6	How do the PGA and Spectra for the design basis and beyond design basis earthquakes compare to USGS results (Frankel et al. 1996), site-specific uniform hazard spectra and a deterministic approach (such as Krinitzsky 1995, Abramson & Silva), including sigma bounds and mean and median values?	The mean PGA and response spectra amplitudes for a return period of 2,000-yr are higher in the Geomatrix than in the Frankel et al. report even after scaling to comparable foundation soil conditions (see Section 2.2 and Figure 2-2 of this report). No "deterministic" estimate of site ground motion is anticipated for this Project. Were one to be done, considering "all reasonable interpretations" of potential site earthquakes sources as advocated by Krinitzsky (<i>Engineering Geology</i> , Vol. 40, pp. 1-7, 1995), ground motions greater than the DBE would likely be found. The only deterministic estimates of DBE ground motions on the Hanford site that have been developed within a regulatory process are the SSE motions for WNP-1/2, the FFTF, and the proposed Skagit-Hanford NAP. The deterministic PGAs for these facilities, which envelop 84%-tile motion estimates at each site, are 0.25 g, 0.25 g, and 0.35 g, respectively. The most recent Abrahamson and Silva paper on strong ground motion attenuation that we know of is in <i>Seismological Research Letters</i> , Vol. 68, pp. 94-127, 1997. It is the published equivalent or update of Abrahamson and Silva (1995) cited and used in the Geomatrix report and was found to be equivalent (see Section 3.1 of this report).

Table A-1. Preliminary Questions Concerning the Geomatrix Report and Dynamic Analysis (sent by the RU following the 12/3/98 Level 1 Meeting){ TC
"A-1. Preliminary Questions Concerning the Geomatrix Report and Dynamic Analysis (sent by the RU following the 12/3/98 Level 1 Meeting)" {f T }

No.	Question/Comment	Response
7	How do the input parameters in your probabilistic seismic hazard analysis compare to USGS values (Frankel et al. 1996)?	As would be expected for a hazard analysis for a very large region, the USGS study uses a less detailed earthquake source model. Specific features of a Geomatrix/Frankel comparison are addressed in responses to question 6 in both Table A-1 and A-2 of this appendix. In general terms, the USGS characterization contains: 1) fewer fault sources (the peak acceleration at the site appears to be dominated by the Rattlesnake Wallula Alignment with no influence of the other YFB structures), 2) more dependence on smoothed areal sources, 3) similar conservation of historical earthquake "budget," 4) a similar model for Cascadia interface source, and 5) use of very similar attenuation relations. The results, corrected for baseline shallow foundation soils, are very similar (see Section 2.2 and Figure 2-2 of the current report).
8	Are there any new geological or seismologic data that postdate the Geomatrix (1996) report that are significant?	We contacted S. Reidel and K. Fecht, experts on Hanford region seismology, tectonics, and geology. No significant new geologic or seismologic data that postdate the Geomatrix report was identified. Post-1991 regional seismicity as cataloged by PNNL (e.g. Hartshorn et al., 1998) has been examined and is discussed in Section 4.1.1 of this report. Several geologic issues known at the time of, but not considered in, the Geomatrix report were identified (the May Junction Fault and alternative estimates of slip rate on two segments of the Saddle Mountains faults). These are discussed in Sections 4.3, 4.4, 6.4 and 6.5 of this report.
9	How do the attenuation relationships used for subduction-zone earthquakes compare to the empirical databases in the range of distances appropriate for this site?	See discussion in Section 6.3.1 and accompanying Figures 6-7 through 6-9 of this report.
10	How were the peak accelerations for subduction-zone earthquakes scaled in the site-specific site response analyses (Appendix A)?	The rock acceleration time histories for Cascadia earthquakes were uniformly scaled such that the acceleration spectral values at long periods (the period in the range of 1 to 2 seconds) matched those expected at Hanford using the empirical attenuation relationships for subduction zone events. See Section 5.1.1.1 of this report.
12	How does historical seismicity relate to geological structure?	The historical seismicity is not directly related to known geologic faults/structure. This was maintained in the 1996b Geomatrix report and confirmed in the current report by updating the regional earthquake catalog (see Section 4.1.1 of the current report).
13	How was "ground truthing," aerial and field reconnaissance, of input parameters to probabilistic seismic hazard analysis accomplished? Where is it documented?	The geologic field studies at and around the Hanford Site are in many documents and are summarized in the original Geomatrix (1996b) report and in Section 3.2 of the current report.

**Table A-1. Preliminary Questions Concerning the Geomatrix Report and Dynamic Analysis (sent by the RU following the 12/3/98 Level 1 Meeting){ TC
"A-1. Preliminary Questions Concerning the Geomatrix Report and Dynamic Analysis (sent by the RU following the 12/3/98 Level 1 Meeting)" \f T }**

No.	Question/Comment	Response
14	Will site-specific site response analyses be conducted with suites of both artificial and scaled recorded accelerograms? How many dimensions would be used (1-, 2-, or 3-dimensional deposit and 1-, 2-, or 3-dimensional accelerograms)? How will you select appropriate rock outcrop motions?	The Geomatrix 2000-yr motion for the 200 East Area defines the ground motion at the ground surface level. This motion will be used to define the DBE. No additional site response analysis will be performed for the purpose of ground motion development. For seismic analysis of structures, seismic soil-structure interaction analysis will be performed. These analyses are expected to be based on three-dimensional models with three components of the design motion applied simultaneously.

Table A-2. Post Meeting RU Comments (from the RU meeting minutes of the 12/14/98 Topical Meeting){ TC "A-2. Post Meeting RU Comments (from the RU meeting minutes of the 12/14/98 Topical Meeting)" \f T }

No.	Question/Comment	Response
5	Research the availability of recorded site seismic data to compare with Geomatrix Report.	Regional microseismic data were updated and Hanford Site strong ground motion data were sought during the current study. Results are presented in Section 4.1.
6	Evaluate how the maximum magnitudes in the USGS report (Frankel, et al, 1996) compare to the range of magnitudes in the Geomatrix report.	Frankel et al. consider three sources contributing shaking hazard to the Hanford Site: specific faults (for example, Rattlesnake-Wallula), the Cascadia subduction zone, and a background area with no specifically identified seismogenic structures. Maximum magnitudes for these sources are 7.1-to-7.4, 8.3, and 7, respectively. The Geomatrix model is more complex and incorporates a wider range of maximum magnitudes for fault, Cascadia, and regional "areal" sources. In gross generalization, these range from 5.0 to 7.8, 8 to 8.7, and 6 to 7, respectively.
9(1)	The Crystalline Basement tectonic model has a significant impact on design motions. Scientific data and analysis of the rift, block and uniform models are lacking. High subjective weight (0.8) is given to the uniform model which results in the least "probabilistic" contribution. A more scientific basis or at least a more sensitive analysis of these subjective weights should be considered.	The basis for weights assigned to the various source models for the crystalline basement beneath the Hanford Site region is discussed in Section 3.2 of the current study. Some sensitivity analysis of the effect of varying these weights is presented in Section 6.2.
9(2)	Yakima Fold sources are affected by whether they are active, coupled or segmented. The activity should have more scientific basis. Faults that are currently uncoupled and segmented may become coupled and segmented.	The basis for weights assigned to the various source models parameters for the YFB sources is discussed in Section 3.2 of the current study. Some sensitivity analysis of the effect of varying these weights for the coupling parameter is presented in Section 6.1.
9(3)	Coupling should not reduce recurrence rates. Why are alternative assumptions, reality checks and sensitivity analysis not considered?	The interplay between coupling and recurrence is complex, but in general coupling does not reduce recurrence rates. Some sensitivity analysis on coupling/uncoupling weights is presented in Section 6.1 of the current report.
9(4)	The Cascadia interface contribution may be too small due to insufficient energy attenuation and site response. However, its impact could be more significant in the long-period range. Has this been analyzed?	Analyses of attenuation and site response issues for the Cascadia subduction zone interface source are discussed in Sections 5.1 and 6.3 of the current study.
9(5)	Would one conclude that the Cascadia interslab and Shallow Basalt sources are relatively unimportant to the overall hazard?	Yes.
9(6)	Attention to the overall model and details is important since the probabilistic seismic hazard analysis is being used to specify an <u>absolute</u> design ground motion, rather than to develop a <u>relative</u> number.	We agree.

Table A-3. Post Meeting RU Comments (from the RU meeting minutes of the 1/7/99 meeting with Geomatrix Consultants){ TC "A-3. Post Meeting RU Comments (from the RU meeting minutes of the 1/7/99 meeting with Geomatrix Consultants)" \f T }

No.	Question/Comment	Response
1	The geological basis for the subjective weights assigned to different fault models in the PSHA logic tree should be elaborated, to provide a clearer logical basis for the weights chosen. For example, the coefficients assigned for coupled vs. uncoupled fault segments, crystalline basement fault characteristics, and Yakima Fold models should be elaborated.	Additional discussion of the basis for assessed weights is presented in Section 3.2 of the current report.
2	Sensitivity calculations to show the effect of different fault model weighting factors on the peak ground acceleration and like seismic spectra should be presented. Representative recurrence intervals of interest, such as 2000 and 10000 year recurrences, are acceptable, rather than a comprehensive sensitivity study.	Sensitivity analyses on selected parameters, with emphasis on those parameters specifically identified as of interest in various RU meetings, are presented in Chapter 6.0 of the current report.
3	The expert reviews regarding the Geomatrix study collected during and after its preparation should be provided to the RU. (Subsequent to the meeting, BNFL has provided this information to the RU.)	Available comments on the Geomatrix Report were forwarded to the RU on January 20, 1999. No further response is required.
4	BNFL will provide an outline of the BNFL/Bechtel evaluation report of the Geomatrix report to the RU once it is available.	An outline of the BNFL evaluation of the Geomatrix Report was forwarded to the RU on January 22, 1999. No further response is required.
5	Figure 4-10 of the Geomatrix study shows the peak ground acceleration attenuation function below the data in the 300-400 KM range. Yet this distance is the range of interest for the TWRS-P site. The effect of using an attenuation estimate in this range that better predicts the data on PGA, and spectra should be discussed.	The suite of attenuation relations used in the Geomatrix report has been plotted against longer period ground motion data for which earthquake shaking hazard from Cascadia interface events is significant. The fit shown is good. See Section 6.3.1 of the current report for discussion.
6	Scoping study should evaluate whether a significant basin effect may exist for the TWRS-P site. The study should consider current research (Frankel, Larsen), and factors such as edge effect, slope of the basin, and basin material.	A review of available literature on this issue appears in Section 4.6 of the current report.
7	The geotechnical SHAKE code runs that were previously performed by Geomatrix to confirm the predominant site periods, empirical relations such as the frequency dependence of attenuation, and the local soil response spectra should be reviewed to confirm the data has been adequately reflected in the Geomatrix report.	All relations cited have been reviewed as part of this report. For predominant site period, see Question 2 of Table A-1 above. Attenuation fit of longer period ground motions to subduction zone earthquakes is discussed in Section 6.3.1 of this report. Confirmation of local soil response spectra developed by Geomatrix is discussed in Section 5.1.2 of this report.
8	A detailed bibliography of data reports that support the Geomatrix 1996 report will be provided in the BNFL/Bechtel evaluation of the Geomatrix report.	This bibliography is provided as Chapter 8.0 of the current report.
9	The records from strong motion instruments in the Hanford vicinity will be reviewed, and the resets of this review provided in the BNFL/Bechtel evaluation of the Geomatrix report.	Efforts to find any strong motion records in the Hanford vicinity are summarized in Section 4.1.2 of the current report. None were found.

